

LYAPUNOV BASED NONLINEAR IMPACT ANGLE GUIDANCE LAW FOR
STATIONARY TARGETS

A THESIS SUBMITTED TO
THE GRADUATE SCHOOL OF APPLIED AND NATURAL SCIENCES
OF
MIDDLE EAST TECHNICAL UNIVERSITY

BY

HAKKI ULAŞ ATEŞ

IN PARTIAL FULFILLMENT OF THE REQUIREMENTS
FOR
THE DEGREE OF MASTER OF SCIENCE
IN
AEROSPACE ENGINEERING

JANUARY 2015

Approval of the thesis:

**LYAPUNOV BASED NONLINEAR IMPACT ANGLE GUIDANCE LAW
FOR STATIONARY TARGETS**

submitted by **HAKKI ULAŞ ATEŞ** in partial fulfillment of the requirements for the degree of **Master of Science in Aerospace Engineering Department, Middle East Technical University** by,

Prof. Dr. Gülbin Dural Ünver
Dean, Graduate School of **Natural and Applied Sciences**

Prof. Dr. Ozan Tekinalp
Head of Department, **Aerospace Engineering**

Assist. Prof. Dr. Ali Türker Kutay
Supervisor, **Aerospace Engineering Dept., METU**

Koray Savaş Erer, M.Sc.
Co-Supervisor, **TMS-G&CD Dept., Roketsan Missiles Inc.**

Examining Committee Members:

Prof. Dr. Ozan Tekinalp
Aerospace Engineering Department, METU

Assist. Prof. Dr. Ali Türker Kutay
Aerospace Engineering Department, METU

Assoc. Prof. Dr. İlkay Yavrucuk
Aerospace Engineering Department, METU

Koray Savaş Erer, M.Sc.
TMS-G&CD Department, Roketsan Missiles Inc.

Prof. Dr. M. Kemal Özgören
Mechanical Engineering Department, METU

Date: 30.01.2015

I hereby declare that all information in this document has been obtained and presented in accordance with academic rules and ethical conduct. I also declare that, as required by these rules and conduct, I have fully cited and referenced all material and results that are not original to this work.

Name, Last Name: HAKKI ULAŞ ATEŞ

Signature:

ABSTRACT

LYAPUNOV BASED NONLINEAR IMPACT ANGLE GUIDANCE LAW FOR STATIONARY TARGETS

Ateş, Hakkı Ulaş

M.S., Department of Aerospace Engineering

Supervisor: Assist. Prof. Dr. Ali Türker Kutay

Co-Supervisor: Koray Savaş Erer

January 2015, 133 pages

In modern guidance law designs, not only capturing but also considering a terminal impact angle while intercepting a target has become an increasingly important necessity in modern guided systems. For several applications such as missiles systems, space explorations or aircraft docking, approaching the target with a specific impact angle is vital requirement for efficiency of the system.

To achieve this requirement, a novel Lyapunov based nonlinear impact angle control guidance law for stationary targets is investigated in this work. In the proposed guidance law, nonlinear line-of-sight dynamics of the engagement geometry and kinematics between target and pursuer is studied and state equations for the line-of-sight angle and its rate are derived. The line-of-sight angle which converges the final flight path angle of the pursuer at the final rendezvous is aimed to be controlled to satisfy impact angle constraints.

The nonlinear time-variant dynamics between target and pursuer is investigated. Then, to control robustly and stably, a first order sliding manifold to force the nonlinear dynamical system to exponential stability and reduce the order of the complex system is introduced. Moreover, Robust Control Lyapunov Function candidate is also investigated to control the dynamical system in order to head towards the desired sliding manifold. The necessary acceleration commands to head towards the target with specified terminal impact angle is carried out by deriving control input of the nonlinear system to have asymptotical stability.

Finally, the results of the proposed guidance law is expressed. Moreover, capturability analysis and capture conditions of the guidance law, robustness and disturbance rejection of the system is investigated. Furthermore, the response of the guidance law to some aspects which can be encountered in practical application is discussed.

Keywords: Impact Angle Control Guidance, Nonlinear Guidance Law, Robust Control Lyapunov Functions, Sliding Manifold, Line-Of-Sight Dynamics

ÖZ

SABİT HEDEFLER İÇİN LYAPUNOV TABANLI DOĞRUSAL OLMAYAN VURUŞ AÇISI KONTROLLÜ GÜDÜM KANUNU

Ateş, Hakkı Ulaş

Yüksek Lisans, Havacılık ve Uzay Mühendisliği Bölümü

Tez Yöneticisi: Assist. Prof. Dr. Ali Türker Kutay

Ortak Tez Yöneticisi: Koray Savaş Erer

Ocak 2015, 133 sayfa

Çağdaş güdümlü sistem teknolojilerinde, güdüm kanunu tasarımı sırasında sadece hedefi yakalamak değil, belirli bir son vuruş açısı düşünmek de giderek artan bir gereklilik olmaktadır. Bir çok pratik uygulama alanında, örneğin füze sistemlerinde, uzay arařtırmalarında veya hava araçlarının kenetlenmesinde, hedefe belirli bir açı ile yaklaşmak sistemin etkinliđi açısından hayati bir gereksinimdir.

Bu gereksinimi karşılamak için bu çalışmada, sabit hedefler için yeni ve özgün, Lyapunov tabanlı, doğrusal olmayan, vuruş açısı kontrollü güdüm kanunu geliştirilmiştir. Takipçinin son uçuş yolu açısına yakınsayan vuruş anındaki görüş hattı açısının kontrol edilmesi ve vuruş açısı gereksiniminin bu sayede karşılanması amaçlanmaktadır.

Kontrol edilmek istenen durum denklemlerini elde etmek için, doğrusal olmayan ve zamanla değişen takipçi-hedef dinamiđi araştırılmıştır. Daha sonra, sistemi gürbüz ve

kararlı şekilde kontrol edebilmek adına, sistemi üssel kararlılığa götürecekt ve öte yandan sistemin derecesini azaltan birinci derece kayma yüzey tanıtılmıştır. Ayrıca, sistemin durumlarını istenen kayma yüzeyine yakınsatacak gürbüz Lyapunov kontrol fonksiyon adayını araştırılmıştır. Hedefe istenen açı ile yaklaşmak için gereken ivme değerleri; sistemin asimptotik kararlılığı için gereken kontrol eforundan analitik olarak hesaplanmıştır.

Son olarak sunulan güdüm kanununun sonuçları gösterilmiştir. Buna ek olarak, yakalayabilme analizi ve yakalama koşulları, gürbüzlük ve bozucu etkilere karşı güdüm kanununun cevapları incelenmiştir. Öte yandan önerilen güdüm kanununun pratik uygulamada karşılaşılabileceği bazı sorunlara karşı davranışı da irdelenmiştir.

Anahtar Kelimeler: Vuruş Açısı Kontrollü Güdüm, Doğrusal Olmayan Güdüm Kanunu, Gürbüz Lyapunov Kontrol Fonksiyonu, Kayma Yüzeyleri, Görüş Hattı Dinamiği

Obscurum per obscurius, ignotum per ignotus.

ACKNOWLEDGEMENTS

First of all, I would like to express appreciation to my supervisor Assist. Prof. Dr. Ali Türker KUTAY for his guidance, deep interest and encouragement throughout this study. I would like to thank my co-supervisor Koray Savaş ERER for enduring and answering my endless questions and his criticisms about this work. Without his contributions and comments, this work has never been so thorough. Also, I would like to gratefully acknowledge Osman MERTTOPÇUOĞLU for his discussions with sliding surfaces.

I also owe my thanks to Alper KAHVECİOĞLU for his helps and understanding and Başak BİNGÖL for her discussions and support during this work.

I would like to extend my appreciation to my dear friends; Mehmet Çağlar ÇÖLMEK, Okan Mete ÇOLUK, Hüseyin Çağlar SARIKAYA and Başar YALÇIN for their invaluable support and friendship.

Above all, I would like to thank my parents Sevim ATEŞ, Mehmet ATEŞ for their endless love, encouragements and support for my whole life. I am also thankful to my sister Özlem SÖNMEZ, my brother-in-law Özgür SÖNMEZ and my two brilliant nephews; Ali Yiğit SÖNMEZ and Kaan Utku SÖNMEZ.

Last but not least important, I owe my deepest gratitude to my dearest Cansu DİREK for her endless support, patience and love. Without her, none of this would have been even possible.

TABLE OF CONTENTS

| | |
|--|------|
| ABSTRACT | v |
| ÖZ | vii |
| ACKNOWLEDGEMENTS | x |
| TABLE OF CONTENTS | xi |
| LIST OF TABLES | xiii |
| LIST OF FIGURES | xiv |
| CHAPTERS | 1 |
| 1. INTRODUCTION | 1 |
| 1.1 Study of Impact Angle Guidance | 1 |
| 1.2 Literature Survey | 2 |
| 1.3 Contribution..... | 7 |
| 1.4 Thesis Structure | 10 |
| 2. PROBLEM DEFINITION | 11 |
| 2.1 Engagement Geometry | 12 |
| 2.2 Geometrical Relationship and Impact Angle Definition | 15 |
| 2.3 Line-Of-Sight Dynamics | 19 |
| 2.4 State-Space Representation of the Dynamical System..... | 24 |
| 3. NONLINEAR GUIDANCE LAW DESIGN | 29 |
| 3.1 Construction of Sliding Manifold..... | 31 |
| 3.2 Robust Control Lyapunov Function | 35 |
| 3.3 Deduction of Guidance Law and Implementation Aspects..... | 38 |
| 3.4 Capturability Analysis of the Guidance Law | 43 |
| 4. SIMULATION RESULTS | 55 |

| | | |
|-----|---|-----|
| 4.1 | Construction of Simulation..... | 56 |
| 4.2 | Ideal Test Scenarios & Results | 58 |
| 4.3 | Successful Mission Criteria..... | 88 |
| 4.4 | Variation of Guidance Constant K | 89 |
| 4.5 | Numerical Robustness and Disturbance Rejection Analyses | 94 |
| 4.6 | Step-size Selection and Integration Scheme..... | 116 |
| 5. | CONCLUSION..... | 123 |
| | REFERENCES..... | 127 |

LIST OF TABLES

TABLES

| | |
|--|-----|
| Table 1. Ideal Engagement Scenarios | 59 |
| Table 2. Nominal Test Scenario | 89 |
| Table 3. Successful Mission Criteria | 89 |
| Table 4. Scenarios for sensor noise & bias | 106 |

LIST OF FIGURES

FIGURES

| | |
|---|----|
| Figure 1: 3-D Engagement Geometry | 13 |
| Figure 2: 2-D Engagement Geometry | 15 |
| Figure 3: Geometrical relationship for LOS angle and behavior of <i>Point g</i> as pursuer moves along the trajectory. | 18 |
| Figure 4: Equilibrium points of the LOS dynamics. | 27 |
| Figure 5. Example phase plane of sliding manifold with chattering phenomenon | 31 |
| Figure 6. Simulation Structure in Simulink Environment..... | 56 |
| Figure 7. Detailed Schematic of Seeker Model..... | 57 |
| Figure 8. Detailed Schematic of Navigation Model..... | 57 |
| Figure 9. Spatial Trajectories of the Pursuer for all scenarios. | 60 |
| Figure 10. LOS Angles for all scenarios | 61 |
| Figure 11. Flight Path Angles of Pursuer for all scenarios | 61 |
| Figure 12. Look Angle between Pursuer and Target for all scenarios | 62 |
| Figure 13. Command Accelerations of Pursuer for all scenarios..... | 62 |
| Figure 14. Speed of the Pursuer for all scenarios..... | 63 |
| Figure 15. Pursuer Trajectory for Scenario 1 | 64 |
| Figure 16. Important Angles in Scenario 1 | 64 |
| Figure 17. Pursuer Speed in Scenario 1 | 65 |
| Figure 18. Guidance Commands in Scenario 1 | 65 |
| Figure 19. Pursuer Trajectory for Scenario 2 | 66 |
| Figure 20. Important Angles in Scenario 2 | 67 |
| Figure 21. Pursuer Speed in Scenario 2 | 67 |
| Figure 22. Guidance Commands in Scenario 2..... | 68 |
| Figure 23. Pursuer Trajectory for Scenario 3 | 69 |
| Figure 24. Important Angles in Scenario 3 | 69 |
| Figure 25. Pursuer Speed in Scenario 3 | 70 |
| Figure 26. Guidance Commands in Scenario 3..... | 70 |

| | |
|---|----|
| Figure 27. Pursuer Trajectory for Scenario 4 | 71 |
| Figure 28. Important Angles in Scenario 4 | 72 |
| Figure 29. Pursuer Speed in Scenario 4 | 72 |
| Figure 30. Guidance Commands in Scenario 4..... | 73 |
| Figure 31. Pursuer Trajectory for Scenario 5..... | 74 |
| Figure 32. Important Angles in Scenario 5 | 74 |
| Figure 33. Pursuer Speed in Scenario 5 | 75 |
| Figure 34. Guidance Commands in Scenario 5..... | 75 |
| Figure 35. Pursuer Trajectory for Scenario 6..... | 76 |
| Figure 36. Important Angles in Scenario 6 | 77 |
| Figure 37. Pursuer Speed in Scenario 6 | 77 |
| Figure 38. Guidance Commands in Scenario 6..... | 78 |
| Figure 39. Pursuer Trajectory for Scenario 7..... | 79 |
| Figure 40. Important Angles in Scenario 7 | 79 |
| Figure 41. Pursuer Speed in Scenario 7 | 80 |
| Figure 42. Guidance Commands in Scenario 7..... | 80 |
| Figure 43. Pursuer Trajectory for Scenario 8..... | 81 |
| Figure 44. Important Angles in Scenario 8 | 82 |
| Figure 45. Pursuer Speed in Scenario 8 | 82 |
| Figure 46. Guidance Commands in Scenario 8..... | 83 |
| Figure 47. Pursuer Trajectory for Scenario 9..... | 84 |
| Figure 48. Important Angles in Scenario 9 | 84 |
| Figure 49. Pursuer Speed in Scenario 9 | 85 |
| Figure 50. Guidance Commands in Scenario 9..... | 85 |
| Figure 51. Pursuer Trajectory for Scenario 10..... | 86 |
| Figure 52. Important Angles in Scenario 10 | 87 |
| Figure 53. Pursuer Speed in Scenario 10 | 87 |
| Figure 54. Guidance Commands in Scenario 10..... | 88 |
| Figure 55. Spatial Trajectories of the pursuer with varying K | 90 |
| Figure 56. LOS Angle between pursuer and target for varying K | 91 |
| Figure 57. Flight Path Angle of Pursuer with varying K | 91 |

| | |
|---|-----|
| Figure 58. Look Angle of Pursuer with varying K | 92 |
| Figure 59. Command Acceleration of Pursuer with varying K..... | 92 |
| Figure 60. Speed of the Pursuer with varying K..... | 93 |
| Figure 61. Spatial Trajectory of the Pursuer with gravitational acceleration..... | 94 |
| Figure 62. Line-of-Sight Angle with gravitational acceleration | 95 |
| Figure 63. Flight path angle of the pursuer with gravitational acceleration | 95 |
| Figure 64. Look Angle of the pursuer with gravitational acceleration | 96 |
| Figure 65. Speed of the pursuer with gravitational acceleration..... | 96 |
| Figure 66. Command Acceleration of Pursuer with gravitational acceleration | 97 |
| Figure 67. Spatial Trajectories of pursuer with first order dynamics..... | 98 |
| Figure 68. LOS Angles with pursuer having first order dynamics | 99 |
| Figure 69. Flight Path Angle with pursuer having first order dynamics..... | 99 |
| Figure 70. Look Angle with pursuer having first order dynamics | 100 |
| Figure 71. Speed of the pursuer with first order dynamics | 100 |
| Figure 72. Command Acceleration on pursuer with first order dynamics | 101 |
| Figure 73. Spatial Trajectory of Pursuer with system lag and limitations | 102 |
| Figure 74. LOS Angle with system lag and limitations | 103 |
| Figure 75. Flight Path Angle with system lag and limitations | 103 |
| Figure 76. Look Angle with system lag and limitations | 104 |
| Figure 77. Speed of the Pursuer with system lag and limitations | 104 |
| Figure 78. Commanded Acceleration with system lag and limitations..... | 105 |
| Figure 79. Spatial Trajectory for all three scenarios with sensor errors | 107 |
| Figure 80. LOS angle for all three scenarios with sensor errors | 108 |
| Figure 81. LOS rate for all three scenarios with sensor errors..... | 108 |
| Figure 82. Flight Path Angle for all three scenarios with sensor errors..... | 109 |
| Figure 83. Look Angle for all three scenarios with sensor errors | 109 |
| Figure 84. Speed of the pursuer for all three scenarios with sensor errors | 110 |
| Figure 85. Command Acceleration for all three scenarios with sensor errors | 110 |
| Figure 86. Spatial Trajectories of Pursuer and constant speed targets..... | 112 |
| Figure 87. LOS angles between pursuer and constant speed targets | 113 |
| Figure 88. Flight Path Angles of Pursuer and constant speed targets | 113 |

| | |
|---|-----|
| Figure 89. Look Angles of pursuer and constant speed targets | 114 |
| Figure 90. Speed of the pursuer for constant speed targets | 114 |
| Figure 91. Command Acceleration for pursuer and constant speed targets..... | 115 |
| Figure 92. Spatial Trajectories for various step-sizes | 117 |
| Figure 93. Important angles for various step-sizes | 117 |
| Figure 94. Speed of pursuer for various step-sizes | 118 |
| Figure 95. Command Acceleration for various step-size..... | 118 |
| Figure 96. Spatial Trajectories for integration schemes..... | 120 |
| Figure 97. Important angles for integration schemes..... | 120 |
| Figure 98. Speed of pursuer for integration schemes..... | 121 |
| Figure 99. Command Acceleration for integration schemes..... | 121 |

CHAPTER 1

INTRODUCTION

1.1 Study of Impact Angle Guidance

Guidance is the process for generating the path of an object towards a given target. Guidance process has been first implemented by building a remotely-guided unmanned boat for military purposes, in the early 1900s. [1] The first successfully operational guided missiles (named “*Lark*” and built in 1944-1950) were developed to effectively counter kamikaze attacks on U.S. vessels at the end of World War II. [2] After the first development of *Lark* missiles in early 1950s, guidance law design becomes an increasingly important criterion in warfare.

In general, missile systems can be categorized as strategic and tactical missile systems. Strategic missiles travel longer distances and designed to intercept stationary, location-known targets. Tactical missiles track and guide shorter range maneuvering and/or moving targets through interception with onboard seekers and guidance algorithms. [3] Thus, guidance and control technology of tactical missile system has more crucial role than strategic missiles in successful interception. Although the history of the guidance process is relatively short, the technological enhancements are immense. The new requirements in modern systems can improve guidance law designs swiftly.

In novel guidance law designs, not only capturing the target, but also considering impact angle while intercepting target has become an increasingly important necessity. In some practical applications, it is desirable to adjust the pursuer

orientation near impact time in addition to interception. For example, in anti-tank or anti-ballistic missile applications, approaching the target with a certain strike angle is a vital requirement for warhead effectiveness. Moreover, in orbital applications, docking multiple spacecraft with each other requires an impact angle guidance law with high precision. Last but not least, modern automated fueling Unmanned Air Vehicles (UAVs) could use impact angle guidance law to approach rotating or fixed wing aircrafts with avoiding lethal collisions.

1.2 Literature Survey

Many guidance laws are studied to satisfy pursuer guidance requirements, yet proportional navigation methods are most widely used among guidance engineers. Proportional navigation methods are simple to implement and effective in intercepting moving and/or stationary targets. [3] Proportional Navigation Guidance Law (PNG) was first studied by C. Yuan during World War II under the support of US Navy. [4] After World War II, the work of US Navy on proportional navigation was declassified and first appeared in the *Journal of Applied Physics*. [5] Mathematical derivation and “optimality” of PNG was studied by Bryson and Ho about 20 years later [6]

PNG basically issues pursuer acceleration commands which are proportional to the line-of-sight rate and closing velocity of the pursuer-target dynamics. The optimality of the guidance law and closed-form solution of guided pursuer dynamics are developed by Bryson & Ho and Guelman respectively. [6, 7, 8, 9]. However, these studies are beyond the scope of this work thus more information about these studies can be found in References.

Several modifications have been studied on Proportional Navigation to improve its effectiveness on various targets. One of the improvements is the augmented (biased) PN laws which are basically adding a bias term in acceleration commands to have successful interceptions with the various targets. [10] Including this bias term,

studies show that the impact angle constraint on pursuer can be achieved. [11, 12] It can be convenient to say that here PN laws deal the problem of target-pursuer dynamic nonlinearly. There may be no linearity assumptions during the development of the guidance law. However, some linear PNG models have also been used to develop and study PNG. [3] Although, linearity assumptions have not been made in most of biased PNG based guidance laws, the need of time-to-go information is appeared in some biased terms in order to achieve impact angle constraints. [13] Time-to-go information is very difficult to measure or estimate accurately in practical applications. A delicate way to overcome this situation is by indirectly calculating impact angle at the final rendezvous, the constant bias is applied at some time interval to achieve desired impact angle. [14]

The final angle orientation of the pursuer can also be seen as a boundary condition at the impact time. Thus, in order to achieve the impact angle constraint, theoretically, the two point boundary value problem of the pursuer-target dynamics should be solved. The impact angle constrained guidance laws were studied not only for modern warfare but also for space explorations as mentioned before. The most iconic example of the utilization of impact angle guidance law is lunar landing of Apollo 11 spacecraft. [3] The guidance algorithm runs in Apollo 11 guidance computer conducts explicit vector calculations to satisfy impact angle constraints. [15] To optimize the terminal landing geometry, the generalized, explicit and optimizing guidance law (sometimes called *E-Guidance*) attempts to shape trajectory of the pursuer while controlling the final orientation of the final velocity vector. Later on, this E-guidance law scheme is used to solve the aforementioned two point boundary value problem with the generalized vector explicit guidance laws and energy-optimal vector explicit angle guidance law accordingly. [16, 17]

Another way to deal with this two point boundary value problem is using optimal control theory. The optimal control theory based solutions to that boundary value problem finds the optimal pursuer acceleration commands to head towards the target. Hence, the pursuer-target dynamics are handled by one sided optimization via

optimal control theory. The general optimal guidance laws (OGLs) have been developed since for ideal [3], for first-order [18] and for second-order [19] pursuer dynamics. Also, higher order pursuer dynamics case has also been investigated. [20] Moreover, the possible acceleration constraints on pursuer in practical application and in the case of maneuvering target have been studied by Rusnak and Meir. [20,21] Although optimal control theory based solutions are good way to find optimal, low-cost acceleration commands, the problem itself is a very challenging task to solve. In literature, optimal control theory based impact angle control problem is first handled in the works of Ryoo et. al.[22] The first-order pursuer dynamic is included and solved for optimal command acceleration in the works of York and Pastric. [23] In the work of Song and Shin, for varying pursuer speed, impact angle constraint is satisfied for stationary targets or slow-moving targets such as ships. However, the small initial heading angle error is needed for successful interception, since some linearization assumptions are done during guidance law synthesis. [24]

The most significant drawback with implementation of OGLs is that the guidance law needs an estimation of target maneuver and/or time-to-go information. Also, for higher-order dynamics, there are no closed-form solutions for the optimization. Yet, the solution of lower-order dynamics optimization problem is only one-sided optimal. In other words, the only control effort of the pursuer is optimized. In order improve this issue, two-sided optimization based guidance law designs are also developed. The differential games approach to design guidance law yielded renowned results as well. [25, 26]

Furthermore, the geometrical approaches to satisfy the impact angle guidance problem have been studied. [27] These geometrical approaches are based on the simple geometrical principles for pursuer to follow a circular arc towards to target that provides wider range of desired impact angles that can be satisfied. [28] The guidance commands are calculated from simple circular trajectory kinematics in order to intercept the target with impact angle constraints.

Moreover, the works of Savkin et. al. showed that linear quadratic regulator and H^∞ formulations are also applicable to guidance law synthesis to achieve desired impact angle. [29] However, these guidance laws rely on a linearized system allowing acceleration of the pursuer in any direction and are not applicable for many practical implementations. Moreover, linearization assumptions cause loss of precision for agile target-pursuer dynamics.

In order to handle guidance and control problem together for agile target-pursuer dynamics, integrated guidance and control synthesis are developed. Integrated guidance and control (IGC) has been a trending topic of research in recent years. Rather than designing guidance law and control method separately, IGC provides designing both guidance and control loops together to eliminate inevitable time-lag existing between two loops. Moreover, IGC synthesis can exploit fully the synergistic relationships between subsystems of the pursuer. In literature, several control methodologies are developed with IGC such as back-stepping [30], the $\theta-D$ method, [31] subspace stabilization, [32] feedback linearization, [33] state-dependent Riccati equation [34] and sliding-mode control [35, 36, 37, 38]. There are few studies which are made on IGC design with terminal impact angle constraints. In the work of Guo and Zhou, an integrated guidance and control system design is presented against ground stationary targets and an adaptive nonlinear control law is derived for target-pursuer dynamics. [39] The sliding-mode control method is introduced for stationary ground targets with suboptimal 3-D guidance law with impact angle constraints in the works of Oza and Padhi. [40] Nonlinear partial integrated guidance and control system is also studied with adaptive MIMO sliding-mode control method to achieve two impact angle constraints in 3-D in the works of Wang and Wang. [41]

It is noted that the linearized pursuer model has often been studied in most of the preceding literature. Hence, it is of great interest to conduct a guidance law design for a nonlinear environment that can achieve both interception and desired impact angles. The Lyapunov based nonlinear guidance laws are studied as a contribution of the nonlinear guidance law design in the works of Yanushevsky. [42] In order to

satisfy Lyapunov stability theory for closed loop nonlinear target-pursuer dynamics, Yanushevsky propose a PNG-like guidance law in order to enhance PNG performance in nonlinear environment. [42, 43] Similar to logic behind PNG laws, the necessary acceleration commands to nullify the line-of-sight angular rate are found with considering asymptotically stable closed-loop target-pursuer dynamics via Lyapunov stability theory. However, due to the LOS kinematics, a singularity when LOS angle becomes $\pm\pi/2$ is appeared in guidance law. Moreover, in work of Lechevin, this singularity of the target-pursuer dynamics is eliminated by using quadratic Lyapunov function candidate. [44]

Moreover, in the works of Sang et. al., impact angle is controlled using similar Lyapunov stability approach. The parameters in time-derivative of Lyapunov functions are calculated using Particle Swarm Optimization (PSO) method to have an asymptotically stable closed-loop system. [45] Even if the impact angle constraints are satisfied theoretically and shown in simulations, the processing CPU requirement to calculate the parameters in guidance law is not applicable for high-frequency processing applications. Another downside of the work of the Sang et. al. is that the Lyapunov function only guarantees the stability of LOS angle and LOS rate. For that reason, the capturability of the guidance law cannot be proven for various targets.

1.3 Contribution

The study represented in this thesis proposes a new nonlinear guidance law to intercept stationary targets with desired impact angle based on Lyapunov stability theory. The proposed guidance law is analytically found without using any linearization assumption. Thus, the guidance law is instinctively expected to give better results than linearized ones.

In order to control pursuer to successfully intercept target with desired impact angle, first, nonlinear dynamics between target and pursuer is investigated. The dynamical equations for pursuer and target kinematics are studied in the sense of line-of-sight geometry. The qualitative studies admit without proof that the pursuer must follow a straight trajectory at the end of the rendezvous. [7, 8, 46] This relationship reveals that the line-of-sight angle between target and pursuer should also converge the flight path angle of the pursuer at the end of the flight. With ground stationary targets, the flight path angle of the pursuer at the end of interception generally determines the impact angle in the literature. The mathematical relationships coming from geometry and kinematics between target and pursuer are investigated with this manner. Thus, these relationships between flight path angle, line-of-sight angle and impact angle construct the basis of this study.

The dynamical system of the target-pursuer engagement kinematics is studied in order to provide the state equations of the nonlinear system. Then the states of this dynamical system are constituted to control stably line-of-sight angle between pursuer and target. Also, state-space representation of this time-variant system is written in order to investigate the equilibrium points or subspaces of the system.

Unlike in the works of Yanushevsky and Lechevin, [42, 44], the line-of-sight angle is the state that is desired to be controlled. With controlling aforementioned state and the time derivative of this state, line-of-sight angular rate is also stably controlled to be zero indirectly. Thus, by controlling both states of the LOS dynamical system, the

pursuer can achieve to capture a stationary target with a specific angle via relationships between impact angle and LOS angle. Thus, the impact angle constraint can be satisfied using LOS dynamics between target and pursuer.

In order to control the desired states of the nonlinear dynamical system, Robust Control Lyapunov Function (RCLF) candidate is introduced. The RCLF method to control nonlinear system is relatively new method to control closed-loop nonlinear dynamical systems with using Lyapunov Stability Theory which is usually applied for open-loop system. Stabilizing systems with RCLF methods implies robustness by definition. [47]

However, in order to control both states of the dynamical system and control the impact angle throughout the flight without acquiring inconvenient chattering phenomenon; a first order sliding manifold which exponentially stabilizes both states is introduced. Unlike the works of Sang et. al., the sliding surface consists of both states and additionally closing velocity. Then, this reduced-order dynamical system is controlled by RCLF methods to achieve asymptotical stability for the system. Once the asymptotical stability is proven, the various targets can be captured with impact angle since the closing velocity term is included in exponentially stable sliding surface. The control inputs which analytically found to lead dynamical system via RCLF to desired exponentially stable sliding manifold are explored. The guidance commands which are the acceleration perpendicular to the line-of-sight vector between target and pursuer are deduced from control inputs of the dynamical system. This kind of acceleration commands is similar to the *True Proportional Navigation* guidance law which is used in many practical applications. [1, 3]

Later on, in order to prove the capturability of the proposed guidance law, capturability analysis is also done via similar Lyapunov stability theory approach. [42] The capture conditions of the proposed guidance law are investigated by using nonlinear capturability analysis. The analysis shows that the guidance law can

capture all targets, and also asymptotic stability of range, closing velocity and look angle between target and pursuer through the flight is proven.

Finally, the simulation which runs in MATLAB®/Simulink environment is constructed to test the proposed guidance law. The criteria of successful interception are set and numerical robustness analysis of the system with proposed guidance law is investigated. Disturbance rejection analysis against sensor errors and disruptive gravitational accelerations are also explored numerically. Some practical application aspect such as integration time-step of the guidance calculations are also carried out.

The papers which are originated with this thesis are given below.

“Sabit Hedefler İçin Lyapunov Tabanlı Doğrusal Olmayan Vuruş Açisi Kontrollü Güdüm Kanunu” at “Havacılıkta İleri Teknolojiler Konferansı HİTEK-2014” conference is about the basic relationships between target and pursuer linearly and nonlinearly. Moreover, a simple RCLF is introduced to control to this linearized and nonlinear dynamical system. [49]

“Lyapunov Based Nonlinear Impact Angle Guidance Law for Stationary Targets” to be published at “SciTech 2015 – Guidance, Navigation and Control” conference is about the first order sliding manifold and more detailed RCLF method to control the nonlinear dynamical system robustly.[50]

The ongoing paper studies are about integrating autopilot loop of the pursuer in the dynamical system equation to avoid inevitable system lag in controlling the pursuer. Lastly, a better RCLF candidate will be investigated to obtain simpler guidance law that can control impact angle.

1.4 Thesis Structure

In the first Chapter, a brief introduction to the importance of guidance process and impact angle guidance for various applications is given. Then, a literature survey about the impact angle control guidance laws in literature is presented. Finally, contribution of the thesis is expressed.

The second Chapter is named problem definition. In this Chapter, the nonlinear target-pursuer dynamics is investigated. Engagement geometry and kinematics between target and pursuer are also explored. Then, the state equations of this dynamical system are carried on. Then, the state-space representation of the time-invariant dynamical system is shown. Finally, the equilibrium subspace of the unforced dynamical system is expressed.

The third Chapter is reserved for deduction of new proposed nonlinear guidance law. A first order sliding manifold is introduced to exponentially stabilize the system. Then, Robust Control Lyapunov Function method is carried out to control the system stably towards the desired sliding manifold. Later, the analytical solution for control input as acceleration commands (i.e. guidance commands) for the pursuer is derived. Finally, capturability analysis and capture conditions of the proposed guidance law are investigated via Lyapunov Stability Theory.

In Chapter 3.4, construction of the simulation to test and prove the proposed guidance law is explained. Then, the successful mission criteria are set for sample engagement geometry. Then, with comparing the results with predefined criteria robustness and disturbance rejection of the system is investigated via numerical analyses. Finally, some practical aspects of the guidance law implementation are discussed and the response of the proposed guidance law is expressed.

In the final Chapter, the thesis is concluded.

CHAPTER 2

PROBLEM DEFINITION

The process of guidance basically depends on position and/or velocity information of the target relative to the pursuer which is the guided object. Analytical guidance laws which date from the eighteenth century are based on geometrical pursuit of the target to capture. [1] In modern guidance laws, the intercepting target is not the main objective anymore. One of the most increasingly important objectives of the modern guidance law design is to approach the target with specified impact angle. For several applications, approaching the target from a certain impact angle with respect to specific reference line is a vital requirement for efficiency.

Guidance is a hierarchical process which may be said to consist of three levels which are listed as geometrical rule, guidance law and control. In the highest one, a geometrical rule is stated in terms of a line-of-sight that passes through the objective of the guidance. [1] Line-of-sight can be visualized as a ray that starts at pursuer and is directed at target along the positive sense. The Line-of-Sight (LOS) concept is widely used as a central pivot in most of the guidance law design and analysis. Thus, in order to design a guidance law which concern impact angle between target and pursuer; the geometry (i.e LOS dynamics) between target and pursuer should be identified.

In this Chapter, first; engagement geometry between target and pursuer is established in 2.1 for use of the rest of the study. Secondly, the impact angle definition and some useful relationships of the geometry are discussed in 2.2. Line-of-sight dynamics between target and pursuer are investigated in 2.3. Finally in section 2.4, the state-space representation of the nonlinear dynamical system is defined on which

nonlinear control approach is applied and equilibrium subspace of this system is investigated.

2.1 Engagement Geometry

The engagement geometry between pursuer and target can be represented in three dimensions. Figure 1 shows three-dimensional engagement geometry between pursuer and target. Three reference coordinate frames are used to define the motion of the pursuer; the inertial reference frame (denoted as I), LOS reference frame (L) with unit vector $[\vec{i}_L, \vec{j}_L, \vec{k}_L]^T$ and pursuer velocity frame (M) with $[\vec{i}_M, \vec{j}_M, \vec{k}_M]^T$. The range vector between target and pursuer is denoted as \vec{r} . The pursuer velocity vector is \vec{v}_m where \vec{a}_{com} is the total acceleration commands of the pursuer. λ_{yaw} and λ_{pitch} denotes the azimuth and elevation components of the LOS angle to the inertial reference frame in spherical coordinates respectively. γ_{yaw} and γ_{pitch} are the azimuth and elevation components of the pursuer velocity vector with respect to the inertial reference frame respectively. These angles are also known as flight path angles of the pursuer, since it gives information about the orientation of the velocity vector of the pursuer.

Directional cosine matrices between aforementioned reference frames are given by

$$C_I^L = R_y(-\lambda_p)R_z(\lambda_y) = \begin{bmatrix} \cos \lambda_p \cos \lambda_y & \cos \lambda_p \sin \lambda_y & \sin \lambda_p \\ -\sin \lambda_y & \cos \lambda_y & 0 \\ -\sin \lambda_p \cos \lambda_y & -\sin \lambda_p \sin \lambda_y & \cos \lambda_p \end{bmatrix} \quad (2.1)$$

$$C_I^M = R_y(-\gamma_p)R_z(\gamma_y) = \begin{bmatrix} \cos \gamma_p \cos \gamma_y & \cos \gamma_p \sin \gamma_y & \sin \gamma_p \\ -\sin \gamma_y & \cos \gamma_y & 0 \\ -\sin \gamma_p \cos \gamma_y & -\sin \gamma_p \sin \gamma_y & \cos \gamma_p \end{bmatrix} \quad (2.2)$$

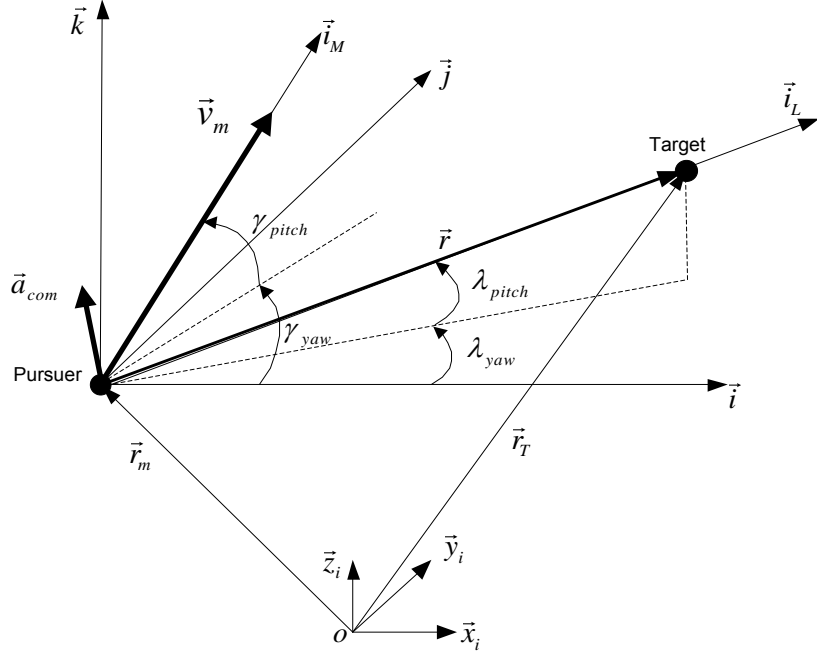


Figure 1: 3-D Engagement Geometry

The transformation matrix between LOS reference vector and pursuer velocity reference vector becomes as follows:

$$C_L^M = C_I^M (C_I^L)^T \quad (2.3)$$

The relative range vector from the target to the pursuer \vec{r} , is given by

$$\vec{r} = R\vec{i}_L = \vec{r}_T - \vec{r}_m \quad (2.4)$$

where \vec{r}_T and \vec{r}_m denote the position vector of the target and pursuer respectively.

The velocity and acceleration vector of the pursuer, \vec{v}_m and \vec{a}_{com} , are defined as

$$\begin{aligned} \vec{v}_m &\triangleq v_m \vec{i}_M \\ \vec{a}_{com} &\triangleq a_x \vec{i}_M + a_y \vec{j}_M + a_z \vec{k}_M \end{aligned} \quad (2.5)$$

For stationary targets, three dimensional dynamic equations becomes

$$\begin{aligned}\frac{\partial \vec{r}_m}{\partial t} &= -\frac{\partial \vec{r}}{\partial t} = -\frac{\partial}{\partial t} (R\vec{i}_L) = -(\dot{R}\vec{i}_L + \vec{\omega}_L \times \vec{r}) \\ &= \vec{v}_m\end{aligned}\quad (2.6)$$

$$\begin{aligned}\frac{\partial \vec{v}_m}{\partial t} &= \frac{\partial}{\partial t} (v_m \vec{i}_M) = \dot{v}_m \vec{i}_M + (\vec{\omega}_L + \vec{\omega}_m) \times \vec{v}_m \\ &= \vec{a}_{com}\end{aligned}\quad (2.7)$$

where $\vec{\omega}_m$ is the rate of the pursuer velocity frame with respect to the LOS reference frame and $\vec{\omega}_L$ denotes the LOS rate with respect to the inertial reference frame.

In general, the impact angle is established by the angle between pursuer's final velocity vector and a reference line or plane which target is located for point mass pursuers. The guidance problem should be studied with three-dimensional engagement geometry accordingly. However, by assuming that the lateral and longitudinal planes of the pursuer are decoupled by means of roll control, it is possible to reduce the three-dimensional engagement geometry to the equivalent two-dimensional planar geometries.

In this study, for simplicity, the engagement geometry is also reduced to two-dimensional planar geometry due to the subject of stationary ground target. Since, the required impact angle is only provided with the longitudinal plane of the 3-D geometry that is proven by taking x-y plane as ground, the engagement geometry between target T and pursuer M in 2-D becomes as shown in Figure 2.

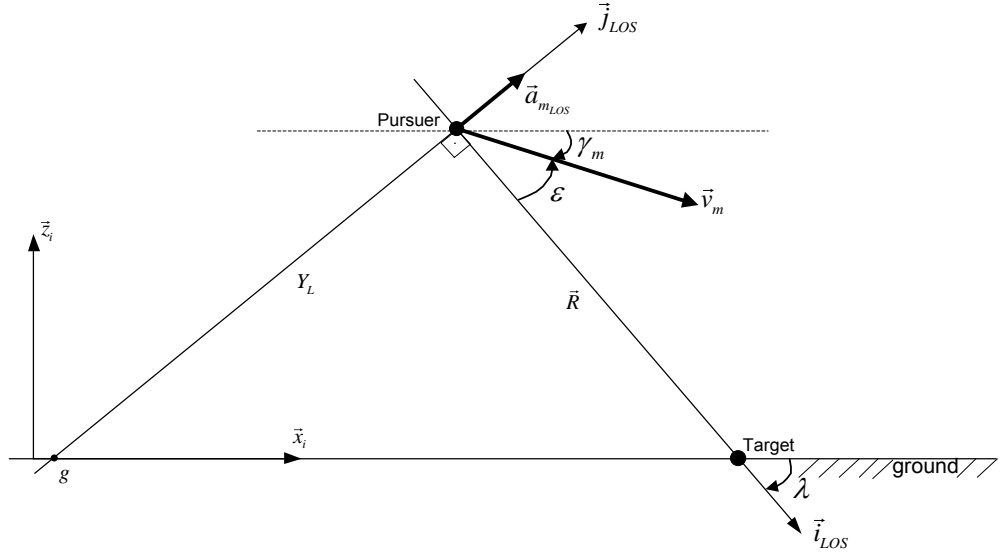


Figure 2: 2-D Engagement Geometry

Similar to 3-D geometry, the velocity vector of the pursuer is \vec{v}_m with γ being the flight path angle of the pursuer. The range vector between target and pursuer is denoted as \vec{R} similarly. The acceleration commands (which can be interpreted as guidance commands) that are perpendicular to the LOS vector; are defined as $\vec{a}_{m_{LOS}}$. The look angle that is defined as the angle between range vector and velocity vector is denoted as ε whereas λ denotes the line-of-sight angle between R and the ground. All angles are positive in counterclockwise direction.

2.2 Geometrical Relationship and Impact Angle Definition

In order to define the impact angle constraint in this study, some geometrical and kinematical relationship of the dynamical system between target and pursuer is examined.

From engagement geometry and kinematics, the relationships between essential angles can be written in 2-D as:

$$\varepsilon = \gamma - \lambda \quad (2.8)$$

The closing velocity which can be taken as the time derivative of the range value is written as

$$\dot{R}(t) = \frac{\partial R(t)}{\partial t} = -v_M(t) \cos \varepsilon(t) \quad (2.9)$$

where v_m denotes the value of pursuer's velocity vector. This velocity vector can be divided into two components represented in LOS reference frame as follows

$$v_r(t) = v_m(t) \cos \varepsilon(t) \quad (2.10)$$

$$v_\lambda(t) = v_m(t) \sin \varepsilon(t) \quad (2.11)$$

The term v_r denotes the velocity parallel to the range vector whereas the term v_λ denotes the velocity perpendicular to range vector. According to qualitative studies that are admitted without proof, the pursuer should follow a straight line trajectory towards the target at the end of the pursuit. [7, 46] If so, the velocity components of the pursuer's velocity vector in LOS frame at the final rendezvous becomes

$$\begin{aligned} \lim_{t \rightarrow t_f} (v_r(t)) &= \lim_{t \rightarrow t_f} (-\dot{R}(t)) = v(t) \\ \lim_{t \rightarrow t_f} (v_\lambda(t)) &= 0 \end{aligned} \quad (2.12)$$

where t_f is the finite capture time. Then, the look angle and its angular velocity must become zero at the final time.

$$\begin{aligned}\lim_{t \rightarrow t_f}(\varepsilon(t)) &= 0 \\ \lim_{t \rightarrow t_f}(\dot{\varepsilon}(t)) &\approx 0\end{aligned}\tag{2.13}$$

So, the relationship between impact angle and LOS angle can be written via using equations (2.8) and (2.13) as follows.

$$\gamma_d = \gamma_f = \lambda_f\tag{2.14}$$

where γ_d is the desired impact angle which can generally established with the final flight path angle which is denoted as γ_f . Moreover, λ_f is the final LOS angle of the target-pursuer dynamics which converges into final flight path angle for stationary targets. This relationship constitutes the basis of this study. In order to control the impact angle in 2-D geometry, LOS angle in final rendezvous can be used as final flight path angle which is widely considered as an impact angle constraint in designing guidance law.

Similarly, from geometrical relationship which can be seen in Figure 2, LOS angle can be represented as follows

$$\tan \lambda(t) = -\frac{Y_L(t)}{R(t)}\tag{2.15}$$

where R is the range value between target and pursuer and it can be deduced as follows:

$$R(t) = \|\vec{R}\| = \|\vec{R}_T - \vec{R}_M\|\tag{2.16}$$

Y_L is the distance value between the center of moving LOS reference frame and the point on stationary target reference line (i.e ground level) with respect to LOS reference frame. It can be demonstrated as follows:

$$Y_L(t) = \|\vec{R}_L\| = \|\vec{R}_M - \vec{R}_g\| \quad (2.17)$$

where \vec{R}_g is the position vector of the *point g* demonstrated in Figure 2. Note that the point *g* is not a stationary point. As the pursuer, as well as the center of LOS reference frame, moves towards the target; the point *g* moves in order to construct the triangular relationship which relates LOS angle. The movement of the point *g* and the triangular relationship can be seen at Figure 3.

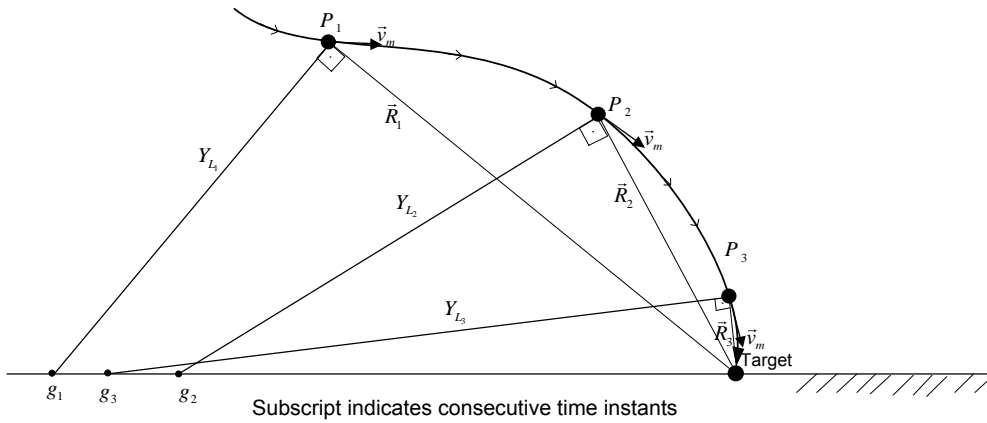


Figure 3: Geometrical relationship for LOS angle and behavior of *Point g* as pursuer moves along the trajectory.

2.3 Line-Of-Sight Dynamics

From equation (2.15), the LOS angle can be represented as the ratio of distance measures between points in engagement geometry. This indicates that the dynamical system which drives LOS angle and LOS angular velocity can be controlled with controlling the position of the pursuer. This could be a challenging task in guidance design since the pursuer needs hard-to-achieve sensor information to control precisely the position of the pursuer and target. However, this position information is hidden in LOS dynamics which can lead to control only pursuer position with respect to target via commanding acceleration on the pursuer indirectly.

In order to examine and define the dynamical system of the LOS dynamics, the time derivative of the LOS angle which is presented in equation (2.15) is obtained as follows

$$\frac{\dot{\lambda}(t)}{\cos^2 \lambda(t)} = -\frac{\dot{Y}_L(t)}{R(t)} + \frac{Y_L(t)\dot{R}(t)}{R(t)^2} \quad (2.18)$$

where $\dot{R}(t)$ is the closing velocity of the pursuer varying with time towards the target. Above equation can be simplified via equation (2.15) as follows

$$\frac{\dot{\lambda}(t)}{\cos^2 \lambda(t)} = -\frac{(\dot{Y}_L(t) + \tan \lambda(t)\dot{R}(t))}{R(t)} \quad (2.19)$$

where $\dot{Y}_L(t)$ is the velocity in the direction of \vec{R}_L . Remember that \vec{R}_L is the vector between pursuer and the point g denoted in (2.17). It can be convenient to state here that the LOS angular velocity can also be written as follows:

$$\dot{\lambda}(t) = -\frac{v_m(t) \sin(\varepsilon(t))}{R(t)} \quad (2.20)$$

Note that the equation (2.20) is a different representation of equation (2.19). The two terms $(\dot{Y}_L(t) + \tan \lambda(t) \dot{R}(t)) \cos^2 \lambda$ and $(v_m \sin \varepsilon)$ are equal to each other since they are both the total velocity components perpendicular to the range vector that changes LOS angular velocity.

The second time derivative of the LOS angle can reveal the LOS angular velocity behavior. So, time derivative of equation (2.19) can be written as:

$$\frac{\ddot{\lambda}}{\cos^2 \lambda} + \frac{2\dot{\lambda}^2 \tan \lambda}{\cos^2 \lambda} = -\frac{\ddot{Y}_L}{R} - \frac{2\dot{\lambda}\dot{R}}{R \cos^2 \lambda} - \frac{\ddot{R} \tan \lambda}{R} \quad (2.21)$$

where \ddot{Y}_L and \ddot{R} is the accelerations in the direction of \vec{R}_L and \vec{R} respectively. For the sake of brevity, time dependent variables are written simply as equation (2.21). Moreover, note that there are no linear assumptions made while obtaining LOS dynamics' equations. Furthermore, nonlinearity of the equations comes from the varying velocity terms and nonlinear angle-angular velocity couples.

To have a better understanding of the LOS dynamics, the terms in differential equations, especially \ddot{R} and \ddot{Y}_L , should be examined. The term \ddot{Y}_L can be interpreted as acceleration perpendicular to the R vector. This acceleration is often used as guidance commands to head towards to target. Most well-known example of this kind of guidance law is known as True Proportional Navigation (TPN) law. [1, 3]

For most of the practical applications, pursuer is generally controlled aerodynamically. For this reason, if the acceleration commands is transformed into pursuer velocity frame, the guidance law commands which is perpendicular to the LOS vector which is presented in pursuer velocity frame, becomes as follows

$$a_{com} = \ddot{Y}_L \rightarrow \begin{cases} \dot{v}_m = a_{com} \sin \varepsilon \\ a_{\perp v_m} = a_{com} \cos \varepsilon \end{cases} \quad (2.22)$$

where $a_{\perp v_m}$ is the acceleration that is perpendicular to the velocity vector of the pursuer and \dot{v}_m being the rate of change of speed of the pursuer. The above equation holds for pursuer that accelerates only by guidance command. Disruptive accelerations like gravitational acceleration are neglected for these equations due to the analytical approach on LOS kinematics.

Moreover, the second term $a_{\perp v_m}$ has a kinematical relationship with the rate of the change of flight path angle with respect to time. [1, 3]

$$a_{\perp v_m} = v_m \dot{\gamma} \quad (2.23)$$

So the equations denoted in (2.22) become as follows

$$\begin{cases} \dot{v}_m = \ddot{Y}_L \sin \varepsilon \\ \dot{\gamma} = \frac{\ddot{Y}_L}{v_m} \cos \varepsilon \end{cases} \quad (2.24)$$

If the acceleration commands and/or the forces effecting pursuer become zero (i.e pursuer travels with constant velocity vector due to Newton's second law of motion), the \ddot{Y}_L term must become null to have a constant velocity vector and also to satisfy equations (2.24).

The other term, \ddot{R} can be thought as the time derivative of the closing velocity which is:

$$\ddot{R} = \frac{\partial \dot{R}}{\partial t} = \frac{\partial}{\partial t}(-v_m \cos \varepsilon) \quad (2.25)$$

Then,

$$\ddot{R} = -\dot{v}_m \cos \varepsilon + v_m \dot{\varepsilon} \sin \varepsilon \quad (2.26)$$

As mentioned before, ε is the look angle, also known as the angle between LOS reference frame and pursuer velocity frame. The relationships shown in equation (2.8) can also be written for time derivatives of the angles as;

$$\dot{\varepsilon} = \dot{\gamma} - \dot{\lambda} \quad (2.27)$$

Then, \ddot{R} can be written as:

$$\ddot{R} = v_m \dot{\gamma} \sin \varepsilon - v_m \dot{\lambda} \sin \varepsilon - \dot{v}_m \cos \varepsilon \quad (2.28)$$

It can be seen from the above equation the \ddot{R} term is affiliated with \dot{v}_m , $\dot{\gamma}$ and $\dot{\lambda}$. If the terms mentioned in equation (2.24) are substituted into equation (2.28) then

$$\ddot{R} = \ddot{Y}_L \sin \varepsilon \cos \varepsilon - v_m \dot{\lambda} \sin \varepsilon - \ddot{Y}_L \sin \varepsilon \cos \varepsilon \quad (2.29)$$

The terms in equation (2.29) cancel each other and equation (2.29) becomes;

$$\ddot{R} = -v_m \dot{\lambda} \sin \varepsilon \quad (2.30)$$

If look angle and LOS angular rate is different than zero, then the \ddot{R} term varies with the geometry throughout the rendezvous without the dependence of the acceleration commands on the pursuer.

If the equations (2.30) and (2.20) are substituted into each other, then the term \ddot{R} becomes

$$\ddot{R} = \dot{\lambda}^2 R \quad (2.31)$$

The equation (2.31) can be interpreted such that when the pursuer is controlled by the acceleration commands perpendicular to range vector or there is no control on pursuer, the closing velocity is always decreasing. Since the term \ddot{R} is always positive, the closing velocity \dot{R} should always increase. That is known that \dot{R} value is negative from equation (2.9) as pursuer goes towards the target. Thus, it can be concluded that if guidance commands are perpendicular to range vector, the pursuer always slows down towards the target while maneuvering. However, when the LOS rate between target and pursuer becomes zero, the closing velocity becomes constant regarding the equation (2.12). So, when LOS rate is not zero –or pursuer is maneuvering– the closing velocity should also be considered throughout the flight in order to intercept with the target.

The relationships between some terms that appear in LOS dynamics can be used in implementation. Moreover, they provide some insights to LOS dynamics and relationships to control it indirectly via controlling only pursuer.

2.4 State-Space Representation of the Dynamical System

The closed form solution of the dynamical system's nonlinear differential equations mentioned in section 2.3 can reveal very important insights of target-pursuer dynamics in designing guidance laws. In literature, even though some linearization assumptions have been made to simplify and solve the system, the general closed form solution of the given differential equation wouldn't be solvable. [7, 8] However, robust nonlinear control methods can control the dynamical system without deducing a closed form solution.

In order to control this nonlinear system with robust nonlinear control methods, the state space representation of the dynamical system should be constituted. To control impact angle by using aforementioned relationship between LOS angle and impact angle, the first state of this dynamical system should be selected as the error between desired and instantaneous value of LOS angle.

$$x_1 = \tan \lambda - \tan \lambda_d \quad (2.32)$$

where λ_d is the desired final LOS angle of the dynamical system or impact angle in stationary target case. If the pursuer-target system converges to the desired LOS angle at the final rendezvous, the pursuer can intercept the target with desired impact angle.

Moreover, in order to converge pursuer's LOS angle to desired one steadily, the angular velocity of the LOS angle should also be considered in state-space representation of this dynamical system. Since, not only converging LOS angle to desired impact angle instantaneously, but also staying the desired LOS angle is a vital requirement in intercepting the stationary target. Also, considering the change in closing velocity; the second state of the dynamical system should be the time

derivative of the first state. Since, desired LOS angle is constant, the time derivative of the first state can be written as follows:

$$x_2 = \dot{x}_1 = \frac{\dot{\lambda}}{\cos^2 \lambda} \quad (2.33)$$

So the time derivative of the second state becomes

$$\dot{x}_2 = \frac{\ddot{\lambda}}{\cos^2 \lambda} + \frac{2\dot{\lambda}^2 \tan \lambda}{\cos^2 \lambda} \quad (2.34)$$

The dynamical system provided in section 2.3 is written via given states in state-space representation as

$$\begin{aligned} \dot{x}_1 &= x_2 \\ \dot{x}_2 &= -\frac{\ddot{Y}_L}{R} - \frac{2x_2 \dot{R}}{R} - \frac{\ddot{R}x_1}{R} - \frac{\ddot{R} \tan \lambda_d}{R} \end{aligned} \quad (2.35)$$

where \ddot{R} is the acceleration in x-direction in LOS reference frame and \ddot{Y}_L is the acceleration perpendicular to range vector as explained in Section 2.3.

In light of this information, the \ddot{R} term is dependent only range and LOS rate for all control inputs. Thus, the only logical course to control the dynamical system in equation (2.35) is to control the acceleration term \ddot{Y}_L . It can be said that the mechanization of the guidance law for practical application could also be similar to the TPN guidance law, since both guidance laws use the accelerations perpendicular to range vector. The mechanization of the guidance law is not explained here since it's not the scope of this study.

If the control input is defined as \ddot{Y}_L in state-space representation, then the dynamical system becomes:

$$\begin{aligned}\dot{x}_1 &= x_2 \\ \dot{x}_2 &= -\frac{u}{R} - \frac{2x_2\dot{R}}{R} - \frac{\ddot{R}x_1}{R} - \frac{\ddot{R}\tan\lambda_d}{R}\end{aligned}\quad (2.36)$$

It can be seen that the nonlinear dynamical system is non-autonomous. Also, the variables in the state equations vary with time.

The matrix form of state equations can be written as follows

$$\begin{bmatrix} \dot{x}_1 \\ \dot{x}_2 \end{bmatrix} = \begin{bmatrix} 0 & 1 \\ -\frac{\ddot{R}}{R} & -\frac{2\dot{R}}{R} \end{bmatrix} \begin{bmatrix} x_1 \\ x_2 \end{bmatrix} + \begin{bmatrix} 0 \\ -\frac{1}{R} \end{bmatrix} u + \begin{bmatrix} 0 \\ -\frac{\ddot{R}}{R} \end{bmatrix} \tan\lambda_d \quad (2.37)$$

The last term in matrix form of state equations can be seen as a disturbance or a bias to the system. So, it can be written as follows:

$$\hat{X} = \hat{A}\hat{X} + \hat{B}_u u + \hat{B}_w w \quad (2.38)$$

Note that the system represented in the equation (2.38) is linear parameter varying (LPV). The terms in \hat{A} , \hat{B}_u and \hat{B}_w matrices are time-variant and depends indirectly on acceleration commands and LOS dynamics.

The phase portrait of the unforced system and/or eigenvalues of the system can be visualized for only instantaneous time since system is non-autonomous and time-variant. However, the equilibrium subspace for the dynamical system can be set. The all states in nonlinear state equations except control input u become zero when

$$\{x \mid x_1 = (\tan\lambda - \tan\lambda_d) = 0, x_2 \approx \dot{\lambda} = 0, \dot{R} < 0\} \quad (2.39)$$

From equations (2.9), (2.12) and (2.13); the above equilibrium point can be rewritten as

$$\{x \mid x_1 = (\tan \lambda - \tan \lambda_d) = 0, x_2 \approx \dot{\lambda} = 0, |\varepsilon| \leq \pi/2\} \quad (2.40)$$

The last condition in condition (2.39) determines the sign of the closing velocity and sets the last condition of the (2.40). Without considering this condition; the equations leads to the equilibrium subspace cannot be defined. There are two conditions that geometrically nullify the states of the system. These equilibrium subspaces are shown in Figure 4. It can be seen that λ_d value is the desired LOS and impact angle for the system. Both states go zero equilibrium geometrically in two conditions. One of them denotes the pursuer goes towards to the target as desired with $\varepsilon = 0$ at final rendezvous. In the other one, which the closing velocity is positive, the pursuer goes away from target but keeping the desired LOS angle and angular velocity with having a look angle as $\varepsilon = \pi$. In order to capture target and satisfy the impact angle constraint, the system should be forced via acceleration commands towards the target and indirectly equilibrium subspace.

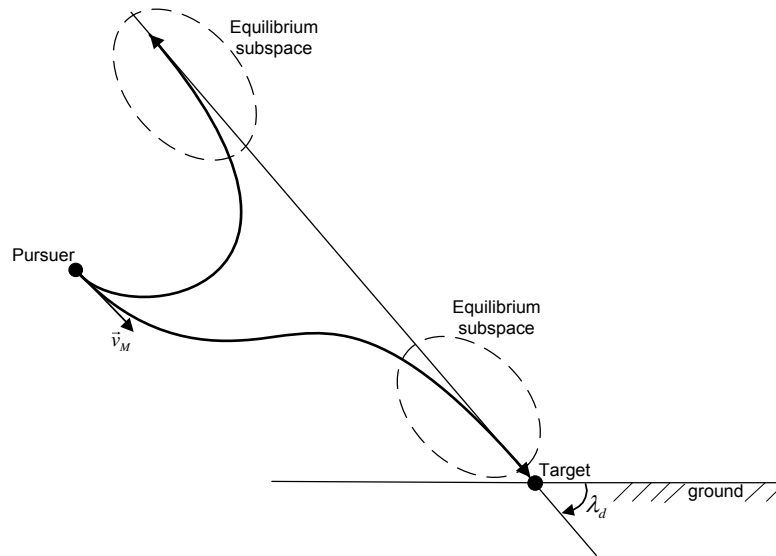


Figure 4: Equilibrium points of the LOS dynamics.

CHAPTER 3

NONLINEAR GUIDANCE LAW DESIGN

There are many ways to control a dynamical system. The main purpose of controlling a system is setting the response of it to a desired value. Thus, in both transient and steady-state region, the response can be shaped using control inputs and feedbacks towards a desired one via understanding the characteristic of the system. In general, this “*character*” of the system could be determined by linear analysis of the system. However, in practical applications, these desired linear characteristics are occasionally not found. Moreover, dynamical systems with feedback (closed-loop systems) are often more complex than systems without feedback (open-loop systems), and the design of feedback controllers involves certain risks.[47] In addition to that nonlinear behavior of the system can also build instabilities which causes difficulties in controlling the desired system.

Therefore, stability theory plays a central role in systems theory and control engineering. There are different kinds of stability problems that arise in the study of dynamical systems. [51] Stability of a dynamical system at near equilibria can usually be found by Lyapunov stability theory (Russian mathematician and engineer who formed the foundation of the theory which is named after him). Although Lyapunov stability theory gives an understanding about the unforced systems’ equilibrium points, the robust nonlinear control methodologies which drive the closed loop system to neighborhood of the equilibrium point become useful in controlling nonlinear system under some disruptive feedback. [47]

Target-pursuer dynamics in guidance law design can also be seen as a nonlinear dynamical system whose detailed analysis is already done in Chapter 2. Novel

guidance law designs are hitherto developed in the context of linear control theory that requires small-angle engagement geometry around an operational point to satisfy linearity assumptions. This required linearity, for example in many practical applications, is provided by small angle changes around zero LOS rate. However, to satisfy challenging precisions in impact angle and/or for very agile pursuer-target kinematics, designing guidance law regarding nonlinear pursuer-target dynamics is instinctively expected to obtain better performance than linear guidance designs with approximations. Thus, the analyzed dynamical system is investigated via nonlinear robust control method called control Lyapunov function with first order sliding manifold to satisfy the impact angle requirements.

The main purpose of the guidance law is to capture the target. Any guidance law design should also be analyzed for capturability for various targets. There are many ways to demonstrate the capturability of the guidance law. One of them is to show the guidance law performance by testing in nonlinear simulation environment for various target-pursuer engagement geometries. However, although this process can reveal most of the characteristics and limitations of the guidance law, it cannot determine the guidance law's capture conditions. In order to prove the capturability and determine the capture conditions of the guidance laws, various mathematical ways are developed. In the early 70s, the closed form solutions of the widely used guidance laws such as proportional navigation laws (PN Laws) are developed to show the capture regions. [7, 8, 46] However, the nonlinear dynamics between target and pursuer makes a challenging task to get closed-form solution of the equation of motion. In order to cope with that problem, the nonlinear capturability analysis based on Lyapunov stability theory is developed by Ryoo et. al. [48] The proposed guidance law is also analyzed by this nonlinear approach to determine the limitations and capture conditions in this study.

This Chapter is formed by four sections. First, in 3.1 construction of first order sliding manifold is explained. Then for robust nonlinear control, Lyapunov function candidate is selected in section 3.2. Section 3.3 is reserved for derivation of the

nonlinear guidance law and some implementation aspects for practical applications. Finally, in section 3.4, nonlinear capturability analysis of the guidance law is performed.

3.1 Construction of Sliding Manifold

In nonlinear control theory, Sliding Mode Control (SMC) is a control method that forces the dynamical system to “slide” along a surface which is the boundary of the control structure. The geometrical locus consisting of the boundary is called the *sliding (hyper) surface or manifold*. [47, 51] Figure 5 shows phase plane trajectory of the system stabilized by SMC on stable sliding manifold. It can be seen from Figure 5 that due to the imperfections of the system, control method generates high-frequency and generally non-deterministic switching control signal that causes the dynamical system to “chatter” in the neighborhood of the sliding manifold.

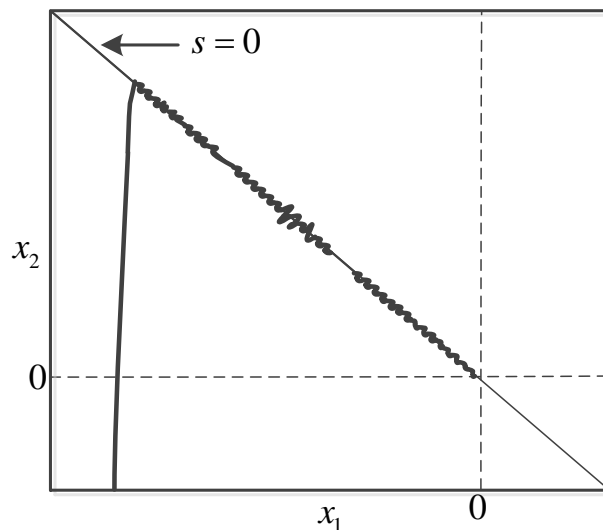


Figure 5. Example phase plane of sliding manifold with chattering phenomenon

Rather than controlling the system on defined sliding manifold with SMC method with discrete control effort, other methods are developed to force the system to

desired sliding manifold more stably. Moreover, the sliding manifold can be an LTI system with desired asymptotical and/or exponential stability. Thus, the system on the sliding manifold should converge desired equilibrium point with asymptotic and/or exponential stability.

Besides these advantages and disadvantages of using sliding manifolds, it can provide the comfort of controlling multiple states with only one surface. In guidance law design, this reduced-order dynamics can be desirable. Since, the pursuer-target dynamic is handled as a control problem of this dynamical system, using sliding manifolds can reduce the number of variables which should be controlled via guidance commands of the pursuer while heading to the target.

The state-space representation of the dynamical system is rewritten as

$$\begin{aligned}\dot{x}_1 &= x_2 \\ \dot{x}_2 &= -\frac{u}{R} - \frac{2x_2\dot{R}}{R} - \frac{\ddot{R}x_1}{R} - \frac{\ddot{R}\tan\lambda_d}{R}\end{aligned}\quad (3.1)$$

where x_1 and x_2 are the states of the system that are affiliated with LOS angle and LOS angular velocity respectively. In order to control both states simultaneously and stably, a first order sliding manifold is introduced as follows

$$s = x_2 - \frac{\dot{R}}{R_{ref}} x_1 \quad (3.2)$$

where \dot{R} is the closing velocity and R_{ref} is a constant named as reference range. In order to be consistent with units in the manifold and also with controlling the closing velocity which affects the equilibrium subspace as explained in Chapter 2, the combination of three variables is used in constructing the first order sliding manifold.

If the system reaches the sliding manifold that also means as $s=0$, then the relationship between states can be defined as

$$s = 0 = x_2 - \frac{\dot{R}}{R_{ref}} x_1 \quad (3.3)$$

The above equation can be written as:

$$x_2 = \frac{\dot{R}}{R_{ref}} x_1 \quad (3.4)$$

where from state equations x_2 is the time derivative of the first state x_1 . Then, above relationship corresponds to the first order linear time varying (LTV) system as follows:

$$\dot{x}_1 = \frac{\dot{R}}{R_{ref}} x_1 \quad (3.5)$$

The solution of this LTV system can be quite simple. If the states is adjoined together and integrated side by side, then equation (3.5) becomes

$$\ln\left(\frac{x_1^*}{x_{1_0}}\right) = \frac{\Delta R}{R_{ref}} = \frac{R^* - R_0}{R_{ref}} \quad (3.6)$$

where x_1^* and R^* is the first state and range of the dynamical system at an arbitrary time. Equation (3.6) can be rewritten as

$$x_1(t) = x_{1_0} e^{\frac{\Delta R}{R_{ref}} t} \quad (3.7)$$

x_{1_0} term denotes the initial value of the first state of the dynamical system. Moreover, the $R^* - R_0$ term can be interpreted as the range difference between an initial time and instantaneous time, denoted as ΔR . From definition of this range difference, it must be negative since the pursuer should head towards the target.

Therefore, it can be seen from equation (3.7) that the first order sliding manifold which corresponds to a first order linear time varying system; exponentially converges to zero if the range difference is negative. Physically, it can be interpreted as once the states of the system reach the sliding manifold (i.e. $s = 0$), they must be forced to go to equilibrium subspace ($x_1 = 0, x_2 = 0$) as explained in Chapter 2 exponentially. And in the neighborhood of this equilibrium subspace the closing velocity \dot{R} should also be negative, so the range difference in equation (3.7) should be negative. Therefore, the exponential stability of the system on provided sliding surface is proven.

3.2 Robust Control Lyapunov Function

In order to force the system to the desired exponentially stable sliding manifold, there are few nonlinear control methods to control dynamical system robustly. SMC is one of them as mentioned before. However, SMC has a chattering problem in essence of imperfections, since the control input is rather discrete. From that reason, more robust and flattened control method could be examined to control dynamical system. Although flattened SMC methods can provide nonlinear control robustly without chattering, the SMC methods are not used in this study.

The Lyapunov stability theory is a powerful tool to investigate the stability of a system. The existence of the Lyapunov function is the most important necessity and sufficient condition for the stability of open loop nonlinear system. [47] The sufficiency was proved by Lyapunov [52] and necessity was established half a century later via so-called converse theorems. [53, 54] Thus, Lyapunov theory deals generally with dynamical system without control inputs. For this reason, it has been traditionally applied only to closed-loop systems or unforced (i.e open loop) systems, that is the input has been eliminated with proper feedback control. However, recently, Lyapunov function candidates are being used to design feedback law itself by making derivative of the Lyapunov function negative. [55, 56, 57, 58] This method introduces the control Lyapunov functions (CLF) for systems with control inputs. The control effort is chosen to make control Lyapunov functions' derivatives negative definite. Therefore, the closed-loop system becomes asymptotically stable.

In order to design a feedback control with control Lyapunov function, first a Lyapunov function candidate should be selected. In this study, the control Lyapunov function should force the LOS dynamics toward to aforementioned desired sliding manifold. So, the Lyapunov function candidate selected to be quadratic-like as follows.

$$V = \frac{1}{2} s^2 \quad (3.8)$$

where s is the sliding manifold which contains states of the system. So,

$$V(x, t) = \frac{1}{2} \left(x_2 - \frac{\dot{R}}{R_{ref}} x_1 \right)^2 \quad (3.9)$$

Lyapunov function is continuously differentiable positive definite for all time and states as expected. To have an asymptotically stable closed-loop system, the derivative of the Lyapunov function (\dot{V}) must be negative definite for all time and states [51, 52]. The time derivative of the Lyapunov function becomes

$$\dot{V}(x, t) = \left(x_2 - \frac{\dot{R}}{R_{ref}} x_1 \right) \left(\dot{x}_2 - \frac{\ddot{R}}{R_{ref}} x_1 - \frac{\dot{R}}{R_{ref}} x_2 \right) \quad (3.10)$$

In order to keep the Lyapunov function candidate's derivative negative definite, as mentioned before, the desired Lyapunov function derivative is defined as follows

$$\dot{V}_d = -KV \quad (3.11)$$

where K is the positive constant which later named as *guidance constant*. Physically, this constant controls the system's speed of convergence to sliding manifold (also indirectly the trajectory of the pursuer) and cannot be less than or

equal to zero for stability concern. If so, since the Lyapunov function candidate is positive definite for all time and states; the desired Lyapunov function candidate will also be negative definite for all time and states. Thus, the desired Lyapunov function candidate becomes explicitly as follows.

$$\dot{V}_d = -\frac{K}{2} \left(x_2 - \frac{\dot{R}}{R_{ref}} x_1 \right)^2 \quad (3.12)$$

Note that the control effort should increase with the constant K , since the system should converge quicker with larger negative definite derivative of the Lyapunov function. If we equate the Lyapunov function candidate's derivative to desired one via equations (3.10) and (3.12) as follows

$$\begin{aligned} \dot{V} &= \dot{V}_d \\ \left(x_2 - \frac{\dot{R}}{R_{ref}} x_1 \right) \left(\dot{x}_2 - \frac{\dot{R}}{R_{ref}} x_2 - \frac{\ddot{R}}{R_{ref}} x_1 \right) &= -\frac{K}{2} \left(x_2 - \frac{\dot{R}}{R_{ref}} x_1 \right)^2 \end{aligned} \quad (3.13)$$

Then

$$\left(\dot{x}_2 - \frac{\dot{R}}{R_{ref}} x_2 - \frac{\ddot{R}}{R_{ref}} x_1 \right) = -\frac{K}{2} \left(x_2 - \frac{\dot{R}}{R_{ref}} x_1 \right) \quad (3.14)$$

The control effort is contained in the \dot{x}_2 term implicitly. So, the equation (3.14) is expanded via equation (3.1) as follows

$$\left(-\frac{u}{R} - \frac{2x_2\dot{R}}{R} - \frac{\ddot{R}x_1}{R} - \frac{\ddot{R}\tan\lambda_d}{R} - \frac{\dot{R}}{R_{ref}}x_2 - \frac{\ddot{R}}{R_{ref}}x_1 \right) = -\frac{K}{2}\left(x_2 - \frac{\dot{R}}{R_{ref}}x_1 \right) \quad (3.15)$$

The above equality can be arranged as follows

$$\begin{aligned} u &= -2x_2\dot{R} - \ddot{R}x_1 - \ddot{R}\tan\lambda_d - \frac{\dot{R}R}{R_{ref}}x_2 - \frac{\ddot{R}R}{R_{ref}}x_1 + \frac{KR}{2}x_2 - \frac{K\dot{R}R}{2R_{ref}}x_1 \\ &= \left(\frac{KR}{2} - 2\dot{R} - \frac{\dot{R}R}{R_{ref}} \right) x_2 - \left(\ddot{R} + \frac{\ddot{R}R}{R_{ref}} + \frac{K\dot{R}R}{2R_{ref}} \right) x_1 - \ddot{R}\tan\lambda_d \end{aligned} \quad (3.16)$$

System is stabilized by control Lyapunov functions as explained. Stabilizing systems with control Lyapunov functions implies robustness by definition. For detailed information, reference [47] can be examined.

3.3 Deduction of Guidance Law and Implementation Aspects

The guidance law can be deduced from the control effort which is found to control dynamical system in section 3.2. To deduct the guidance acceleration commands, some parameters should be clarified. First of all, in constructing the sliding manifold, the R_{ref} term should be set. In order to define R_{ref} , sliding manifold equation (3.6) can be divided by R_0 as follows:

$$\ln\left(\frac{x_1^*}{x_{1_0}}\right) = \frac{\left(\frac{R^*}{R_0} - 1\right)}{\frac{R_{ref}}{R_0}} \quad (3.17)$$

As mentioned before, x_{1_0} is the initial value of state x_1 which equates the value of x_{1_0} as follows

$$x_{1_0} = \tan \lambda_0 - \tan \lambda_d \quad (3.18)$$

Furthermore, x_1^* can be interpreted as error amplitude (preferably predefined near zero) for shaping the sliding surface. Physically, x_1^* can be demonstrated as the LOS angle error between desired and arbitrary one. The control Lyapunov function forces the system to that angle error while converging on the desired sliding manifold. Not only this error amplitude of the first state should go zero equilibrium exponentially by CLF, but also setting this error amplitude value can shape the trajectory of the pursuer indirectly.

The range value R^* can also be predefined. Note that this predefined range value cannot exceed initial range value between target and pursuer. After defining necessary values in the sliding manifold, it can be shown that the left hand side of the equation (3.17) and R^*/R_0 ratio is constant.

Then, let the ratio of the reference range and initial range R_{ref}/R_0 be η ,

$$\ln\left(\frac{x_1^*}{x_{1_0}}\right) = \frac{\left(\frac{R^*}{R_0} - 1\right)}{\eta} \quad (3.19)$$

Then

$$\eta = \frac{\left(\frac{R^*}{R_0} - 1\right)}{\ln\left(\frac{x_1^*}{x_{1_0}}\right)} \quad (3.20)$$

To construct the range ratio η in the sliding surface, the error amplitude can be predefined near zero as mentioned since the system should be on zero equilibrium subspace for successful mission. Note that the selections of these error amplitude and range value are independent from the system or its states. It has only a relationship with the sliding manifold. So, it can be used as a constant predefined value for all initial and boundary conditions. Once the system is on the provided sliding surface, it's already proven that the system is exponentially stable. The range ratio η depends only on initial conditions of engagement kinematics once the R^* and x_1^* are predefined. Thus, let the term λ^* be near zero as follows:

$$\lambda^* = \lambda_d \pm 0.004 \text{ rad} \quad (3.21)$$

Then the term x_1^* becomes

$$x_1^* = \tan \lambda^* - \tan \lambda_d \quad (3.22)$$

Furthermore, the range value can be predefined as quarter of the initial range value for every initial condition as follows

$$R^* = 0.25R_0 \quad (3.23)$$

Then, the range ratio η becomes

$$\eta = \frac{-0.75}{\ln\left(\frac{x_1^*}{x_{1_0}}\right)} \quad (3.24)$$

With calculating the η , the sliding manifold becomes

$$s = x_2 - \frac{\dot{R}}{R_{ref}}x_1 = x_2 - \frac{\dot{R}}{\eta R_0}x_1 \quad (3.25)$$

$$R_{ref} = \eta R_0 \quad (3.26)$$

The necessary values in sliding surface are complete. It is convenient to say here that; the initial condition dependence of the in sliding surface with constant η and R_0 grants the nonlinear guidance law robustness against various initial conditions.

The control input which is found in section 3.2 can be rewritten as

$$\begin{aligned}
u &= \frac{KR}{2} x_2 - 2x_2 \dot{R} - \ddot{R} x_1 - \ddot{R} \tan \lambda_d - \frac{\dot{R}R}{\eta R_0} x_2 - \frac{\ddot{R}R}{\eta R_0} x_1 - \frac{K\dot{R}R}{2\eta R_0} x_1 \\
&= \left(\frac{KR}{2} - 2\dot{R} - \frac{\dot{R}R}{\eta R_0} \right) x_2 - \left(\ddot{R} + \frac{\ddot{R}R}{\eta R_0} + \frac{K\dot{R}R}{2\eta R_0} \right) x_1 - \ddot{R} \tan \lambda_d
\end{aligned} \tag{3.27}$$

As mention before, the control input of the dynamical system is the acceleration command perpendicular to the range vector. This acceleration command consist the information of LOS angle and LOS angular rate via states of the system. Thus the acceleration commands which defined in equation (3.27) can be rewritten explicitly as follows

$$\begin{aligned}
a_{com} &= \frac{KR\dot{\lambda}}{2\cos^2 \lambda} - \frac{2\dot{\lambda}\dot{R}}{\cos^2 \lambda} - \ddot{R} \tan \lambda - \frac{\dot{R}R\dot{\lambda}}{\eta R_0 \cos^2 \lambda} - \\
&\quad - \left(\frac{\ddot{R}R}{\eta R_0} + \frac{K\dot{R}R}{2\eta R_0} \right) (\tan \lambda - \tan \lambda_d)
\end{aligned} \tag{3.28}$$

The \ddot{R} term in the guidance command denotes the acceleration in the direction towards the target. This term which is found in Chapter 2, is affiliated with range and LOS angular rate between target and pursuer.

Thus, the \ddot{R} term can be rewritten as

$$\ddot{R} = \dot{\lambda}^2 R \tag{3.29}$$

Therefore, proposed guidance law becomes explicitly as follows.

$$a_{com} = \frac{KR\dot{\lambda}}{2\cos^2\lambda} - \frac{2\dot{\lambda}\dot{R}}{\cos^2\lambda} - \dot{\lambda}^2 R \tan\lambda - \frac{\dot{R}R\dot{\lambda}}{\eta R_0 \cos^2\lambda} - \left(\frac{\dot{\lambda}^2 R^2}{\eta R_0} + \frac{K\dot{R}R}{2\eta R_0} \right) (\tan\lambda - \tan\lambda_d) \quad (3.30)$$

To use the guidance commands in practical applications, initial and instantaneous range between pursuer and target and LOS angle and angular rate information should be provided. These information could be gathered from on-board sensors (i.e seekers, gyroscopic sensors, accelerometers, range-finders etc.) attached to the pursuer. The closing velocity should be calculated with an on-board flight computer for every instant. The equations for closing velocity is stated in equation (2.9). The velocity vector of the pursuer that appears in closing velocity equation can be integrated from total acceleration vector which can be sensed from on-board inertial measurement units. The \ddot{R} term can be calculated from LOS rate and range as stated in equation (2.31). If the LOS angle & angular rate could not be gathered from sensors, necessary information can be calculated by navigational equations. These equations can be found easily in the literature and are not scope of this study.[1, 3]

To conclude, after explaining all contributory parameters in the guidance commands for practical applications; the analytical formulation for nonlinear impact angle control guidance law is completed.

3.4 Capturability Analysis of the Guidance Law

There are many ways to prove the capturability of a guidance law in the literature. The first works of capturability of a guidance law is closed-form solution approach developed by Guelman M. [7] for True PN law. In his work, the conditions necessary

for the pursuer to reach the target are determined via getting time-dependent closed form solutions of the equations of the motion between target and pursuer. Yet, the equations of motion of the dynamical system are purely nonlinear and only solvable for some conditions. Because of that reason, the closed form solution of the Pure PN laws were developed some time later due to requirement of challenging mathematical manipulations. [8] Both closed-form solution approaches can determine the capturability for only some conditions. Due to that nonlinear approaches are developed to prove the capturability of the more general guidance law. [48, 59] Moreover, some geometrical approaches are developed again for PN laws to prove capturability without solving the differential equations of the motion in nonlinear environment. [60]

The nonlinear approach based on Lyapunov stability theory is studied to prove capturability analyses for True PN, Pure PN and Augmented PN laws in the work of Ryoo et al. [48] The beauty of that approach is to determine the stability of the pursuer with guidance commands without getting the closed-form solutions of the dynamics between target and pursuer. The range state is also transformed to avoid singularity at $R = 0$ in the work of Ryoo et al. Then, the asymptotical stability of the system at the neighborhood of the equilibrium subspace is achieved and boundedness of the guidance commands near the target is proven.

The equation of motion between target and pursuer is investigated similarly in Chapter 2. However, in the view of Lyapunov stability approach, the look angle, which should also converge to null equilibrium at the end of rendezvous; is also included in the equation of motion to investigate closed-loop system at the near equilibrium subspace. Thus, the general equation of motion of the pursuer in three dimensions and states of the dynamical system become as follows

$$\begin{aligned} \dot{z} &= f(t, z) \\ z &= [R \quad \varepsilon_p \quad \varepsilon_y \quad \lambda_p \quad \lambda_y]^T \end{aligned} \quad (3.31)$$

Then, the $f(t, z)$ becomes:

$$f(t, z) = \begin{bmatrix} -v_m \cos \varepsilon_p \cos \varepsilon_y \\ \frac{a_{z_m}}{V_m} + \frac{v_m \cos \varepsilon_p \sin^2 \varepsilon_y \sin \theta_L}{R \cos \theta_L} + \frac{v_m \sin \varepsilon_p \cos \varepsilon_y}{R} \\ \frac{a_{y_m}}{V_m \cos \varepsilon_p} - \frac{v_m \sin \varepsilon_p \sin \varepsilon_y \cos \varepsilon_y \sin \lambda_p}{R \cos \lambda_p} + \frac{v_m \sin \varepsilon_y}{r \cos \varepsilon_p} \\ -\frac{v_m \sin \varepsilon_p}{R} \\ -\frac{v_m \cos \varepsilon_p \sin \varepsilon_y}{R \cos \lambda_p} \end{bmatrix} \quad (3.32)$$

As defined before, ε_p and ε_y are the elevation and azimuth components of the look angle between pursuer velocity vector and range vector and λ_p and λ_y are also the elevation and azimuth components of the LOS angle. The terms a_{z_m} and a_{y_m} are the acceleration components which are represented in velocity frame. To avoid the singularity point at $R = 0$, the range state R is transformed to R_T as follows

$$R_T = (R - R_c)^2 \quad (3.33)$$

where R_c is an arbitrary chosen positive constant and satisfies;

$$0 < R_c \leq R_0 \quad (3.34)$$

Since, investigated system is in 2-D in this work, the transformed states becomes as follows

$$\begin{aligned} \dot{h} &= g(t, h) \\ h &= [R_T \quad \varepsilon \quad \lambda]^T \end{aligned} \quad (3.35)$$

Then, the equations of motion for given states becomes

$$g(t, h) = \begin{bmatrix} -2v_m \operatorname{sgn}[R - R_c] \sqrt{R_T} \cos \varepsilon \\ \frac{a_{zm}}{v_m} + \frac{v_m \sin \varepsilon}{\left(R_c + \operatorname{sgn}[R - R_c] \sqrt{R_T} \right)} \\ - \frac{V_m \sin \varepsilon}{\left(R_c + \operatorname{sgn}[R - R_c] \sqrt{R_T} \right)} \end{bmatrix} \quad (3.36)$$

where sign function $\operatorname{sgn}[\alpha]$ is defined as

$$\operatorname{sgn}[\alpha] = \begin{cases} +1 & \text{if } \alpha \geq 0 \\ -1 & \text{if } \alpha < 0 \end{cases} \quad (3.37)$$

It can be convenient to note that here the equilibrium subspaces of the dynamical system are similar to that explained in Chapter 2. The only difference between these

equilibrium subspaces is the impact angle constraints. The equilibrium subspace determination for proposed guidance law includes the error difference between desired and instantaneous LOS angle. This constraint in equilibrium subspace is excluded for capturability analysis since the only concern is capturing the target. Even though the stability of the closed loop LOS dynamic is guaranteed with CLF method, the stability of range, look angle should also be checked by capturability analysis.

In order to keep the brevity of the study, the domain in which the capturability analysis of the transformed states is performed, is determined as follows

$$D = \left\{ h \mid 0 \leq R_r \leq R_0^2, |\varepsilon| < \frac{\pi}{2}, |\lambda| < \frac{\pi}{2} \right\} \quad (3.38)$$

Then it can be said that the region D contains the equilibrium subspace of the system. Thus, let Lyapunov function candidate for stability analysis V_C be

$$V_C(R_r, \varepsilon) = \frac{R_r}{R_0^2} + (1 - \cos \varepsilon) \quad (3.39)$$

Then Lyapunov function candidate V_C satisfies positive definiteness in region D except $\{R_r = 0, \varepsilon = 0\}$. Moreover, since it is bounded by 2, local stability test for nonlinear dynamical system can be applied. [51]

In the proposed guidance law, the guidance commands are perpendicular to the range vector, so, the a_{zm} term in the equations of motion becomes

$$a_{zm} = a_{com} \cos \varepsilon \quad (3.40)$$

Note that the other component of the acceleration command is parallel to velocity vector and makes the speed of the pursuer non-constant. Nevertheless, aforementioned capturability test is suitable for varying speed. [48]

The $\{R_r = 0, \varepsilon = 0\}$ condition is the equilibrium subspace for the system. The proposed Lyapunov function candidate can be used to prove the capturability and determine capture conditions for proposed guidance law. Note that the domain of the state related to the equilibrium subspace is not yet specified.

For $0 < R_c \leq R \leq R_0$, the time derivative of the Lyapunov function candidate is

$$\dot{V}_C = \frac{\dot{R}_r}{R_0^2} + \dot{\varepsilon} \sin \varepsilon \quad (3.41)$$

The time derivative terms in the above equation can be replaced via equation of motion given in equation (3.36). Then the Lyapunov derivative becomes

$$\dot{V} = -\frac{2v_m \sqrt{R_r} \cos \varepsilon}{R_0^2} + \frac{a_{com} \cos \varepsilon \sin \varepsilon}{v_m} + \frac{v_m \sin^2 \varepsilon}{(R_c + \sqrt{R_r})} \quad (3.42)$$

Let the function W_4 be

$$W_4 = \frac{2v_m \sqrt{R_T} \cos \varepsilon}{R_0^2} \quad (3.43)$$

It can be seen that the function W_4 is a positive definite function in region D.

Moreover, the terms in guidance commands a_{com} can be rewritten as;

$$\dot{R} = -v_m \cos \varepsilon \quad (3.44)$$

and

$$\dot{\lambda} = -\frac{v_m \sin \varepsilon}{R} = -\frac{v_m \sin \varepsilon}{\left(R_c + \operatorname{sgn}[R - R_c] \sqrt{R_T}\right)} \quad (3.45)$$

Then, the guidance commands acting on the pursuer becomes as follows

$$\begin{aligned}
a_{LOS} = & - \left(\frac{K(R_c + \sqrt{R_T})}{2} + 2v_m \cos \varepsilon + \frac{v_m \cos \varepsilon (R_c + \sqrt{R_T})}{R_{ref}} \right) \\
& \left(\frac{v_m \sin \varepsilon}{(R_c + \sqrt{R_T}) \cos^2 \lambda} \right) - \ddot{R} \tan \lambda - \\
& \left(\frac{\ddot{R}(R_c + \sqrt{R_T})}{\eta R_0} + \frac{K(R_c + \sqrt{R_T}) v_m \cos \varepsilon}{2\eta R_0} \right) (\tan \lambda - \tan \lambda_d)
\end{aligned} \tag{3.46}$$

Therefore, the derivative of the Lyapunov function V_C becomes

$$\begin{aligned}
\dot{V}_C = & -W_4 - \left(\frac{K(R_c + \sqrt{R_T})}{2} + 2v_m \cos \varepsilon + \frac{v_m \cos \varepsilon (R_c + \sqrt{R_T})}{R_{ref}} \right) \\
& \left(\frac{\sin^2 \varepsilon \cos \varepsilon}{(R_c + \sqrt{R_T}) \cos^2 \lambda} \right) + \frac{v_m \sin^2 \varepsilon}{(R_c + \sqrt{R_T})} - \frac{\ddot{R} \tan \lambda \cos \varepsilon \sin \varepsilon}{v_m} - \\
& - \left(\frac{\ddot{R}(R_c + \sqrt{R_T}) \cos \varepsilon}{v_m \eta R_0} + \frac{K(R_c + \sqrt{R_T}) \cos^2 \varepsilon}{2\eta R_0} \right) \sin \varepsilon (\tan \lambda - \tan \lambda_d)
\end{aligned} \tag{3.47}$$

It can also be rearranged via some mathematical manipulation as follows:

$$\begin{aligned}
\dot{V}_C = & -W_4 - \left(\frac{K}{2} + \frac{v_m}{(R_c + \sqrt{R_T}) \cos \varepsilon} (2 \cos^2 \varepsilon - \cos^2 \lambda) + \frac{v_m \cos \varepsilon}{R_{ref}} \right) \\
& \left(\frac{\sin^2 \varepsilon \cos \varepsilon}{\cos^2 \lambda} \right) - \frac{\ddot{R} \tan \lambda_d \cos \varepsilon \sin \varepsilon}{v_m} - \\
& - \left(\frac{\ddot{R} \cos \varepsilon}{v_m} + \frac{\ddot{R} (R_c + \sqrt{R_T}) \cos \varepsilon}{v_m \eta R_0} + \frac{K (R_c + \sqrt{R_T}) \cos^2 \varepsilon}{2 \eta R_0} \right) \\
& \sin \varepsilon (\tan \lambda - \tan \lambda_d)
\end{aligned} \tag{3.48}$$

Let again function W_5 be

$$W_5 = \left(\frac{K}{2} + \frac{v_m}{(R_c + \sqrt{R_T}) \cos \varepsilon} (2 \cos^2 \varepsilon - \cos^2 \lambda) + \frac{v_m \cos \varepsilon}{R_{ref}} \right) \left(\frac{\sin^2 \varepsilon \cos \varepsilon}{\cos^2 \lambda} \right) \tag{3.49}$$

It can be seen that the function W_5 is a positive definite function in region D for all time and states. Thus, the derivative of the Lyapunov function becomes

$$\begin{aligned}
\dot{V}_C = & -W_4 - W_5 - \left(\frac{\ddot{R} \cos \varepsilon}{v_m} + \frac{\ddot{R} (R_c + \sqrt{R_T}) \cos \varepsilon}{v_m \eta R_0} + \frac{K (R_c + \sqrt{R_T}) \cos^2 \varepsilon}{2 \eta R_0} \right) \\
& \sin \varepsilon (\tan \lambda - \tan \lambda_d) - \frac{\ddot{R} \tan \lambda_d \cos \varepsilon \sin \varepsilon}{v_m}
\end{aligned} \tag{3.50}$$

Note that the term \ddot{R} is positive definite for all time states as seen in equation (3.29).

Then,

$$\begin{aligned}\dot{V}_C &\leq -W_4 - W_5 - W_6 \sin \varepsilon (\tan \lambda - \tan \lambda_d) \\ &\leq -W_3\end{aligned}\quad (3.51)$$

Note that W_6 is a positive definite function as follows:

$$W_6 = \left(\frac{\ddot{R} \cos \varepsilon}{v_m} + \frac{\ddot{R} (R_c + \sqrt{R_T}) \cos \varepsilon}{v_m \eta R_0} + \frac{K (R_c + \sqrt{R_T}) \cos^2 \varepsilon}{2 \eta R_0} \right) \quad (3.52)$$

And

$$W_3 = W_4 + W_5 + W_6 \sin \varepsilon (\tan \lambda - \tan \lambda_d) \quad (3.53)$$

Therefore, $\dot{V}_C \leq 0$ is satisfied only for the region given by

$$\operatorname{sgn} \varepsilon (\operatorname{sgn} (\lambda - \lambda_d)) \geq 0 \quad (3.54)$$

So, the domain D for proposed guidance law becomes as a combination of ε , λ and λ_d as follows

$$D = \left\{ h \mid R \geq 0, \operatorname{sgn} (\varepsilon (\lambda - \lambda_d)) \geq 0, |\varepsilon| < \frac{\pi}{2}, |\lambda| < \frac{\pi}{2} \right\} \quad (3.55)$$

For given domain D ,

$$W_1 = V_c = W_2 \quad (3.56)$$

And

$$\frac{\partial V_c}{\partial t} + \frac{\partial V}{\partial h} f(t, h) \leq -W_3(t) \quad (3.57)$$

The equations (3.56) and (3.57) proves that the closed-loop system's equilibrium subspace is uniformly asymptotically stable for $R \geq R_c$, since Lyapunov function is uniformly bounded and derivative of the Lyapunov function is negative definite for all time and states. [51]

Physically, starting at any initial conditions in domain D, the pursuer tends to approach the equilibrium subspace for $R \geq R_c$. In finite time, $R = R_c$ is achieved because \dot{R} is always negative. (i.e. $|\varepsilon| < \pi/2$) In the case of $R \leq R_c$, Lyapunov stability theory can't indicate the stability of the system. However, from establishing guidance law, the equation $R_c = R_{ref}$ can be satisfied, since the predefined term R_{ref} should be smaller than initial range value R_0 . Then it can be said that the system approaching the equilibrium subspace asymptotically stable; is also on the defined sliding surface at $R = R_c = R_{ref}$ which is established during guidance law development. Since, the defined sliding manifold as explained before is exponentially stable, the system with proposed guidance law can be said to be stable throughout the flight.

CHAPTER 4

SIMULATION RESULTS

The performance and the robustness of the proposed guidance law are examined by simulations in this chapter. First, some ideal test scenarios are tested to investigate proposed guidance law behavior under various engagement geometries. The tunable parameters of guidance law are changed to see the effect of them on trajectories and/or the behavior of the guidance law. After setting the necessary precision value for impact angle and selecting a nominal scenario from ideal test scenarios, some disturbances in sensor feedback are added to the simulation to check the impact angle precision with guided system for numerical robustness and disturbance rejection analyses.[†]

In practical applications, integration scheme and selection of step size is essential parameters in guidance law performance. Normally, step size is selected as 1/5 or 1/10 of the fastest dynamics of the system for accuracy. However, this step size selection can also depend on integration scheme. For that reason, various integration scheme and step size are tried to investigate the limits of the proposed guidance law for practical applications in nominal scenario.

In this Chapter, in section 4.1, construction of simulation is explained. Next, some ideal test scenarios and results are shown in section 4.2. Then section 4.3 is reserved for determining successful mission criteria for nominal scenario. The effect of guidance constant K on trajectories is investigated in section 4.4. In section 4.5,

[†] The robustness and disturbance rejection of the guidance law are determined only via numerical analyses and there could not be no claim about guidance law being robust.

disturbance rejection and robustness against various disturbances of the proposed guidance law are investigated. Lastly, effects of integration scheme and step size selection on flight computer calculations are examined in section 4.6

4.1 Construction of Simulation

The simulation model is constructed in MATLAB®/Simulink environment using MATLAB R2009a and Simulink 7.3. The general outline of the simulation is shown in Figure 6.

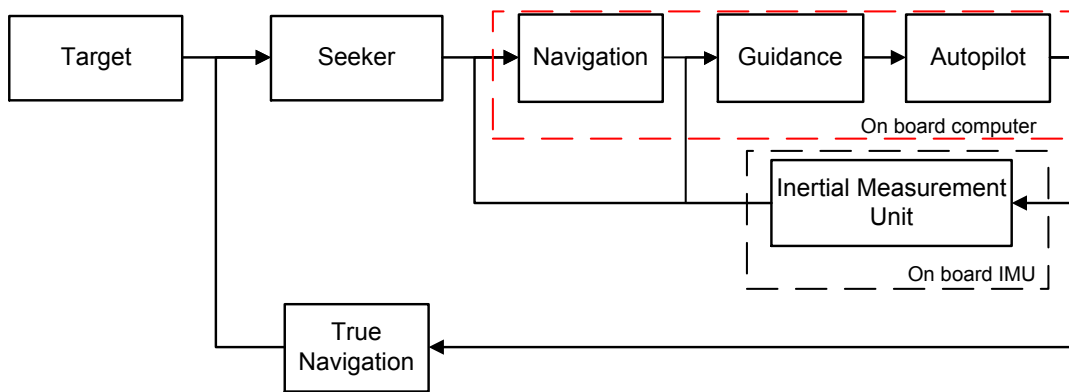


Figure 6. Simulation Structure in Simulink Environment

In detail, the target model consist the information about target position and velocity in 2-D. The LOS angle, angular rate and range information related to target-pursuer geometry is calculated in Seeker Model. Inputs and outputs of the seeker model can be viewed in detail in Figure 7. The relationships between position/velocity information and LOS angle/rate can be examined thoroughly in reference 3. In practical applications, this LOS angle and rate information can be gathered via gimbaled seekers. These gimbal systems have their own stabilization algorithm to always look towards the target. Thus, the angle and rate information between gimbal frame and inertial frame is generally calculated on-board and transferred to pursuer's flight computers. These relationships are not given in detailed since it is not the scope of this study. Moreover, some sensor related errors in LOS angle and first

order gimbal dynamics for LOS rate are also modeled in Seeker Model. Perfect signals that has no error/lag and denoted as “*True*” in Figure 7. However, both Navigation and Guidance models don’t use these perfect signals in non-ideal scenarios.

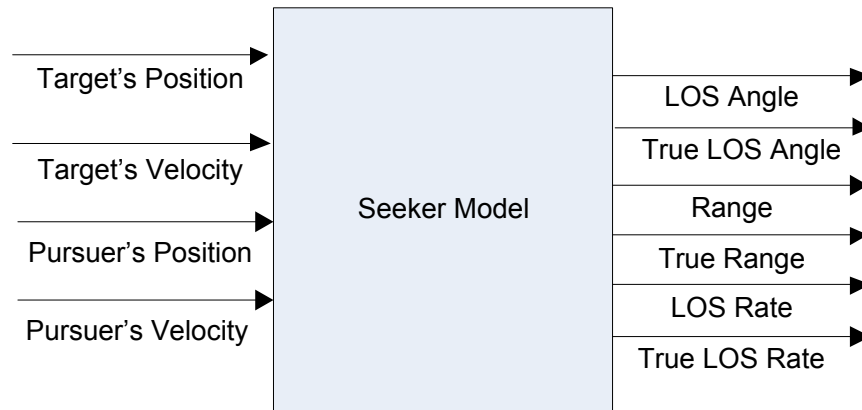


Figure 7. Detailed Schematic of Seeker Model

In Navigation model, the necessary information which is fed to guidance model is calculated from information coming from seeker model. The detailed scheme of Navigation Model can be seen in Figure 8. All calculations runs in Navigation Model are explained in previous Chapters.

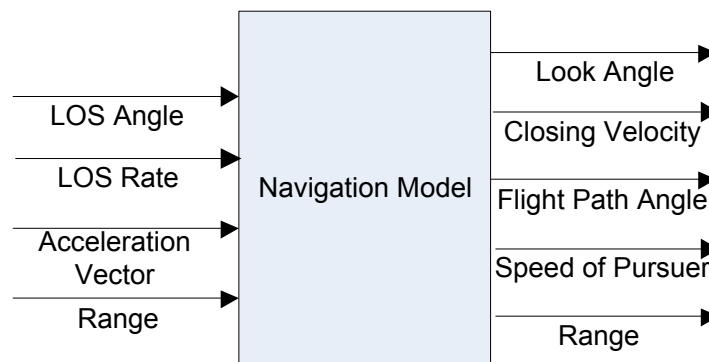


Figure 8. Detailed Schematic of Navigation Model

The guidance commands from proposed guidance synthesis are calculated in guidance model. To calculate necessary commands, the states of the dynamical system are constituted in model, and then necessary constants of guidance law are calculated from input file of the simulation. After, they are introduced to calculations in guidance model. In inertial measurement unit model, the disturbance coming from sensors is added to the acceleration of pursuer to examine the robustness of the guidance law numerically. In autopilot model, the delay on acceleration commands is modeled as first order system to simulate autopilot and aerodynamics. Finally, in True Navigation model, the acceleration, velocity and position information of pursuer is calculated in a “Real-World” manner.

The simulation parameters are configured to use Euler (ode1) solver with fixed step size. The step size is selected as 0.002 seconds (500 Hz) for all test scenarios. It is assured that a step size of 0.002 seconds is adequate to accurately simulate the system. The real world calculations run in a continuous manner with same selected fixed step-size. Note that in practical applications, the dash-lined parts in Figure 6 are calculated in discrete time. For that reason, in discussions of practical aspects; the on-board calculations run with various step-times with discrete integration schemes that are explained in section 4.6.

4.2 Ideal Test Scenarios & Results

To simulate and verify the proposed guidance law, the guidance law is examined for ideal system[‡] with 10 scenarios in this section. The scenarios presented in this section are variants of several air-to-ground and ground-to-ground like engagement geometries. Pursuer’s cross-range value is 1000 m and 100 m for air-to-ground and ground-to-ground scenarios respectively. Target is located 1000 m downrange as well for both sets of scenarios. For all scenarios, the pursuer initial velocity is also set to be 250 m/s. Initial flight path angle of the pursuer is set to three different values for air-to-ground engagement as -45° , 0° and 30° degrees respectively. Since

[‡] Ideal system has no system delay or lag, no disruptive sensor feedback and no limitations.

pursuer's initial position is close to the ground level in ground-to-ground engagement geometry, the initial flight path angle varies with two values such as 0° and 45° degrees respectively. Two desired impact angles for both engagement geometries are set as 30° and 60° respectively. Summaries of these ideal scenarios can be detailed in Table 1. Simulations stops when range between target and pursuer goes below 0.1 meters. The guidance constant K of the proposed guidance law is taken as 10 in air-to-ground engagement geometries and 4 in ground-to-ground engagements geometries for ideal scenarios.

Table 1. Ideal Engagement Scenarios

| Scenario # | Initial Pursuer Position[m] | Target Position[m] | Pursuer Velocity[m/s] | Initial Flight Path Angle[deg] | Desired Impact Angle[deg] |
|------------|-----------------------------|--------------------|-----------------------|--------------------------------|---------------------------|
| 1 | (0,1000) | (1000,0) | 250 | 0 | 60 |
| 2 | (0,1000) | (1000,0) | 250 | 0 | 30 |
| 3 | (0,1000) | (1000,0) | 250 | -45 | 60 |
| 4 | (0,1000) | (1000,0) | 250 | -45 | 30 |
| 5 | (0,1000) | (1000,0) | 250 | 30 | 60 |
| 6 | (0,1000) | (1000,0) | 250 | 30 | 30 |
| 7 | (0,100) | (1000,0) | 250 | 45 | 60 |
| 8 | (0,100) | (1000,0) | 250 | 45 | 30 |
| 9 | (0,100) | (1000,0) | 250 | 0 | 60 |
| 10 | (0,100) | (1000,0) | 250 | 0 | 30 |

The performed simulations show that target is captured with desired impact angle for all scenarios. The simulation results for all scenarios can be seen from Figure 9 to Figure 14. It can be observed from trajectories that even if the pursuer initial condition varies with the scenarios, the trajectories converge to each other in order to stabilize the system around the equilibrium point. Since the flight time varies in scenarios, the time values are normalized for demonstraion purposes. It can be seen from Figure 10 that the LOS angle error is controlled and LOS angle converges to desired value like a cascade-controlled system. It is intuitively expected that LOS angle response of the guidance law can be tuned by changing the parameters in guidance law and/or sliding surface (such as K , λ^* and R^*). It can be observed from

Figure 11 that flight path angle of the pursuer follows LOS angle behavior and converges desired impact angle. Look angle obeys the relationship between LOS and flight path angles which can be seen in Figure 12. It can be interpreted from figures that the LOS angle rises towards the desired value in the 30 percent of total time. This feature comes with the cost of huge instantaneous acceleration commands at the beginning of the flight up to $800g$'s. The command accelerations for given scenarios can be seen in Figure 13. However, it can be seen that when LOS angle converges to desired impact angle, command acceleration tends to zero. This behavior can grant some robustness against disturbances and counter-measurements in practical applications. The speed of the pursuer varies with time since the command accelerations are applied perpendicular to range vector. The speed of pursuer can be seen in Figure 14. For the scenarios with drastic maneuvering, the speed of the pursuer decrease severely. As mentioned before, with tuning the parameters of the guidance law, these undesirable result can intuitively be avoided.

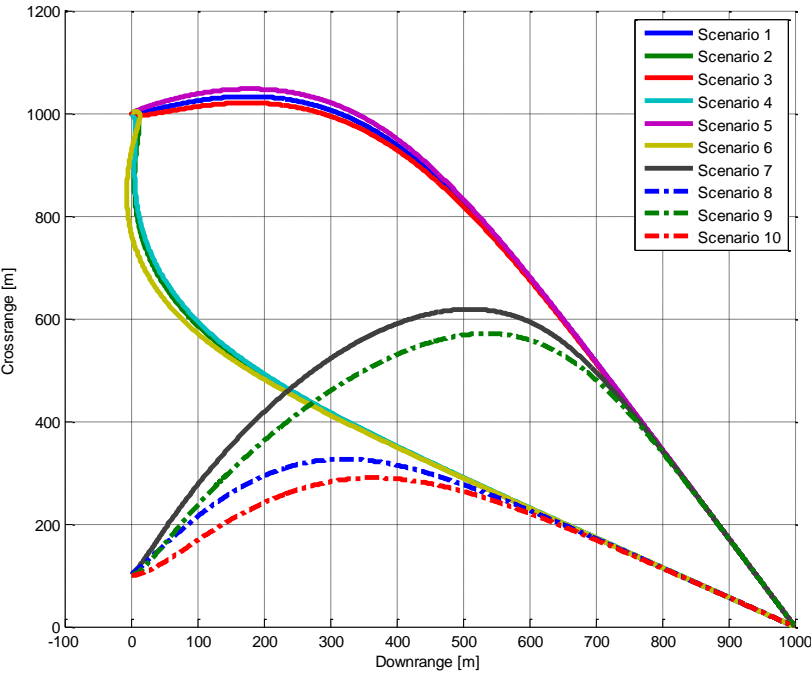


Figure 9. Spatial Trajectories of the Pursuer for all scenarios.

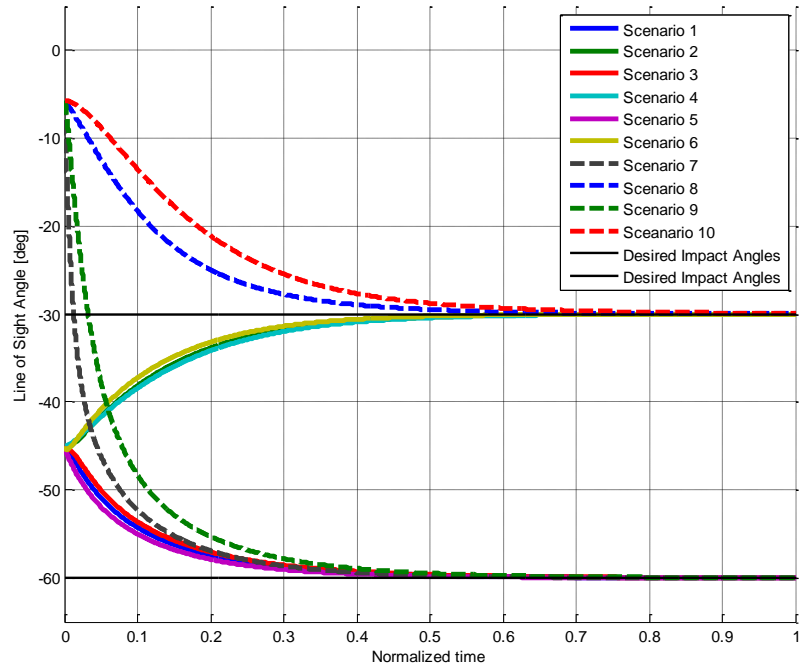


Figure 10. LOS Angles for all scenarios

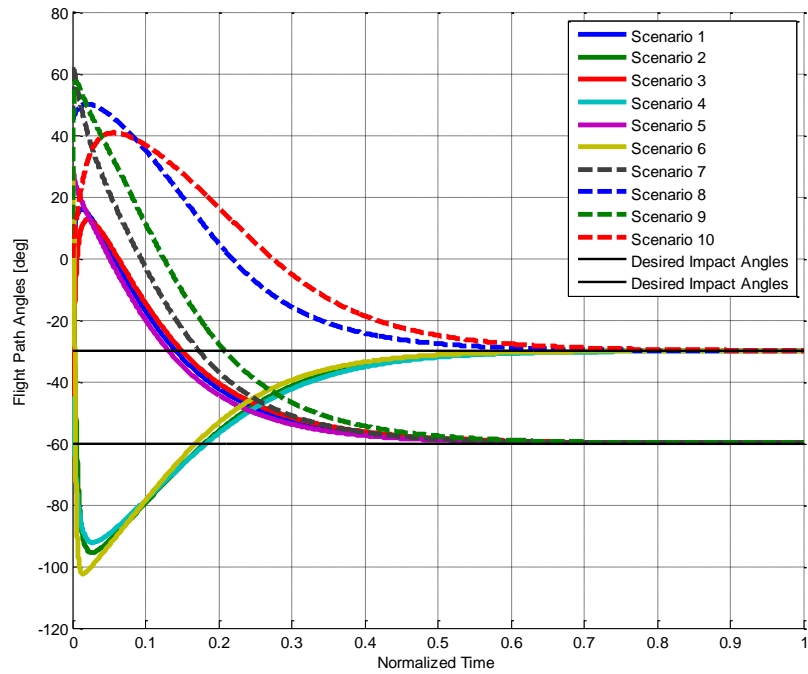


Figure 11. Flight Path Angles of Pursuer for all scenarios

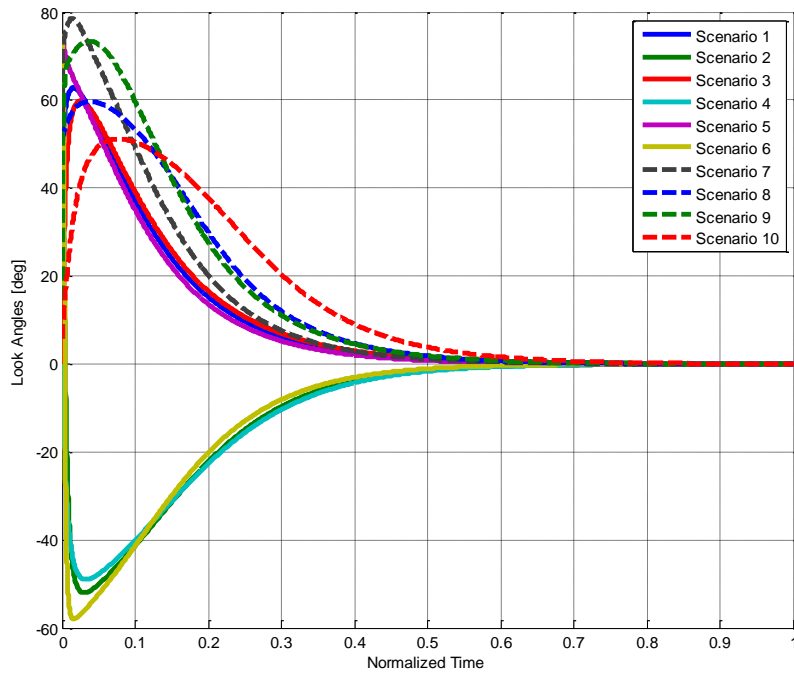


Figure 12. Look Angle between Pursuer and Target for all scenarios

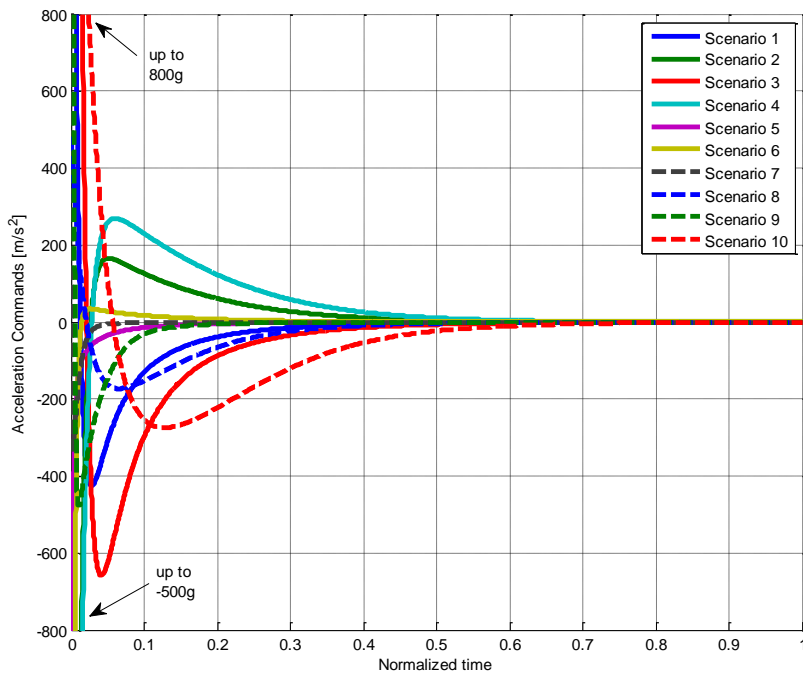


Figure 13. Command Accelerations of Pursuer for all scenarios

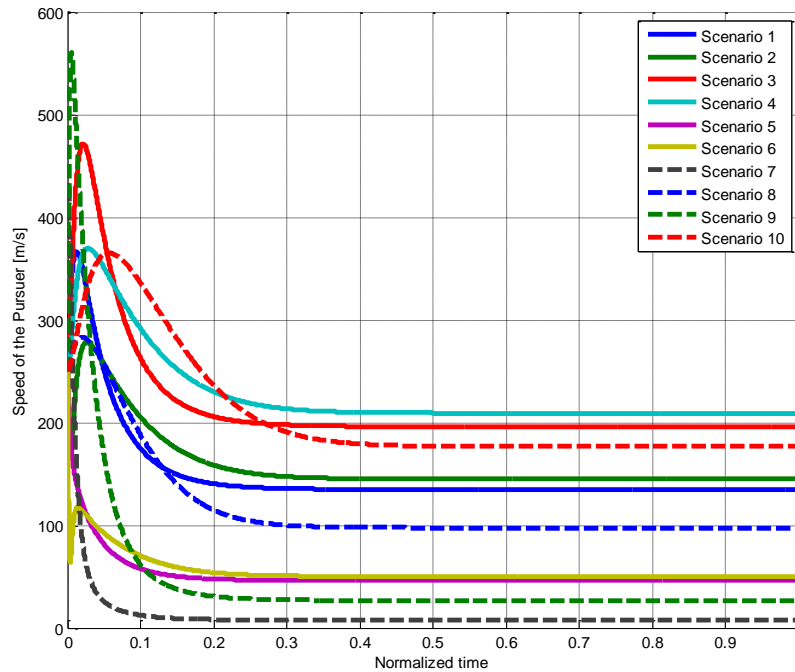


Figure 14. Speed of the Pursuer for all scenarios

The simulation results for scenario 1 are shown in figures from Figure 15 to Figure 18. Figure 15 shows that the target is successfully captured for that scenario. Figure 16 demonstrates the important angles for proposed guidance law such as LOS angle, flight path angle and look angle. It shows that characteristic of the proposed guidance law that is closing LOS error primarily while approaching the target. The look angle which should go null at near impact time can be also seen in Figure 16. Since the commanded accelerations are perpendicular to the range vector, the speed of the pursuer also varies due to this effect. Thus, Figure 17 shows changes in pursuer's speed for first scenario. Moreover, acceleration commands tend to zero long before the final time. The acceleration commands for proposed guidance laws for first scenario can be seen from Figure 18.

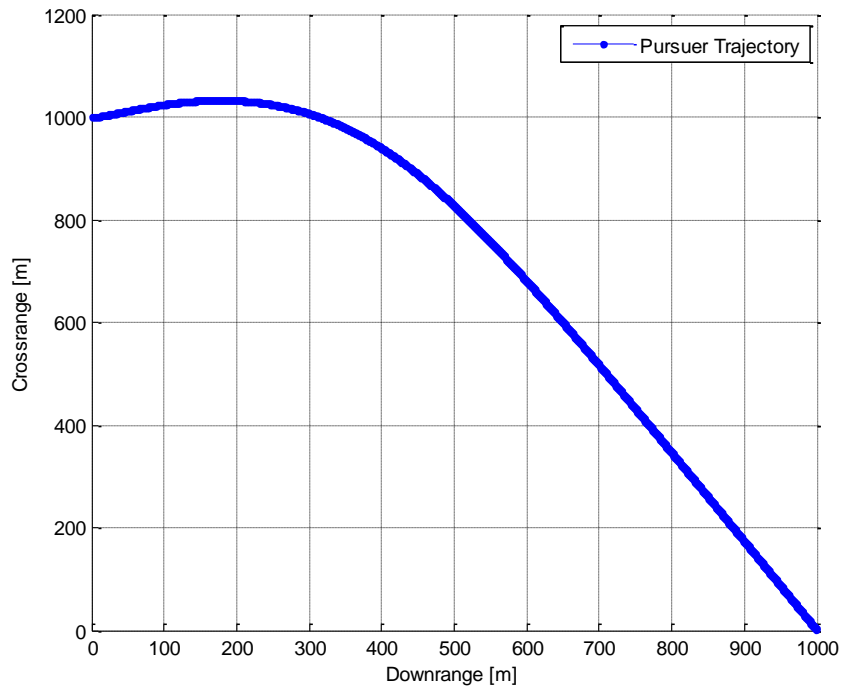


Figure 15. Pursuer Trajectory for Scenario 1

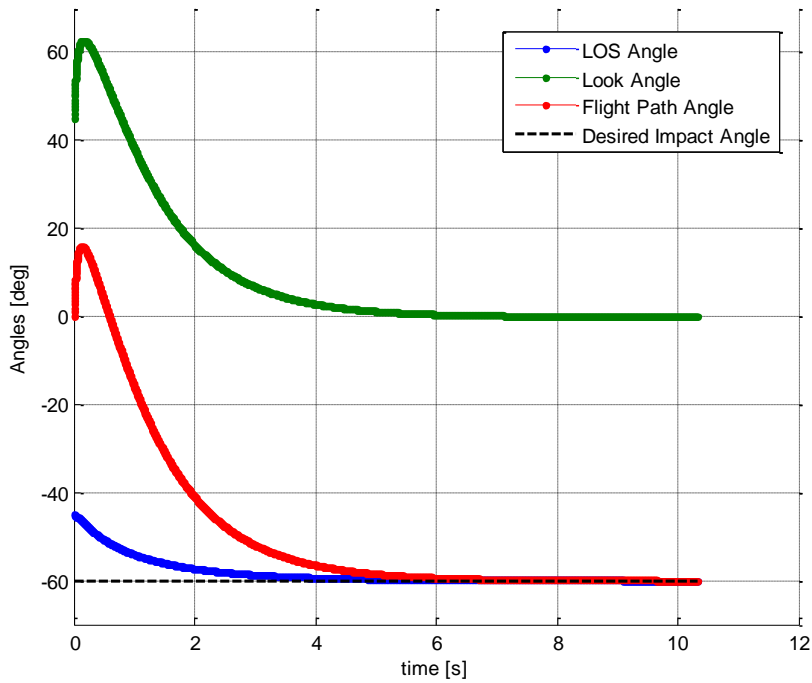


Figure 16. Important Angles in Scenario 1

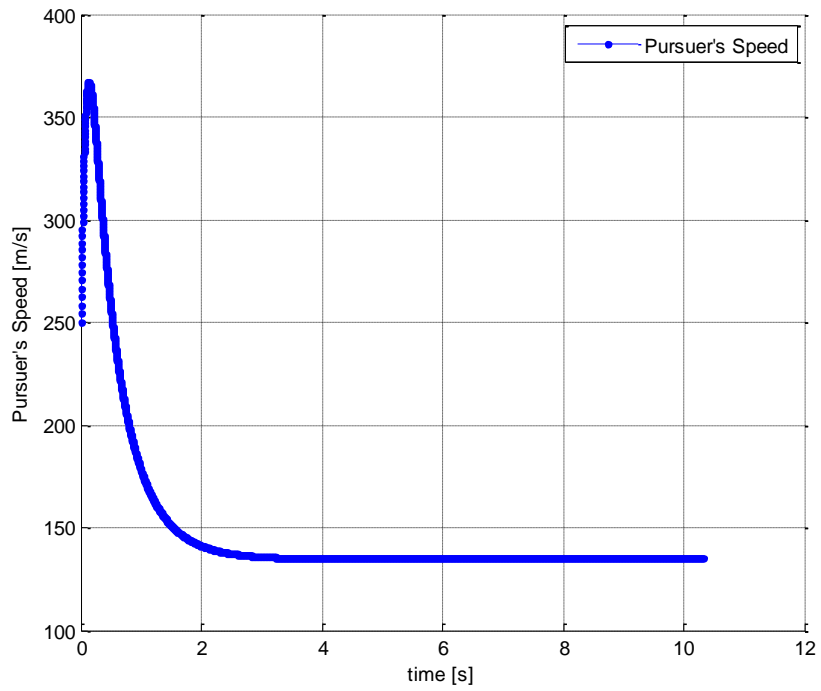


Figure 17. Pursuer Speed in Scenario 1

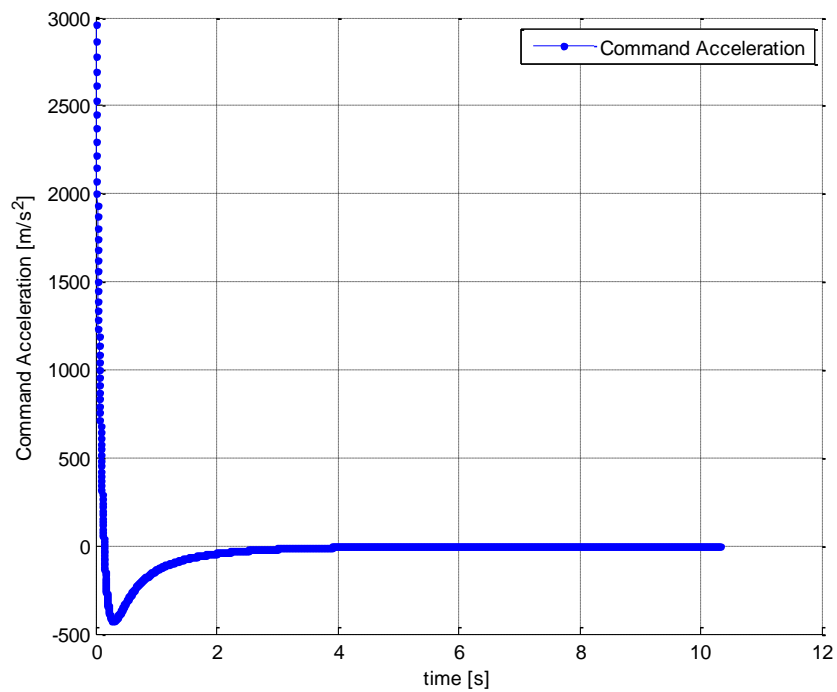


Figure 18. Guidance Commands in Scenario 1

The simulation results for second scenario are shown in figures from Figure 19 to Figure 22. Spatial trajectory of the pursuer can be seen in Figure 19. Figure 20 demonstrates the important angles for proposed guidance law. The speed of the pursuer can be seen in Figure 21. Moreover, acceleration commands of the pursuer with proposed guidance laws for second scenario can be observed from Figure 22. It can be seen from Figure 22 that in order to close the angle difference between LOS angle and impact angle which is the first state of the dynamics, pursuer goes directly below the target to achieve desired LOS angle in the cost of huge instant acceleration commands at the beginning of the flight. However, once the states of the system are at equilibrium subspace, then there is no need to change the trajectory of the target, hence acceleration command tends to go zero long before the impact. Furthermore, the commands perpendicular to range vector varies the speed of the pursuer while maneuvering as expected.

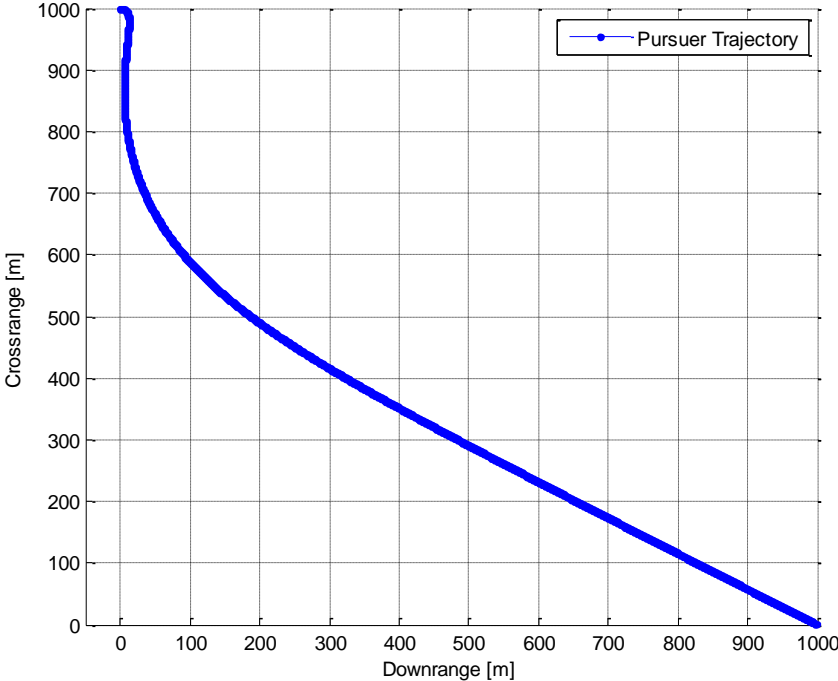


Figure 19. Pursuer Trajectory for Scenario 2

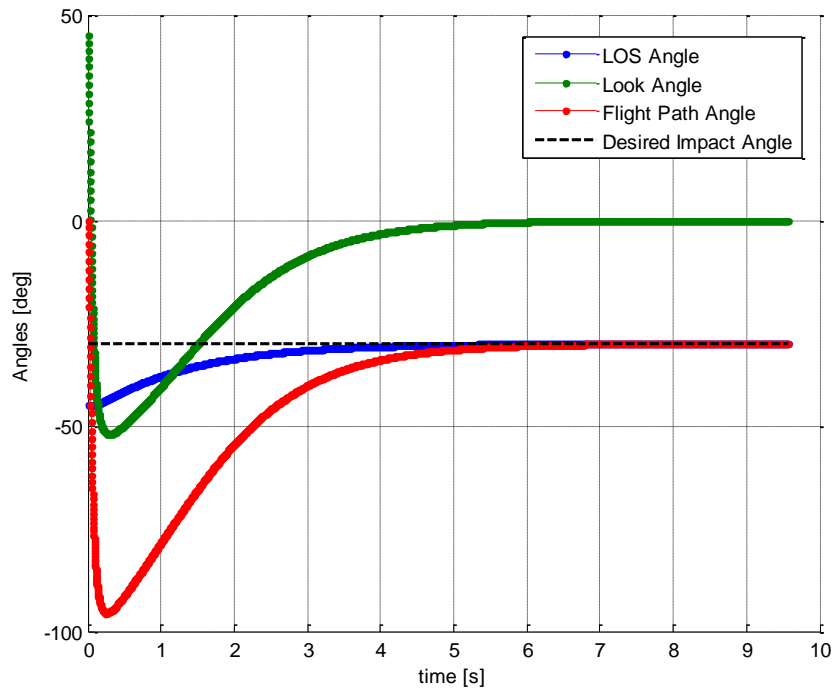


Figure 20. Important Angles in Scenario 2

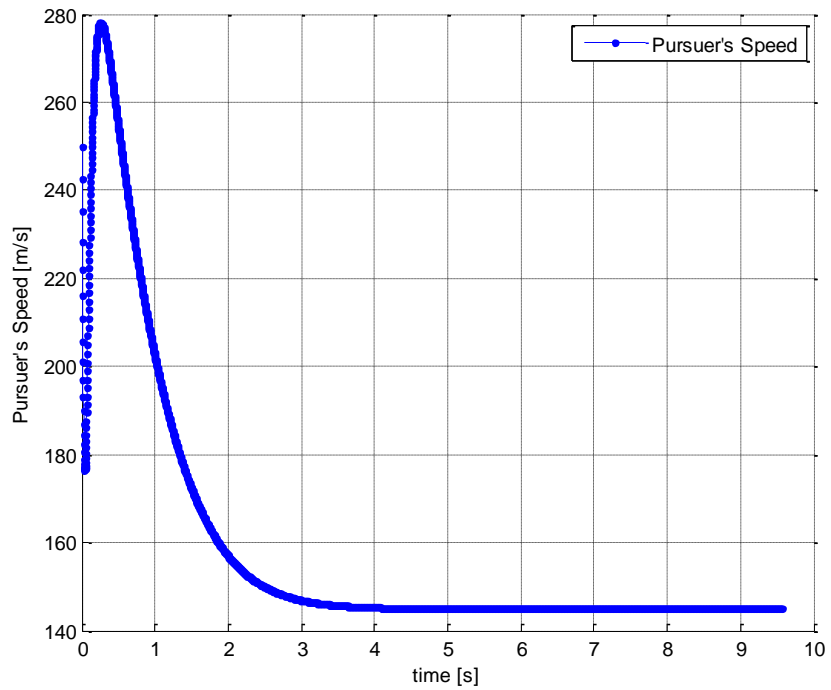


Figure 21. Pursuer Speed in Scenario 2

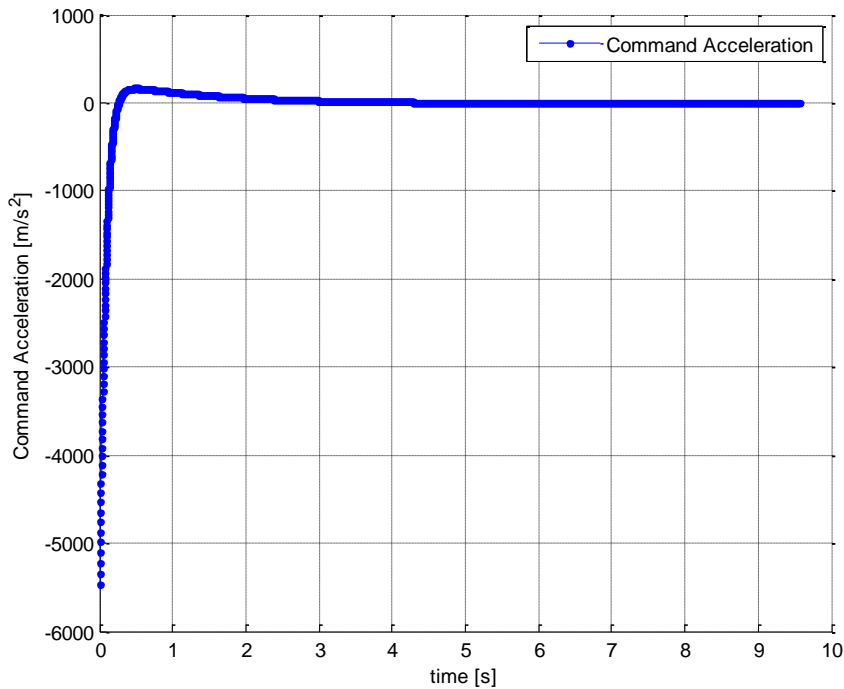


Figure 22. Guidance Commands in Scenario 2

The spatial trajectory of the pursuer for scenario 3 can be seen in Figure 23. Target is successfully captured for scenario 3. Since the pursuer begins the flight with negative flight path angle which can be seen in Figure 24; the higher acceleration commands to achieve desired LOS angle are needed at the beginning of the flight. The acceleration commands of the pursuer can be seen in Figure 26. Similar to previous scenarios, the acceleration commands tends to zero once the states of the dynamical system goes null equilibrium. The LOS angle and look angle of the pursuer-target geometry can be seen in Figure 24. Controller-like behaviour of the guidance law on LOS angle can be observed from Figure 24. Furthermore, since the commands to go above the target accelerates the pursuer's velocity, the speed of the pursuer at the near impact is higher than scenario 1. The speed of the pursuer for scenario 3 can be seen in Figure 25.

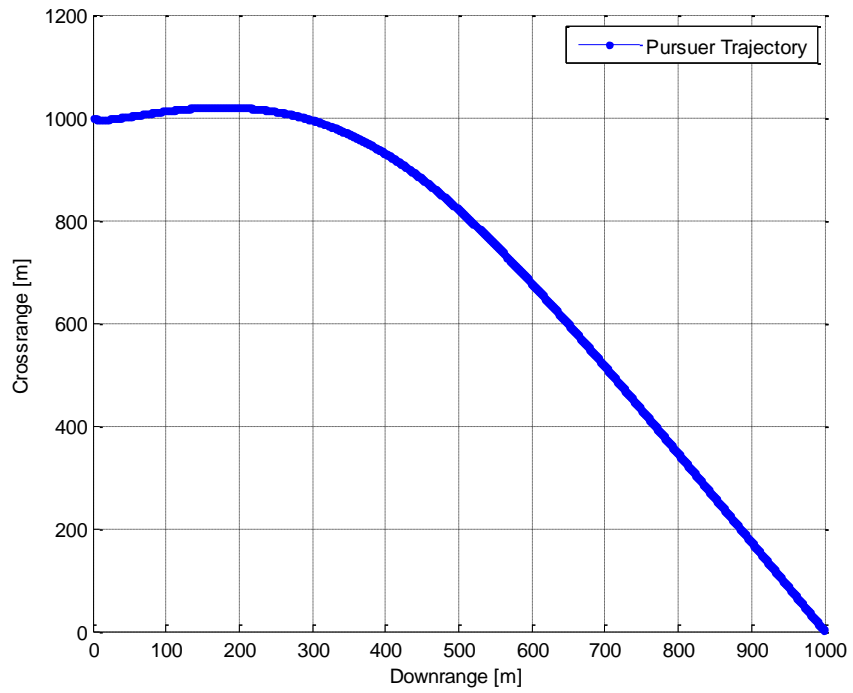


Figure 23. Pursuer Trajectory for Scenario 3

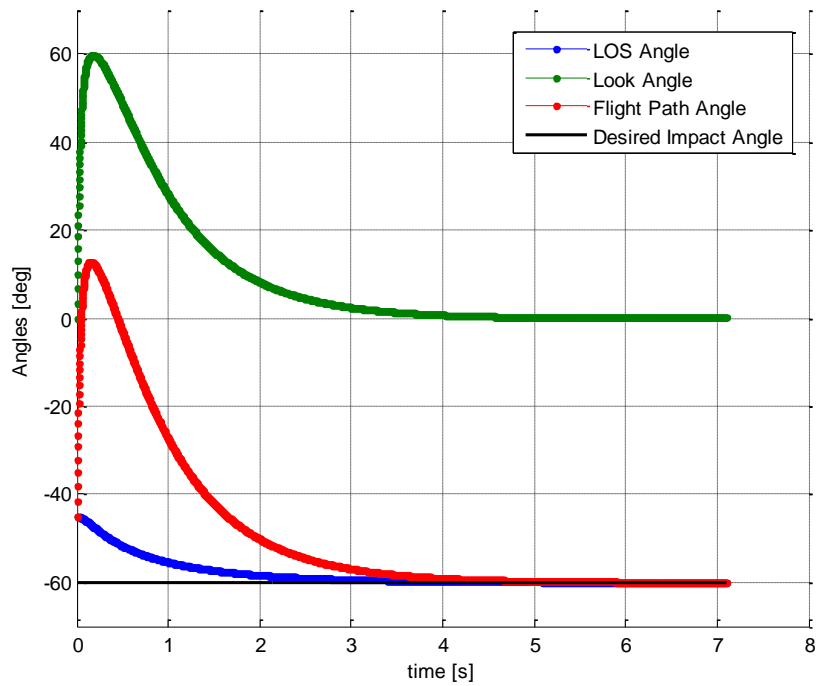


Figure 24. Important Angles in Scenario 3

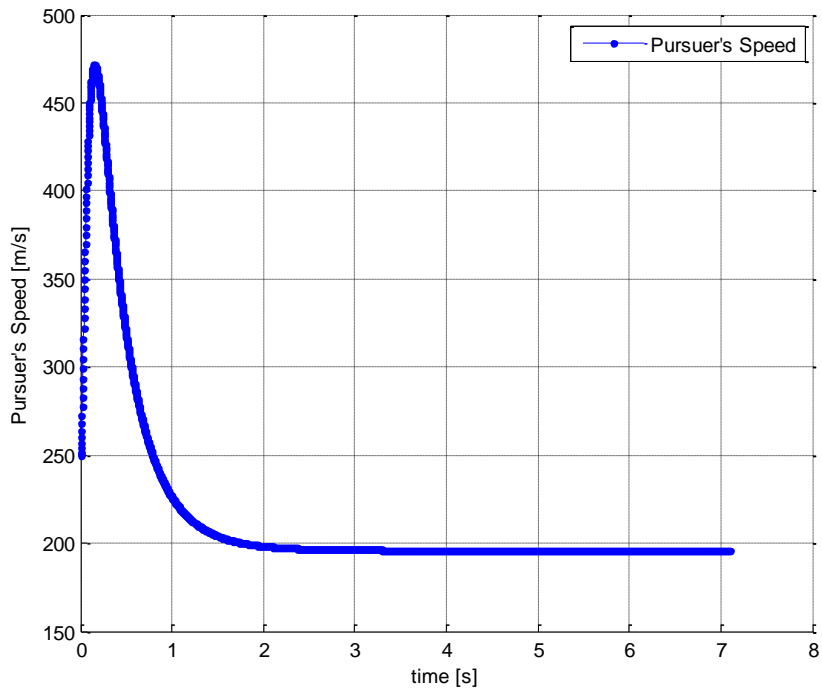


Figure 25. Pursuer Speed in Scenario 3

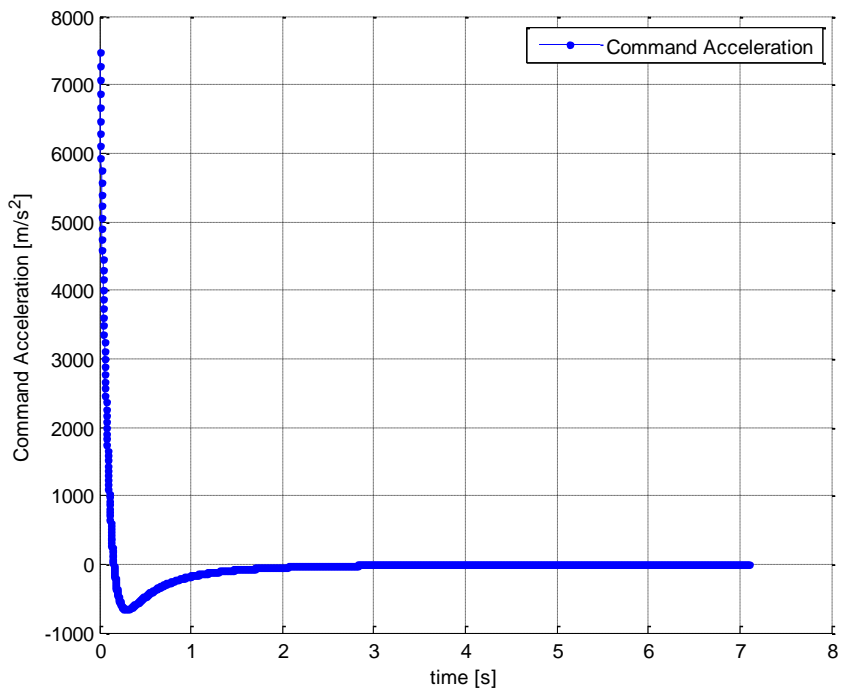


Figure 26. Guidance Commands in Scenario 3

The simulation results for scenario 4 can be seen in figures from Figure 27 to Figure 30. The spatial trajectory of the pursuer is shown in Figure 27. It can be seen that the target is again successfully captured. The pursuer begins the flight with negative flight path angle. From that reason, the required acceleration commands in the beginning of the flight to achieve desired LOS angle decreased for this scenario. The acceleration commands of the proposed guidance law can be seen in Figure 30. Moreover, the flight path angle, look angle and LOS angle of the pursuer-target geometry is presented in Figure 28. Note that since the flight path angle and initial LOS angle is same for this scenario, the look angle value starts from zero. The speed of the pursuer can be seen in Figure 29. The less acceleration commands provides less alteration in pursuer speed.

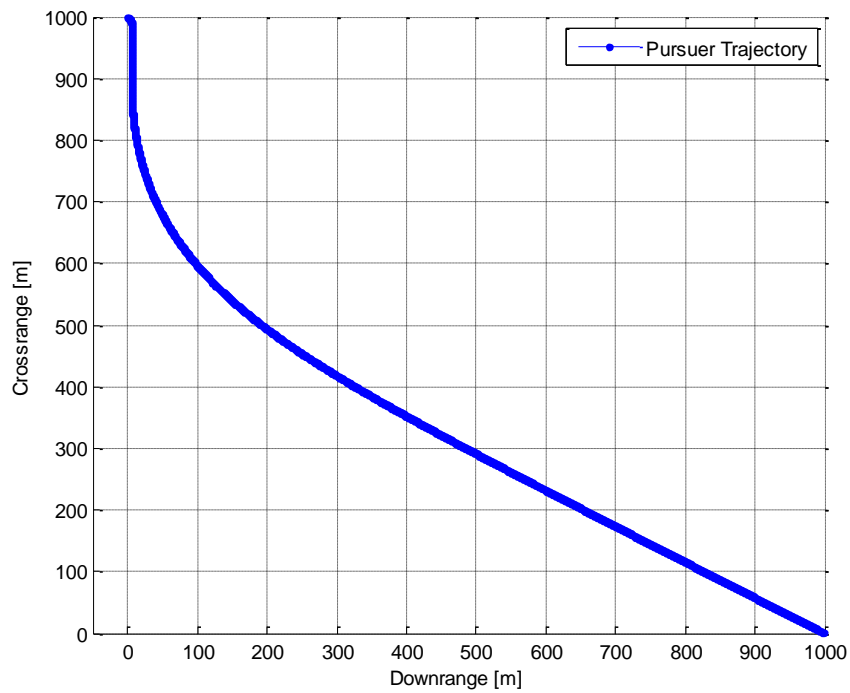


Figure 27. Pursuer Trajectory for Scenario 4

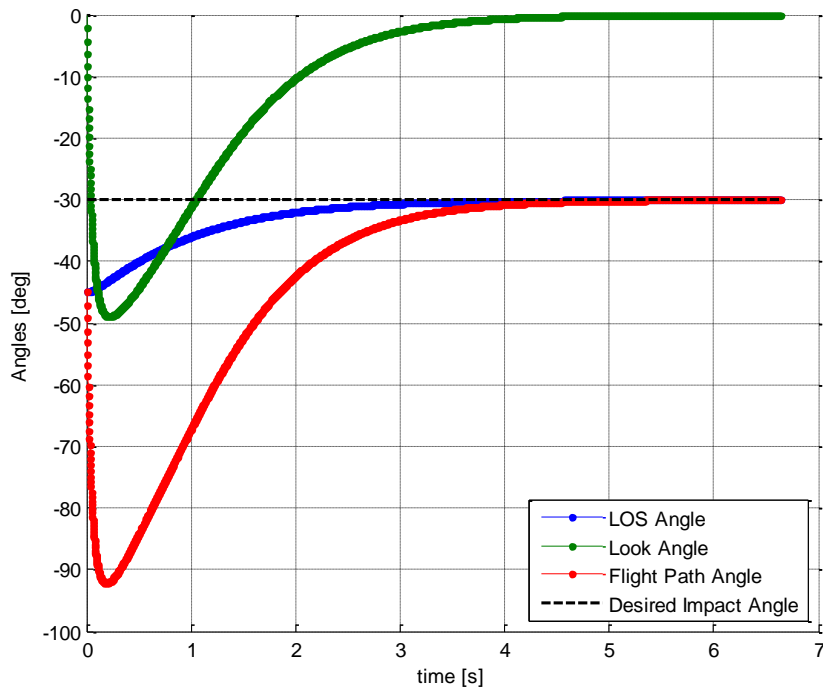


Figure 28. Important Angles in Scenario 4

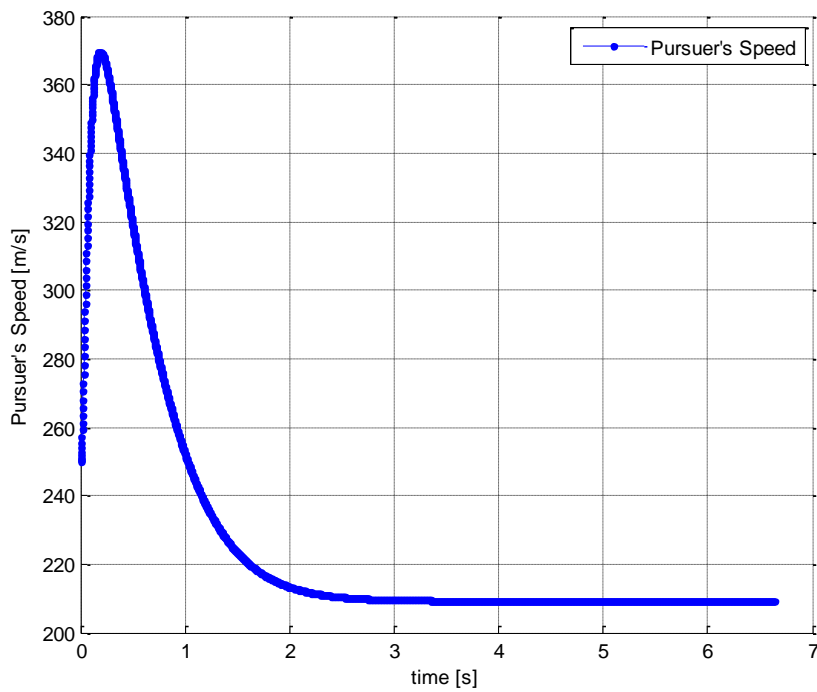


Figure 29. Pursuer Speed in Scenario 4

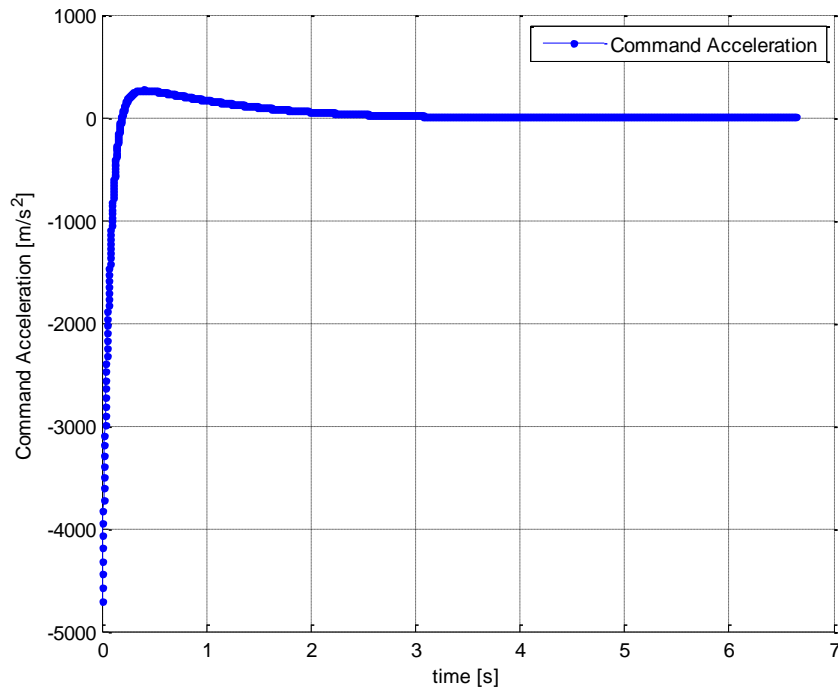


Figure 30. Guidance Commands in Scenario 4

The simulation results for scenario 5 can be seen figures from Figure 31 to Figure 34. The spatial trajectory of the pursuer is shown in Figure 31. Since the pursuer starts the flight with positive flight path angle, the acceleration commands become less than previous scenarios at the beginning of the flight. Moreover, the desired impact angle is higher than initial one, so pursuer should go above the target to achieve desired LOS angle. Initial flight path angle aids the guidance law and less guidance commands needed for the flight. The change in LOS, flight path and look angles can be seen in Figure 32. It can be seen from Figure 32, the initial look angle is near $\pi/2$ because of the positive flight path angle. Note that proposed guidance law operates in the look angle region of $(-\pi/2, \pi/2)$. Physically, as the look angle goes near $\pm\pi/2$, the closing velocity becomes zero and pursuer no longer proceed towards the target. This manner should be taken into consideration in launching conditions of pursuer.

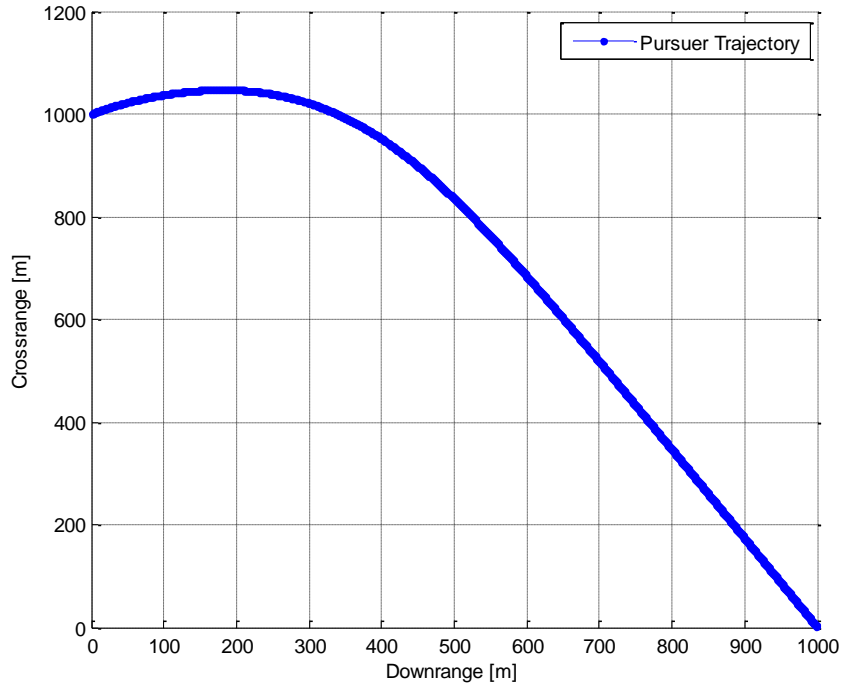


Figure 31. Pursuer Trajectory for Scenario 5

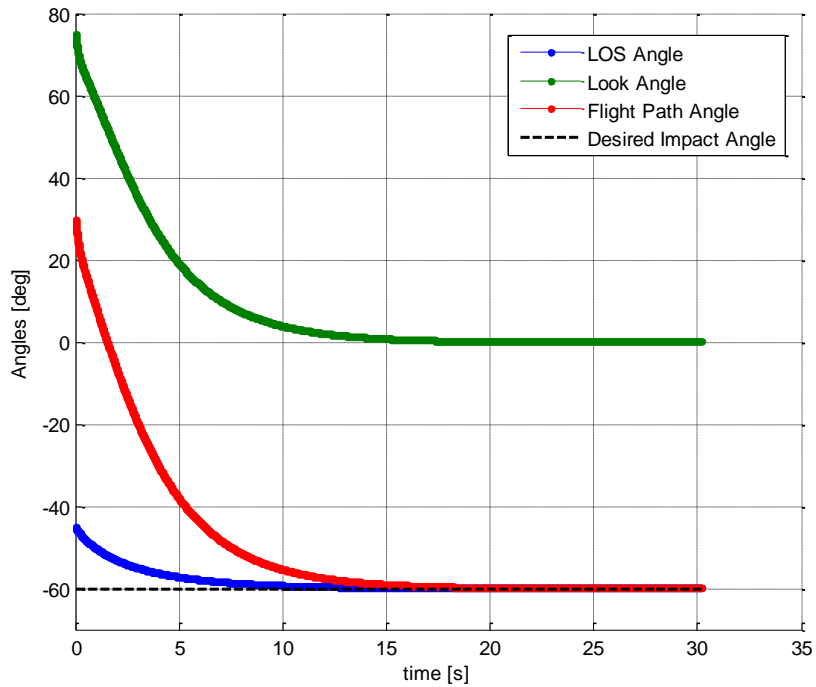


Figure 32. Important Angles in Scenario 5

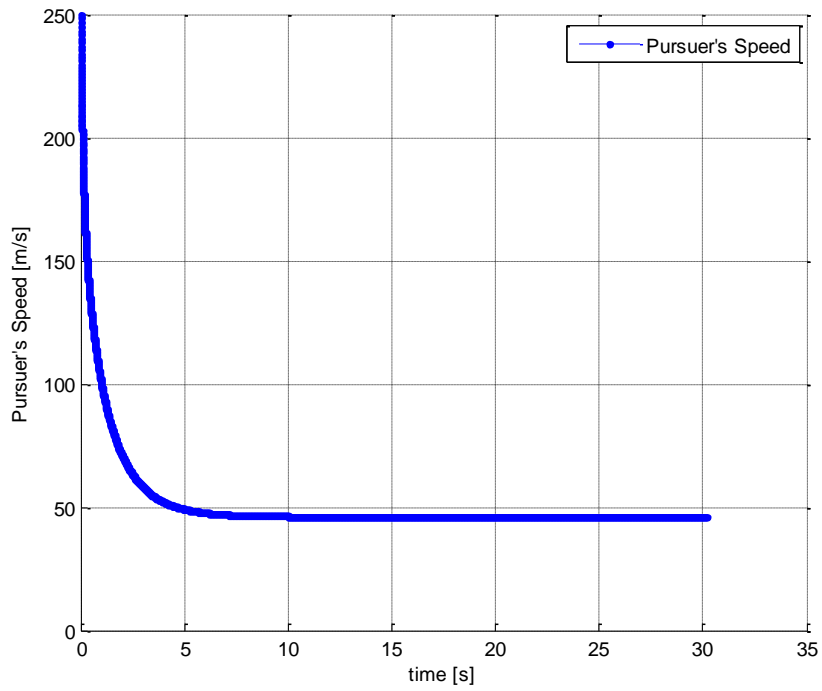


Figure 33. Pursuer Speed in Scenario 5

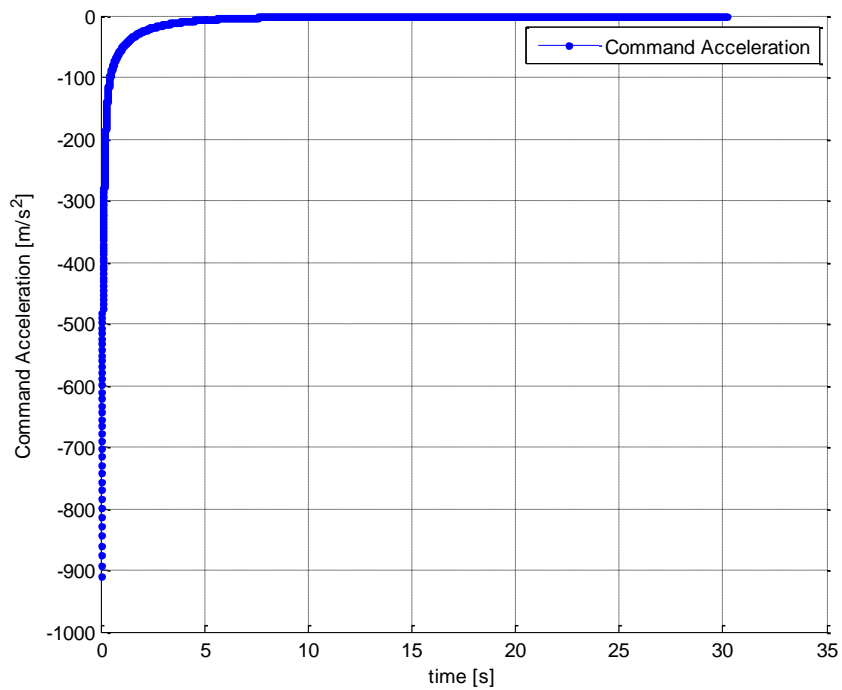


Figure 34. Guidance Commands in Scenario 5

The simulation results for scenario 6 can be seen figures from Figure 35 to Figure 38. The spatial trajectory of the pursuer is exhibited in Figure 35. The flight path, LOS and look angles of the pursuer-target geometry can be seen in Figure 36. Note that again for this scenario, the initial flight path angle is selected as positive. Thus, the desired impact angle or LOS angle is less then initial one. Because of that reason, pursuer makes a huge pull down maneuver to go below the target to satisfy impact angle criterion in the cost of huge negative acceleration commands. Since the acceleration commands of the pursuer is perpendicular to the range vector, the speed of the pursuer degrades too. The speed of the pursuer can be seen in Figure 37. The guidance commands is also shown in Figure 38.

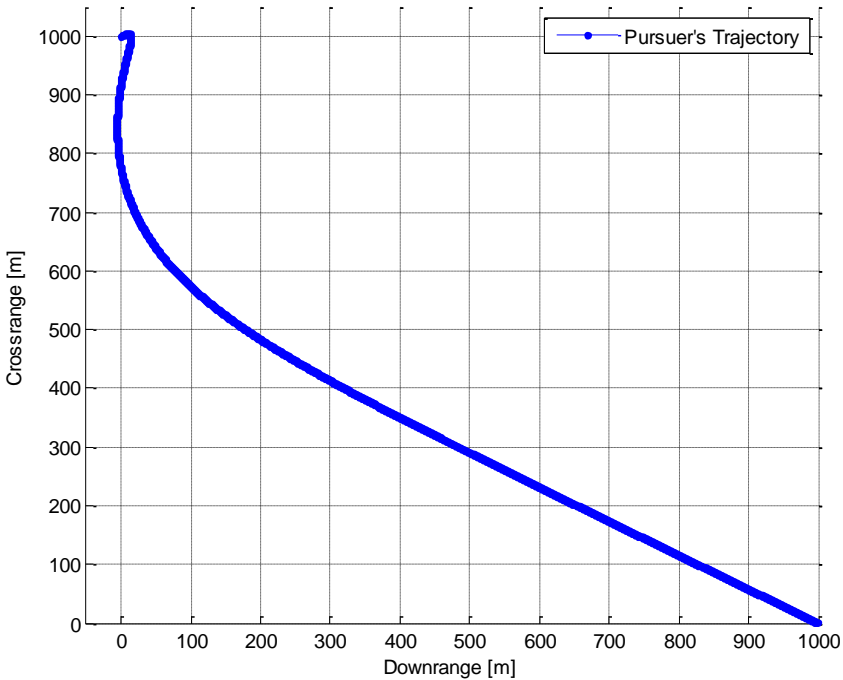


Figure 35. Pursuer Trajectory for Scenario 6

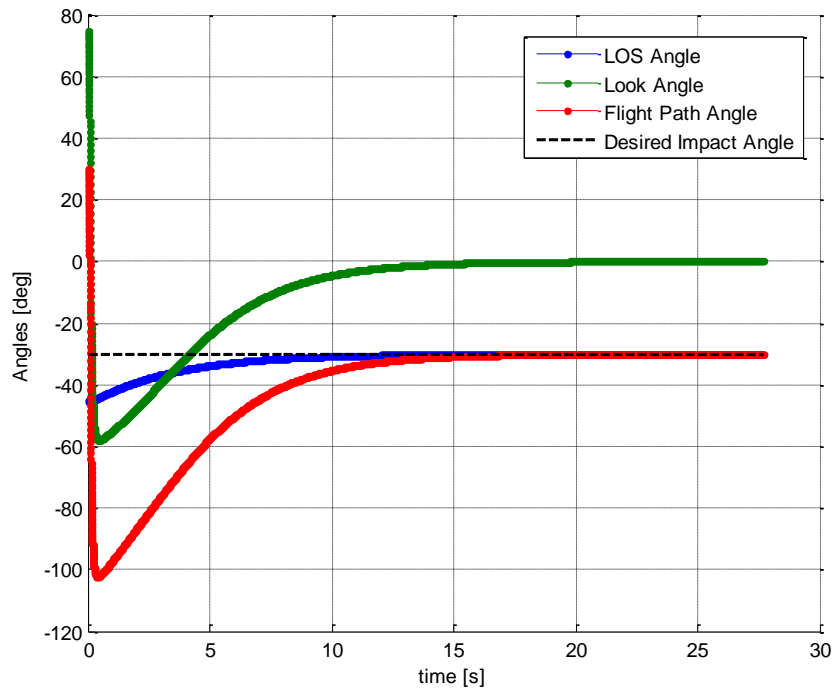


Figure 36. Important Angles in Scenario 6

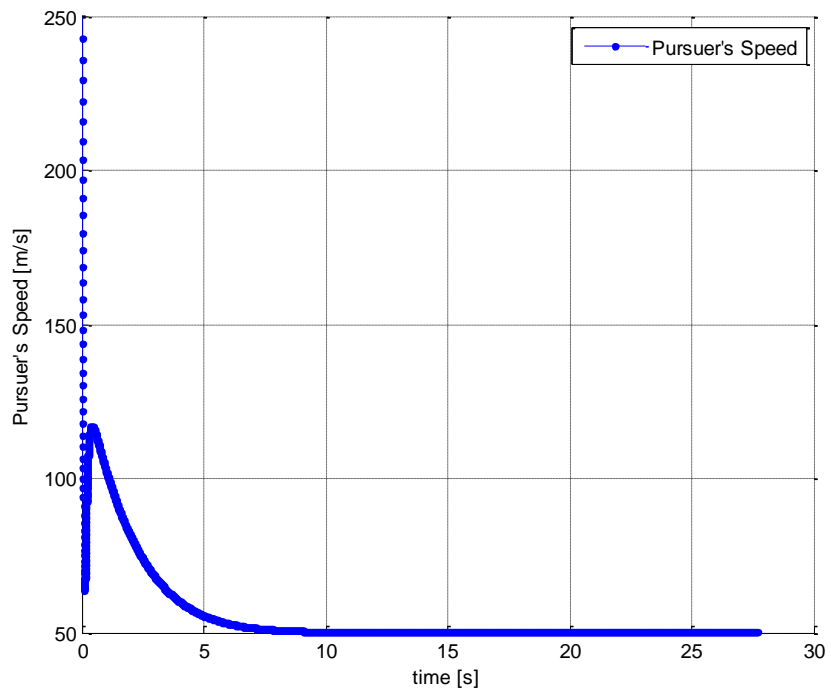


Figure 37. Pursuer Speed in Scenario 6

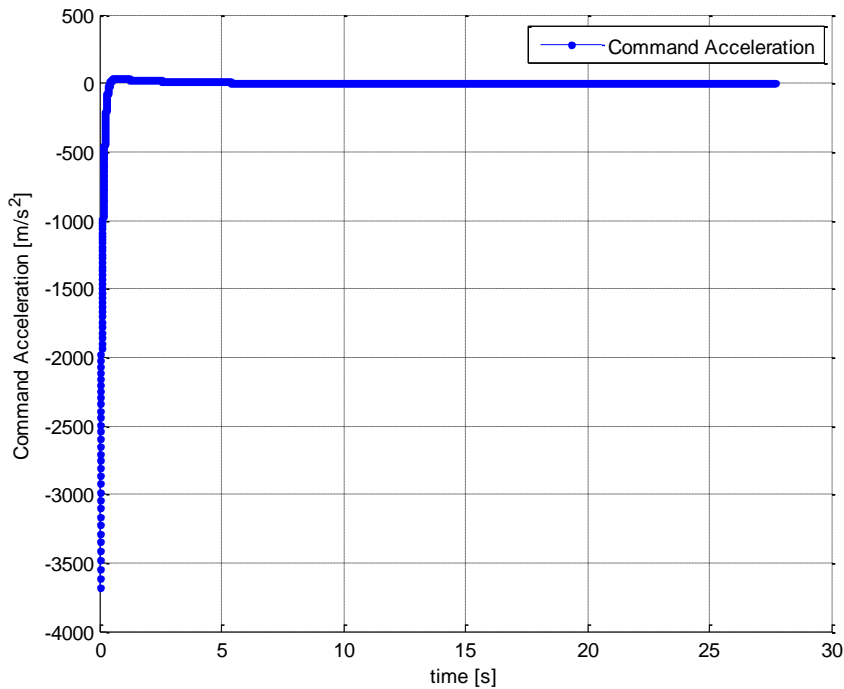


Figure 38. Guidance Commands in Scenario 6

The scenario 7 shows a ground-to-ground engagement geometry. The simulation results for this scenario can be seen figures from Figure 39 to Figure 42. The spatial trajectory of the pursuer can be seen in Figure 39. The target is again captured successfully. With the positive initial flight path angle, pursuer directly climb above the target to satisfy the desired LOS angle. The flight path angle, LOS angle and look angle can be seen in Figure 40. The initial LOS angle is near zero because of the ground-to-ground engagement scenario. However, from the controller-like characteristics of the proposed guidance law, LOS angle converges the desired one as the pursuer heads towards the target. In order to catch up this angle difference between instantaneous LOS angle and desired one, the massive acceleration commands –up to 350g– are needed. The guidance commands can be seen in Figure 42. Moreover, due to this severe acceleration, the speed of the pursuer decreases dramatically near zero. The speed of the pursuer can be seen in Figure 41.

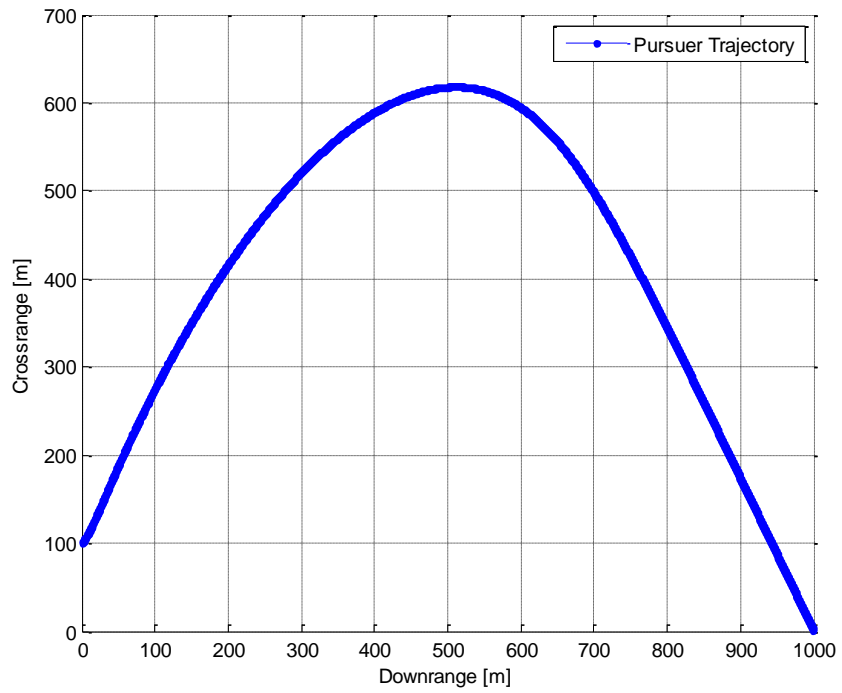


Figure 39. Pursuer Trajectory for Scenario 7

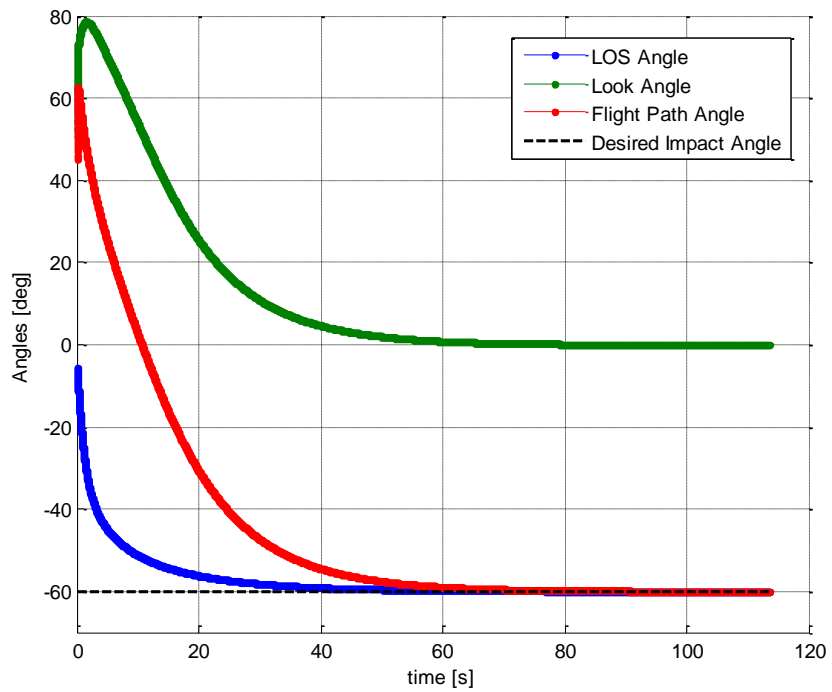


Figure 40. Important Angles in Scenario 7

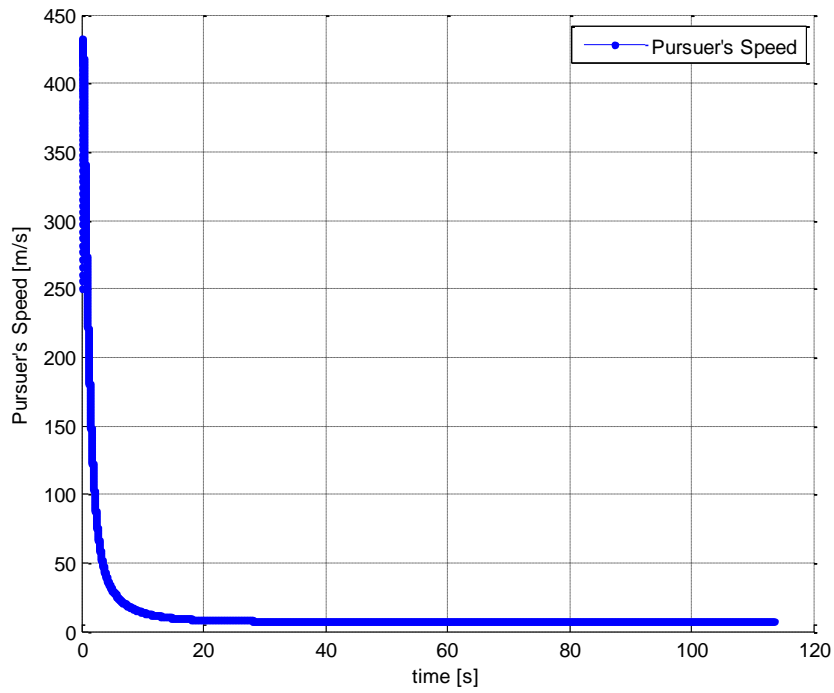


Figure 41. Pursuer Speed in Scenario 7

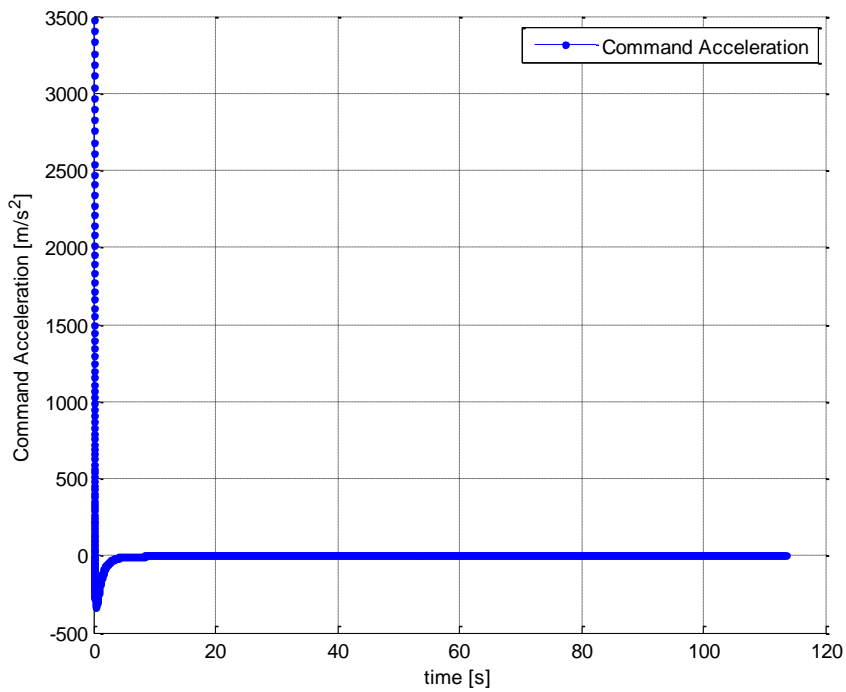


Figure 42. Guidance Commands in Scenario 7

The simulation results of the scenario 8 can be seen figures from Figure 43 to Figure 46. The smaller impact angle is needed in this scenario with again positive initial flight path angle. From that reason, the pursuer climbs less while heading towards the target to achieve impact angle criterion. The spatial trajectory of the pursuer can be seen in Figure 43. The important angles such as flight path angle, LOS angle and look angle are shown in Figure 44. It can be seen from Figure 44 that after a short period of time, the pursuer climbs above the target and flight path angle and look angle decrease towards the equilibrium. The necessary acceleration commands for that maneuver can be seen in Figure 46. The pull down maneuver decreases the pursuer speed as expected. However, the final impact speed is higher than previous ground-to-ground engagement geometry since the desired impact angle is smaller. The speed of the pursuer can be seen in Figure 45. Note that again the acceleration commands tends to go null long before impact time. This feature of the guidance law can grant robustness against counter-measures of the target and sensor errors in the feedback.

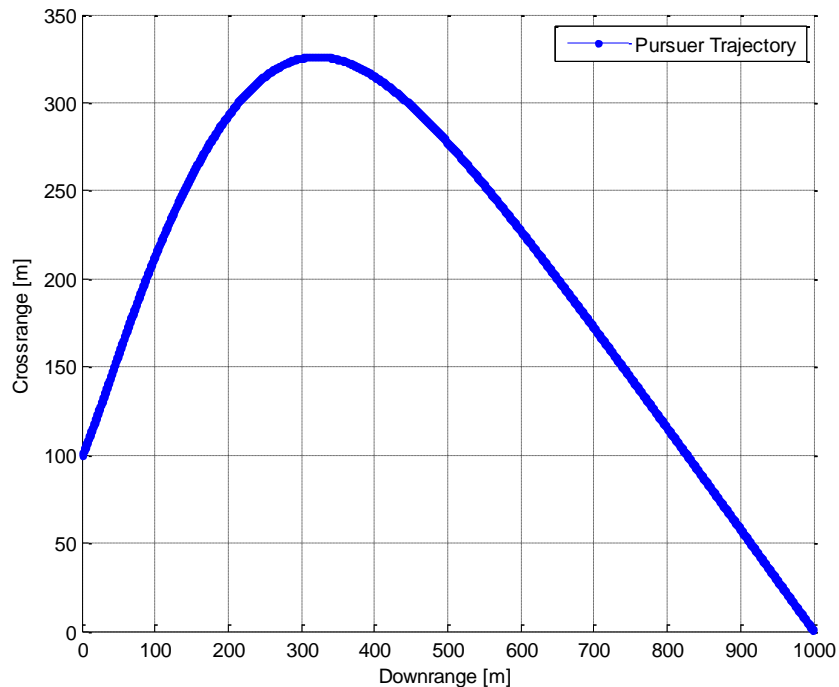


Figure 43. Pursuer Trajectory for Scenario 8

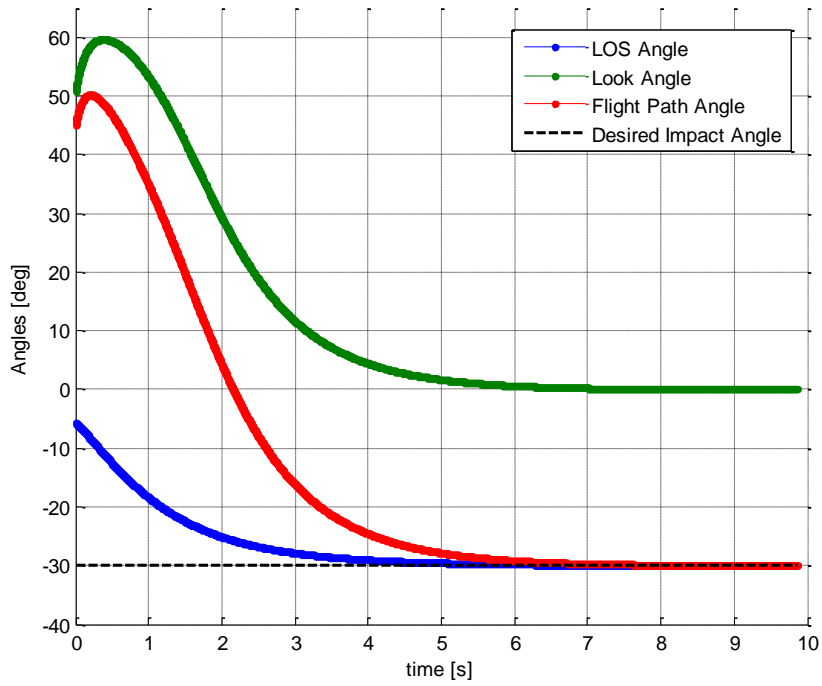


Figure 44. Important Angles in Scenario 8

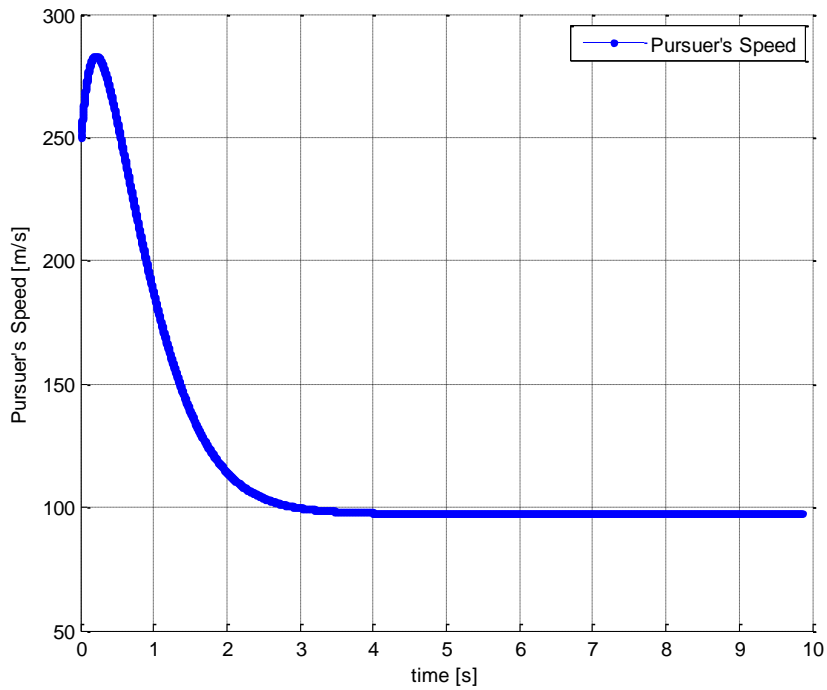


Figure 45. Pursuer Speed in Scenario 8

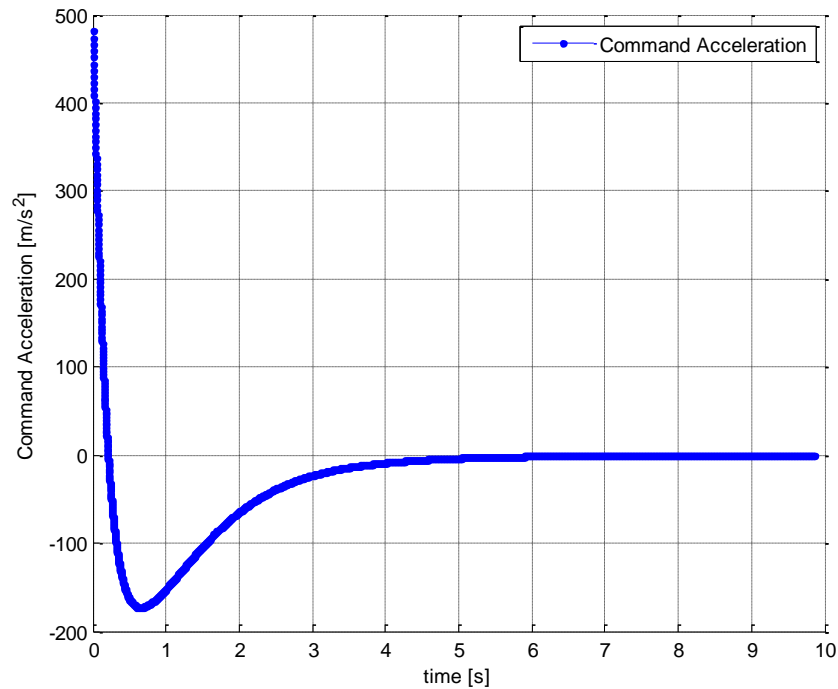


Figure 46. Guidance Commands in Scenario 8

The simulation results for scenario 9 can be seen in figures from Figure 47 to Figure 50. The spatial trajectory of the pursuer is shown in Figure 47. The initial flight path angle is set to be zero in this scenario to investigate the behaviour of the guidance law in horizontal launch ground-to-ground engagement. The target is again successfully captured for this scenario. The flight path angle, LOS angle and look angle of the pursuer-target dynamical system can be seen in Figure 48. Similar to the scenario 7, the pursuer climbs above the target to satisfy the impact angle. However, due to null initial flight path angle, the pursuer climbs less while heading to target since the range value between target and pursuer is less than previous. The acceleration commands can be seen in Figure 50. The commanded accelerations increases since the pursuer launched horizontally. Moreover, the speed of the pursuer can be seen in Figure 49.

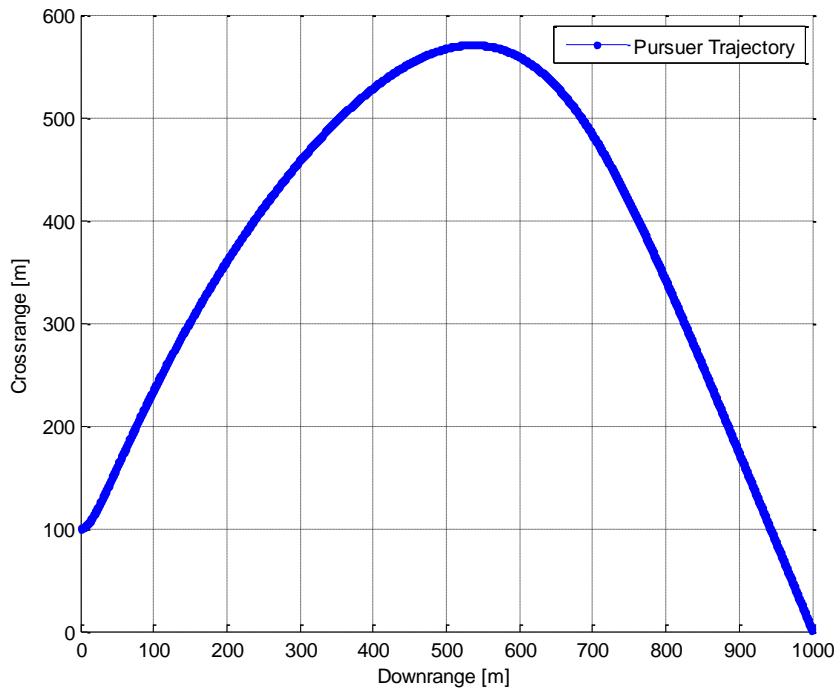


Figure 47. Pursuer Trajectory for Scenario 9

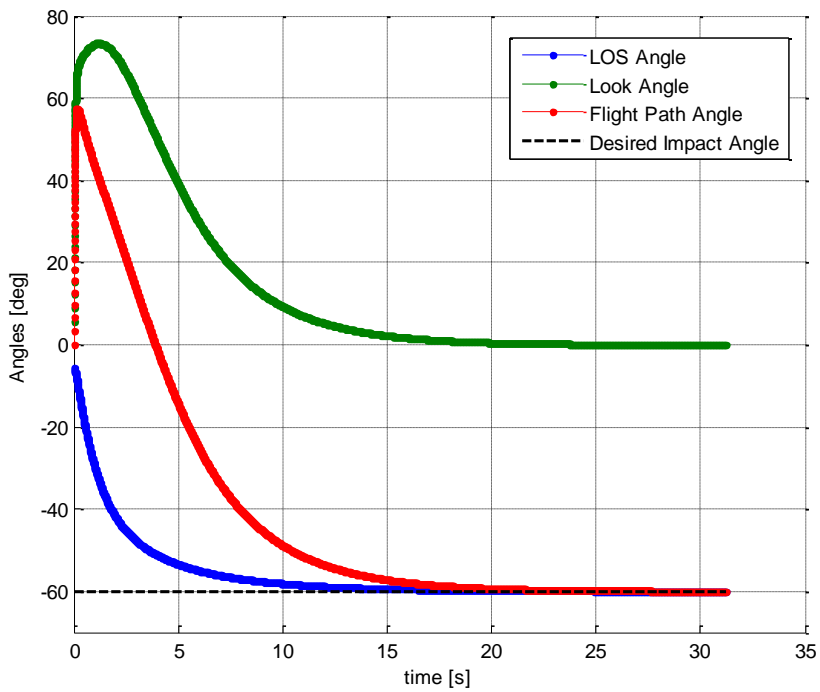


Figure 48. Important Angles in Scenario 9

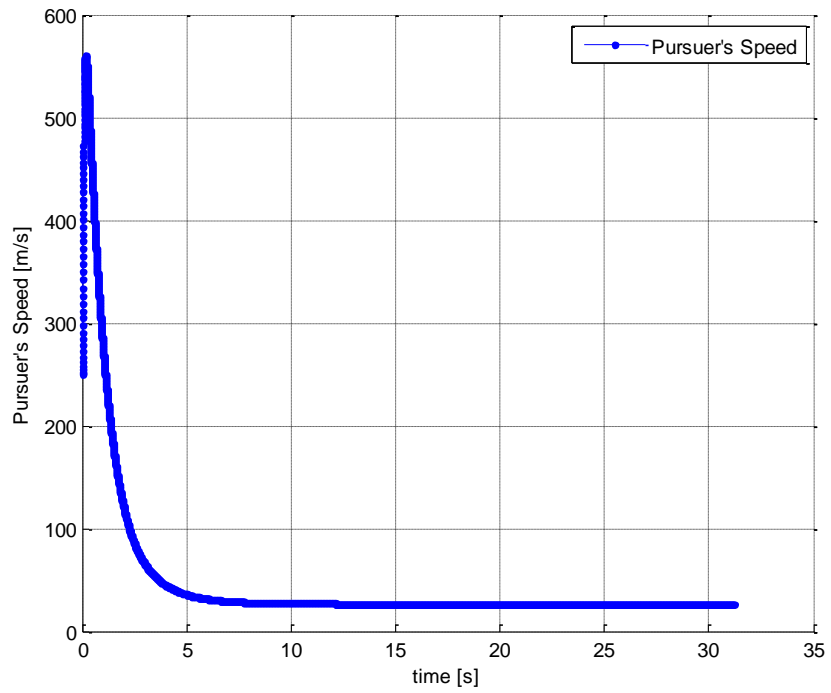


Figure 49. Pursuer Speed in Scenario 9

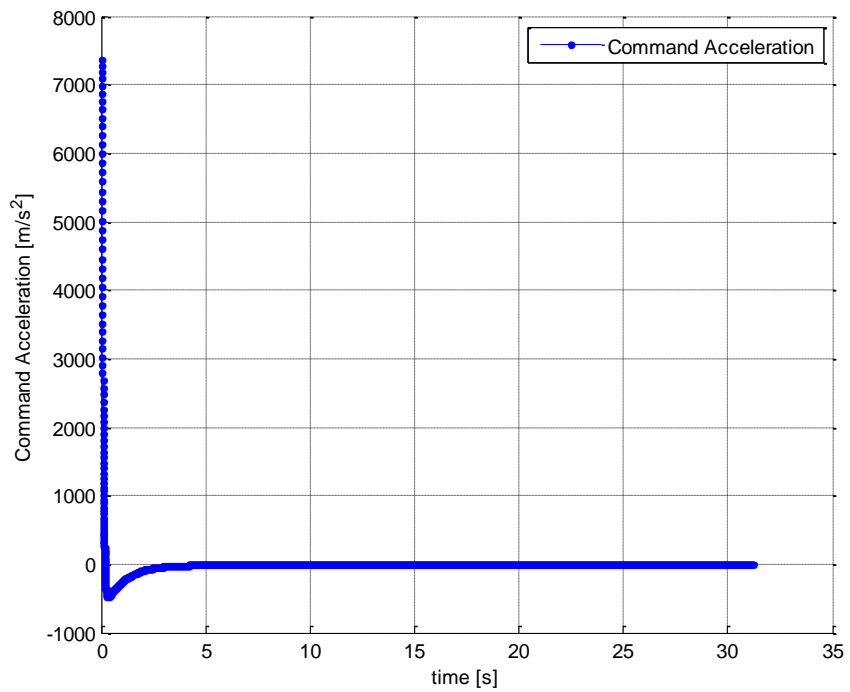


Figure 50. Guidance Commands in Scenario 9

The simulation results for the last scenario can be seen in figures from Figure 51 to Figure 54. The spatial trajectory of the pursuer can be observed in Figure 51. The flight path angle, LOS angle and look angle of the pursuer-target dynamics are demonstrated in Figure 52. Since the pursuer is launched with zero flight path angle and desired LOS angle is less than the one in previous scenario, less altitude is required to satisfy the impact angle constraint. Hence, the less acceleration commands are needed to capture the target. The acceleration commands perpendicular to the range vector is shown in Figure 54. The speed of the pursuer is also shown in Figure 53.

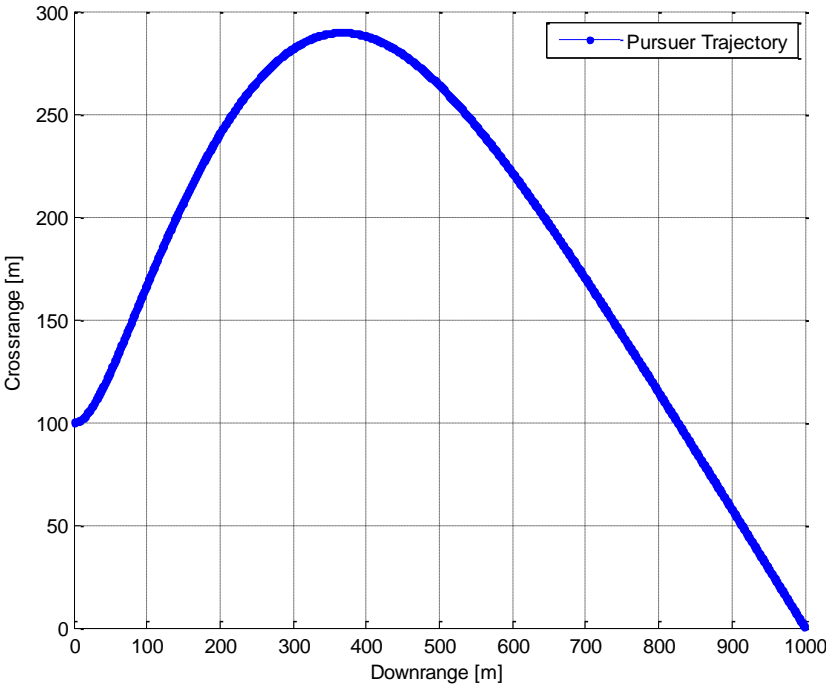


Figure 51. Pursuer Trajectory for Scenario 10

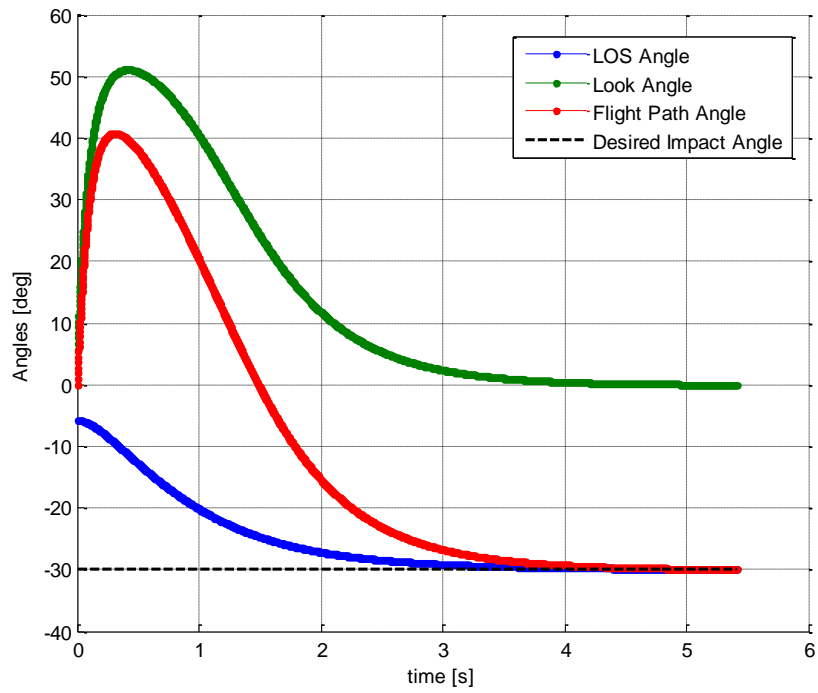


Figure 52. Important Angles in Scenario 10

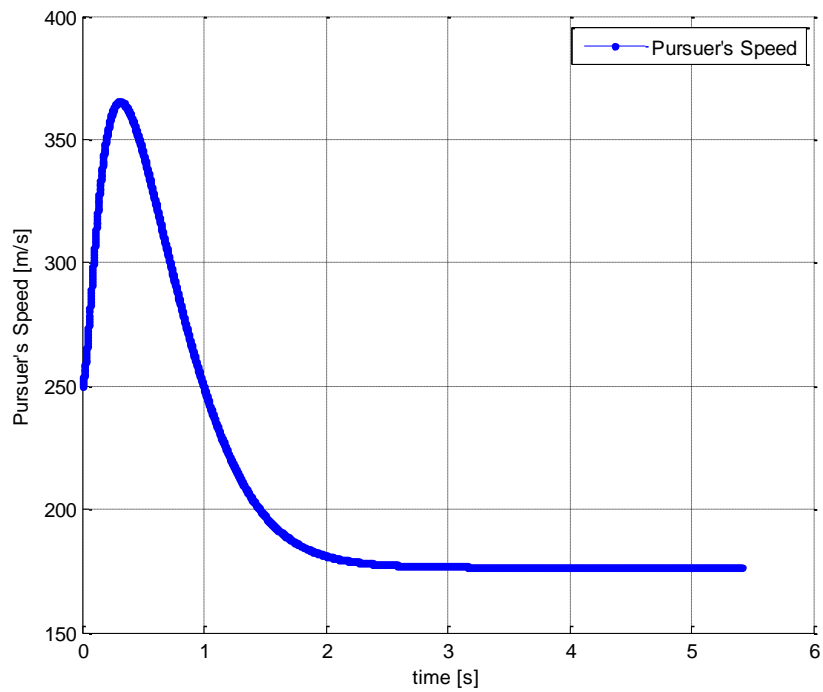


Figure 53. Pursuer Speed in Scenario 10

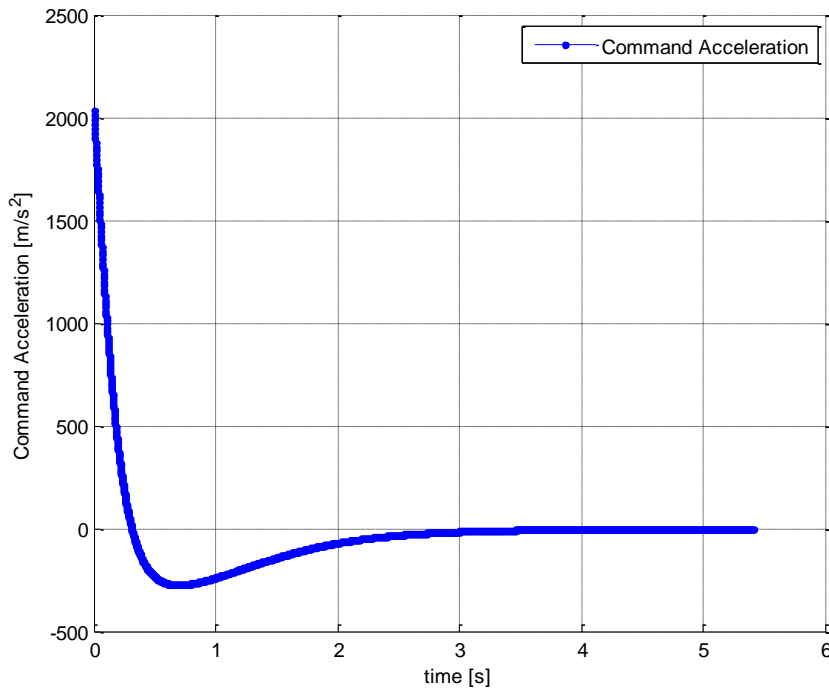


Figure 54. Guidance Commands in Scenario 10

4.3 Successful Mission Criteria

To test the proposed guidance law against system lag and disturbances in simulation environment, a nominal scenario is selected. Then, for that scenario, a reasonable successful mission criterion needs to be defined. In testing robustness and/or disturbance rejection behaviors of the proposed guidance law numerically; the error between desired and actual impact angle, LOS angle and look angle are required to be evaluated. Moreover, the final range value between target and pursuer must also be lower than 0.1 meters for successfully capturing the target.

Various engagement geometries are tried in ideal scenarios in section 4.2. In the light of this information, it can be said that the proposed guidance law is more practical for air-to-ground engagement geometries, since the required acceleration commands are relatively smaller in air-to-ground engagements and speed of the pursuer does not

decrease severely. Thus, the nominal scenarios are selected as ideal scenario #1 and listed in Table 2 as follows.

Table 2. Nominal Test Scenario

| Initial Pursuer Position [m] | Target Position [m] | Pursuer Velocity [m/s] | Initial Flight Path Angle [deg] | Desired Impact Angle [deg] |
|-------------------------------------|----------------------------|-------------------------------|--|-----------------------------------|
| (0,1000) | (1000,0) | 250 | 0 | 60 |

After selecting the nominal test scenario, the criteria in important angles such as LOS angle, LOS rate, flight path angle and look angle are also considered. The successful mission criteria for pursuer are listed in Table 3.

Table 3. Successful Mission Criteria

| | LOS Angle | Flight Path Angle | Look Angle | LOS Rate |
|--------------------------|------------------|--------------------------|-------------------|-----------------|
| Absolute Error in | 0.5 deg | 0.5 deg | 0.5 deg | 0.1 deg/s |

The error of LOS angle and flight path angle in final rendezvous is set as ± 0.5 degree deviation from desired value. The desired value for LOS angle and Flight Path angle is same as desired impact angle for stationary target as noted in Table 2. The look angle should go zero at the impact time. Thus, the acceptable region for successful mission is also selected as 0.5 degree for look angle. Furthermore, the acceptable region for LOS rate is chosen as 0.1 degree per second. Thus, the final LOS rate should not exceed ± 0.1 deg/s. Finally, the range between target and pursuer at the final rendezvous cannot exceed 0.1 meters as mentioned before.

4.4 Variation of Guidance Constant K

The guidance constant K is another variable in behavior of the guidance law. In order to see the effect of constant K on acceleration commands, trajectory and on LOS controlling, simulations are performed. The nominal test scenario is selected and

guidance constant K is increased from 1 to 10 consecutively. The other parameters in sliding surfaces remain same since the concern is merely on guidance constant. The nominal test scenario in this section runs in ideal case environment which system has no delay, disturbance and limitations.

The spatial trajectories of the pursuer can be seen in Figure 55. It can be seen that as the constant K increases, the trajectories tends to converge logarithmically a single one. That's because when the error in LOS angle is zero, the trajectory becomes straight line. Furthermore, when K decreases, the precision in controlling LOS angle also decreases. LOS angle deviation with constant K can be seen in Figure 56. The variation on K also affects the guidance commands acting on pursuer. The variation of acceleration commands can be observed from Figure 59. The severe acceleration commands tends to decrease as K decreases, from that reason the speed of the pursuer also varies and can be seen in Figure 60.

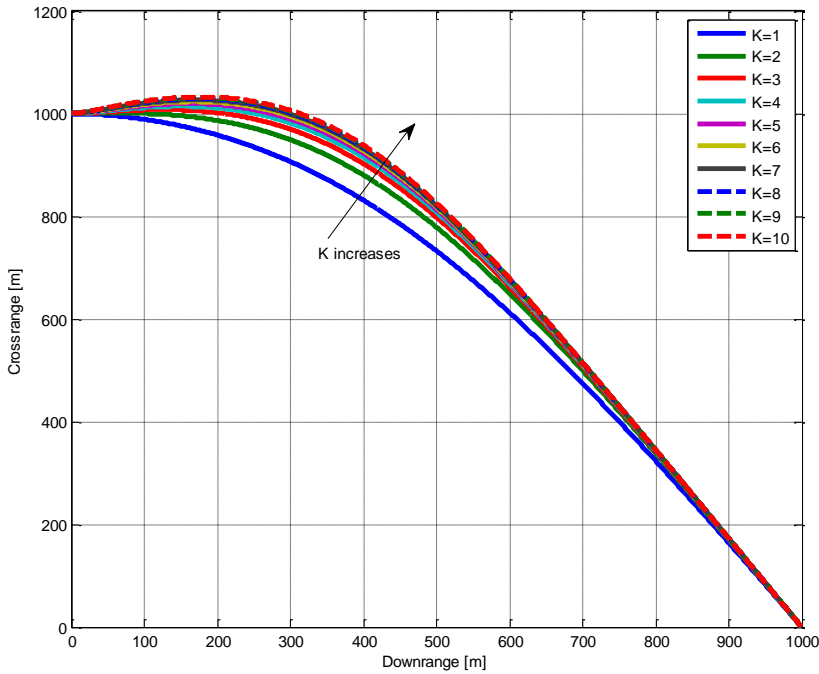


Figure 55. Spatial Trajectories of the pursuer with varying K

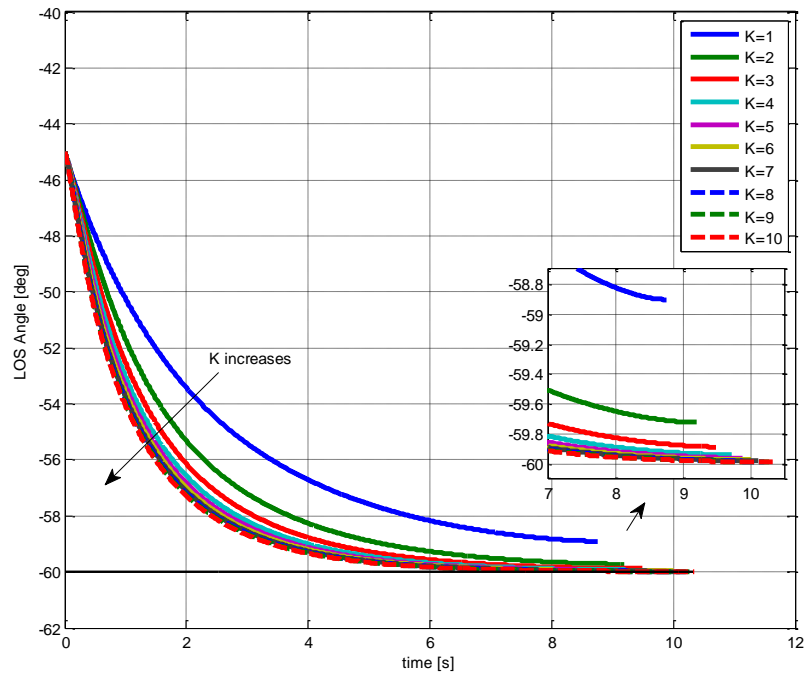


Figure 56. LOS Angle between pursuer and target for varying K

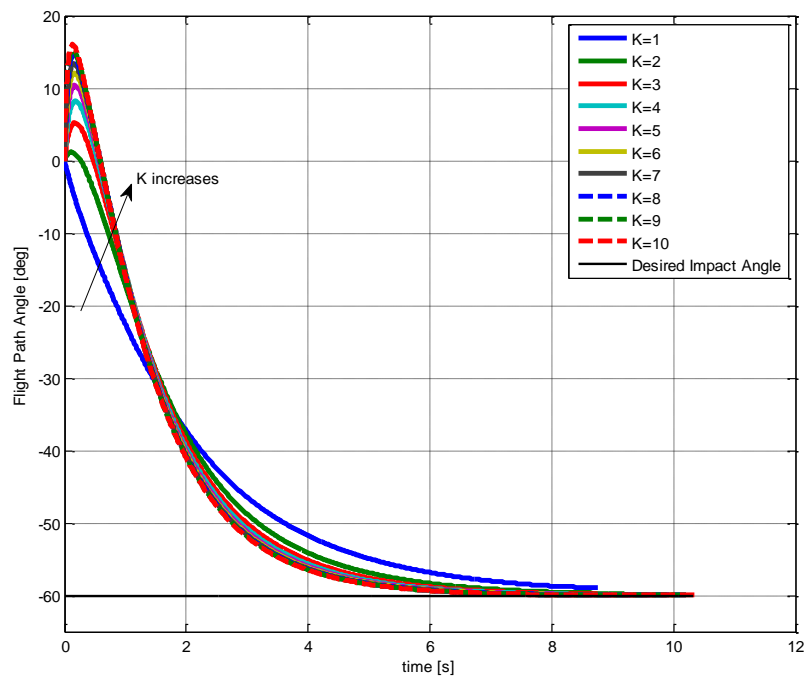


Figure 57. Flight Path Angle of Pursuer with varying K

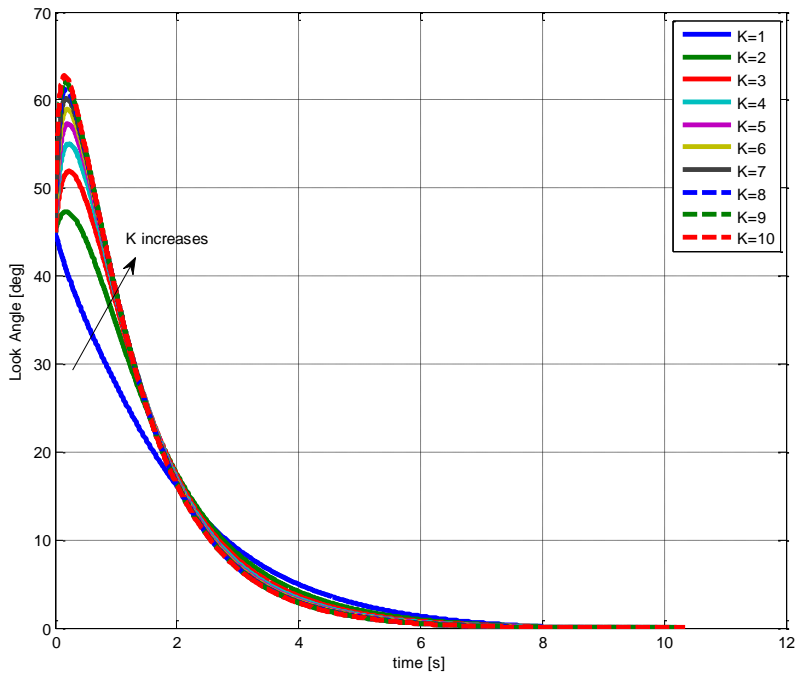


Figure 58. Look Angle of Pursuer with varying K

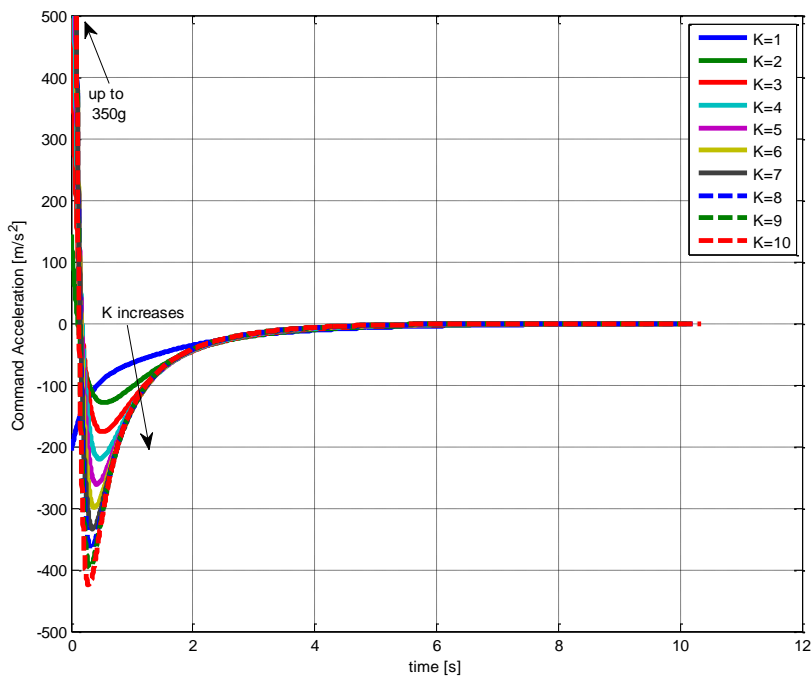


Figure 59. Command Acceleration of Pursuer with varying K

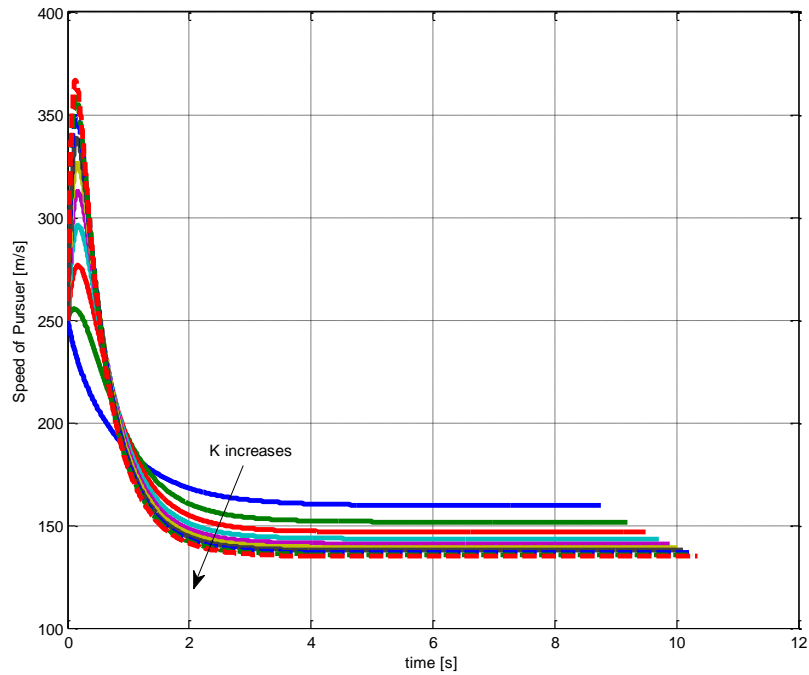


Figure 60. Speed of the Pursuer with varying K

It can be observed that the elapsed time for closing LOS angle error decreases when the guidance constant K increases. This classical-controller-like behavior of the proposed guidance law makes sense since time derivative of the Lyapunov function becomes large and system converges the desired sliding manifold faster with higher values of K . However, the acceleration commands are directly amplified by guidance constant K and required acceleration commands are also getting higher for high values of K . Furthermore, the constant K multiplies directly with the LOS angle and angular rate. Thus, if this sensed information has any disturbances, not only state equations of the nonlinear system are disrupted, but also guidance commands directly amplified by that disturbance.

To conclude that the guidance constant K should be tuned by guidance engineer with respect to mission requirements. Although low values of K requires reasonable acceleration demands and can grant some robustness against disturbances, precision

on impact angle loosen. On the other side, high K values can provide precise impact angles, but the system is expected to become less robust against disturbances. This trade-off should be made concerning the area of expertise.

4.5 Numerical Robustness and Disturbance Rejection Analyses

For testing robustness and disturbance rejection characteristics, numerical analyses are done for nominal scenario which is selected in section 4.3. Disruptive effect of the gravitational acceleration is investigated. Then, the system lag is introduced to ideal system. Next, the limitation on pursuer model is examined. After that, the effects of some sensor error and bias on proposed guidance law are shown. Finally, the behavior of the guidance law for moving targets is investigated. First, gravitational acceleration is taken into account as -9.81 m/s^2 in z-direction on inertial frame. Note that the guidance gain K stay same as 10 for this analysis.

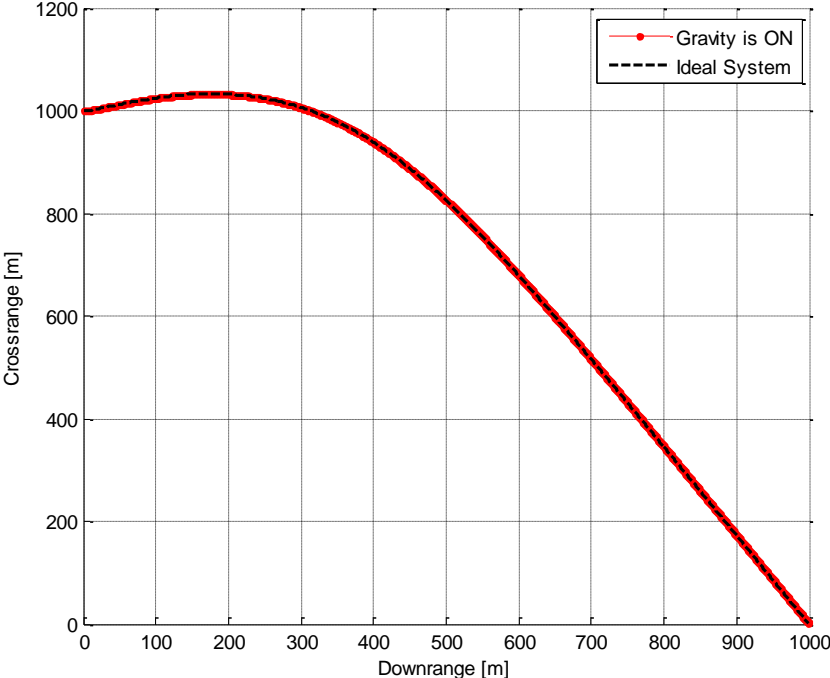


Figure 61. Spatial Trajectory of the Pursuer with gravitational acceleration

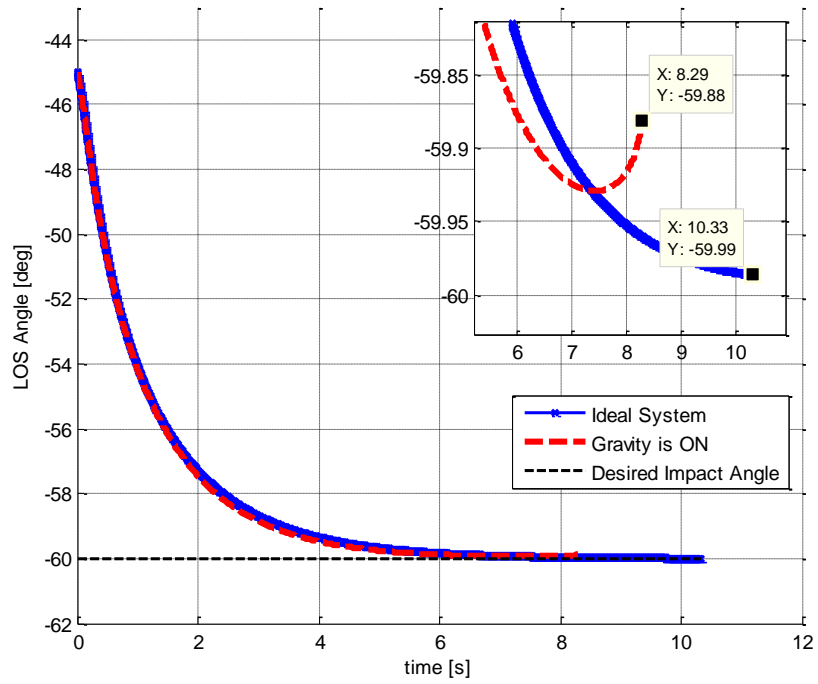


Figure 62. Line-of-Sight Angle with gravitational acceleration

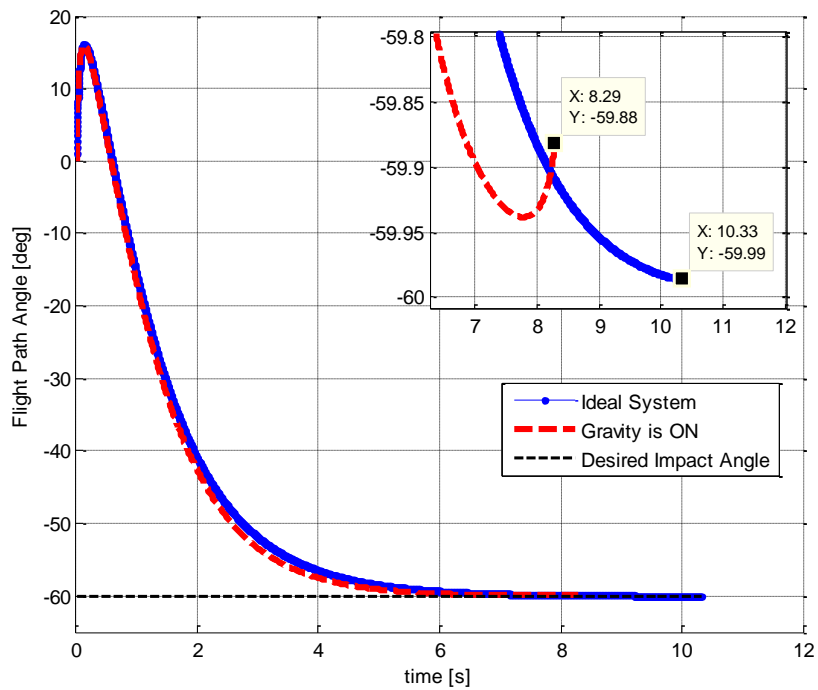


Figure 63. Flight path angle of the pursuer with gravitational acceleration

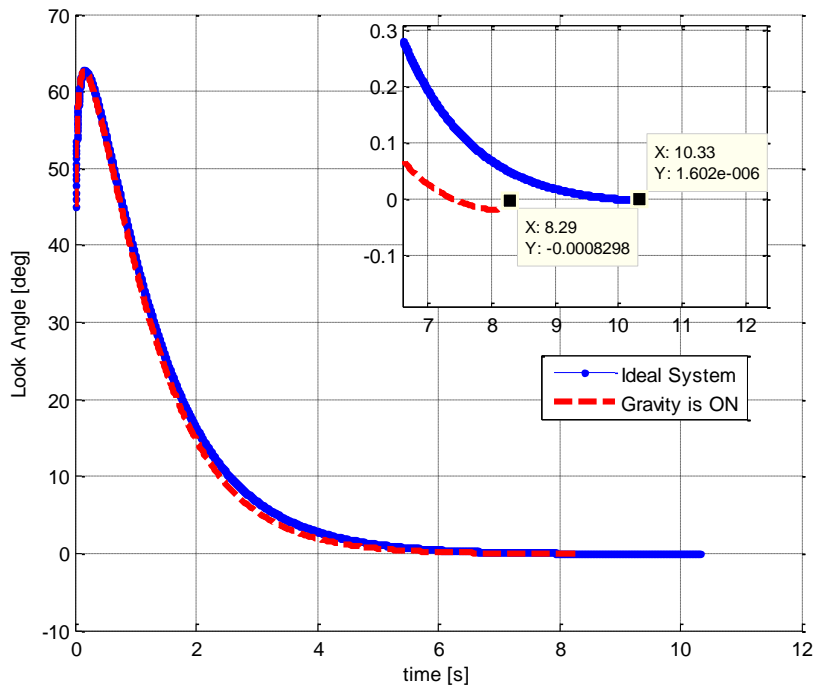


Figure 64. Look Angle of the pursuer with gravitational acceleration

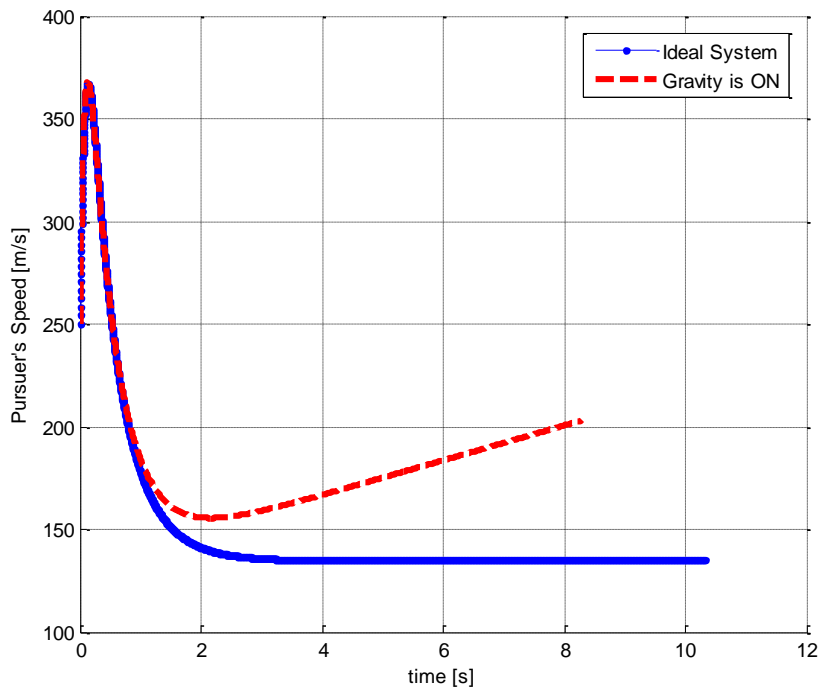


Figure 65. Speed of the pursuer with gravitational acceleration

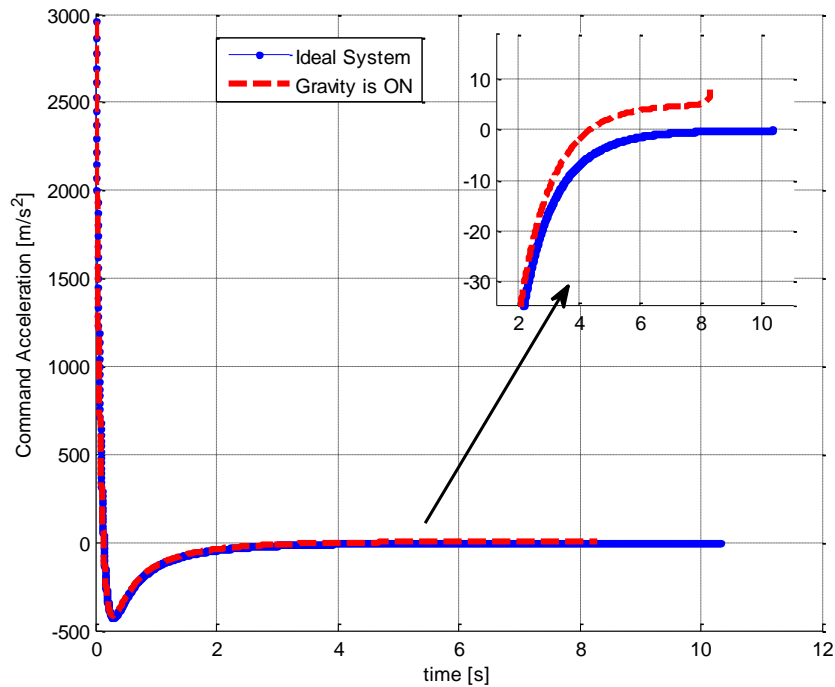


Figure 66. Command Acceleration of Pursuer with gravitational acceleration

The simulation results for effects of gravitational acceleration on proposed guidance law can be observed from Figure 61 to Figure 66. As it can be seen from figures, the successful mission criteria for LOS angle, flight path angle and look angle is satisfied and target is also successfully captured. The speed of the pursuer can be seen in Figure 65. It can be seen from figure that due to gravitational acceleration, the speed of the pursuer is increasing unlike ideal system. Thus, the impact speed of the pursuer is higher. The guidance commands of the pursuer is shown in Figure 66 for both ideal and gravitation accelerating system. Note that, the gravitation acceleration is compensated without subtracting gravity from guidance commands. This feature is provided from controlling closed-loop pursuer-target dynamical system. The gravity compensation is not needed for proposed guidance law, since the guidance law tries to control dynamical system in closed-loop. Thus, it can be seen from Figure 66 that the acceleration commands go constant gravity compensating value for acceleration at the near impact time.

Next, effects of having a first order dynamics in pursuer model on proposed guidance law is investigated through numerical analysis. The time constants for first order dynamical system are chosen as 0.1, 0.2, 0.4 and 0.8s respectively. For this analysis guidance constant K is reduced because the value of the guidance constant K determines how aggressively control inputs forces the system to stability. For that reason, guidance constant K is reduced as 3 concerning robustness against system lag and control effort of the pursuer.

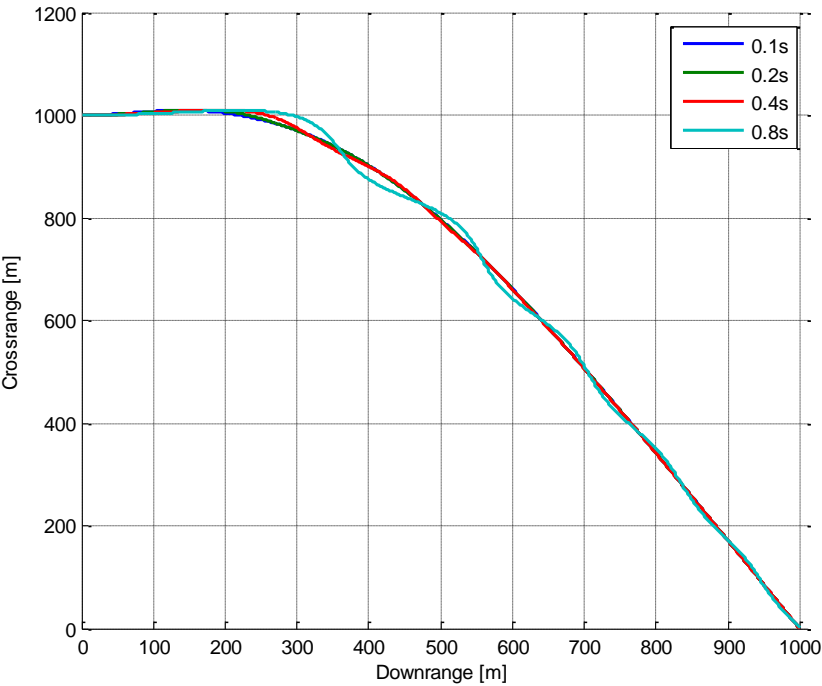


Figure 67. Spatial Trajectories of pursuer with first order dynamics

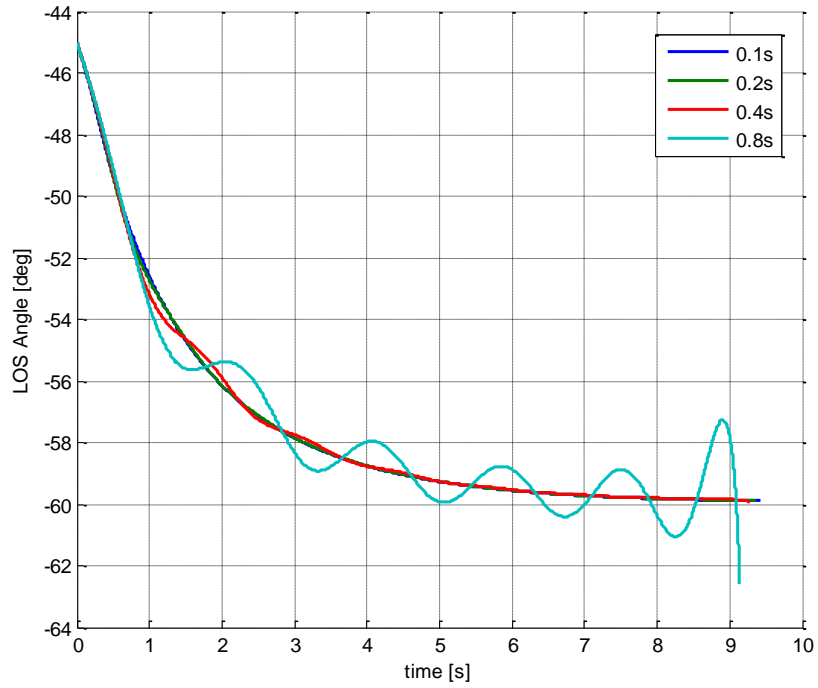


Figure 68. LOS Angles with pursuer having first order dynamics

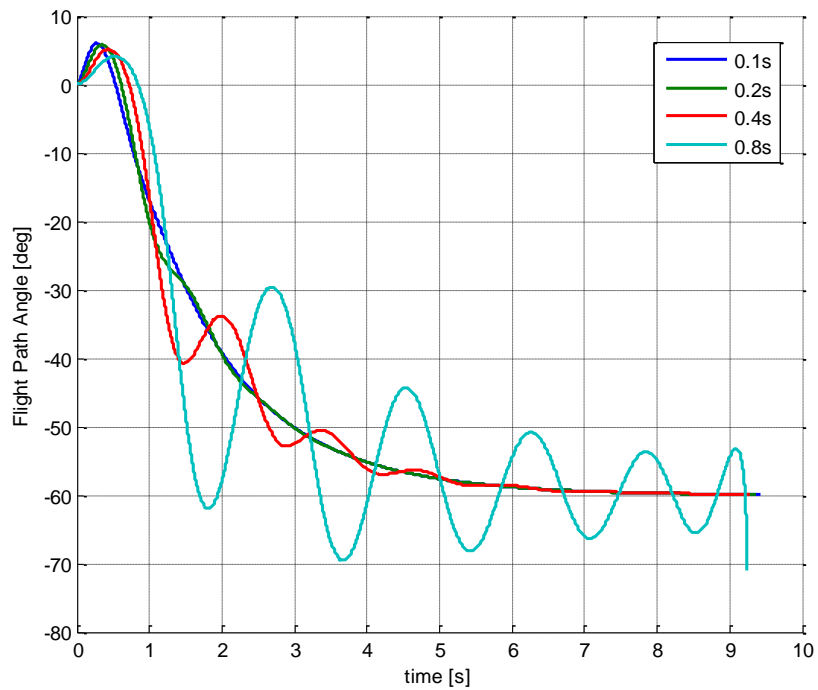


Figure 69. Flight Path Angle with pursuer having first order dynamics

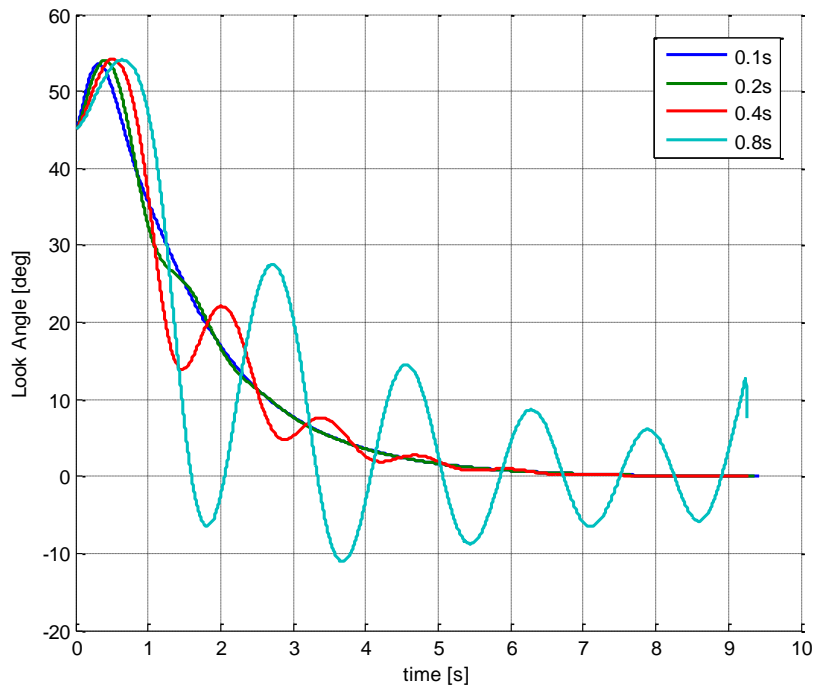


Figure 70. Look Angle with pursuer having first order dynamics

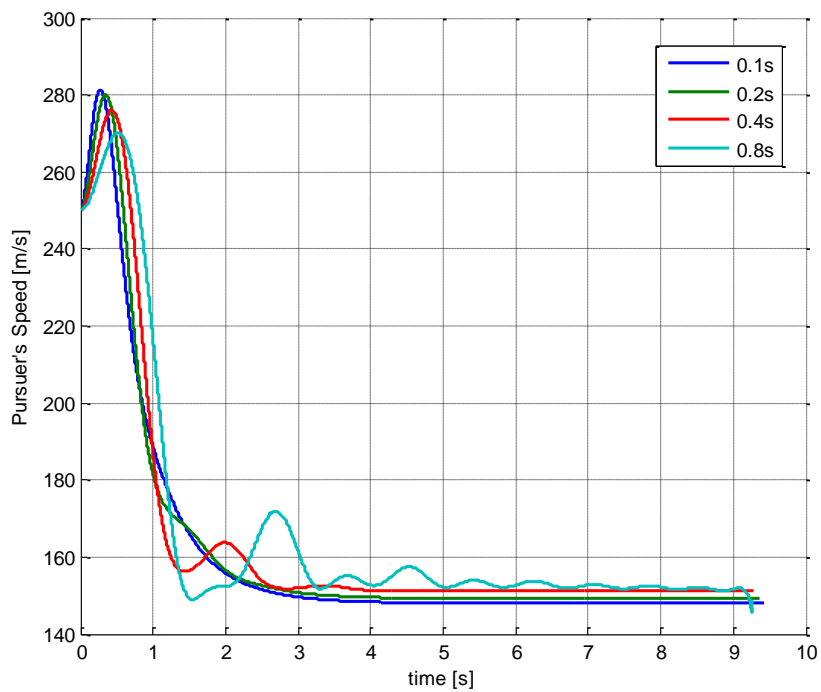


Figure 71. Speed of the pursuer with first order dynamics

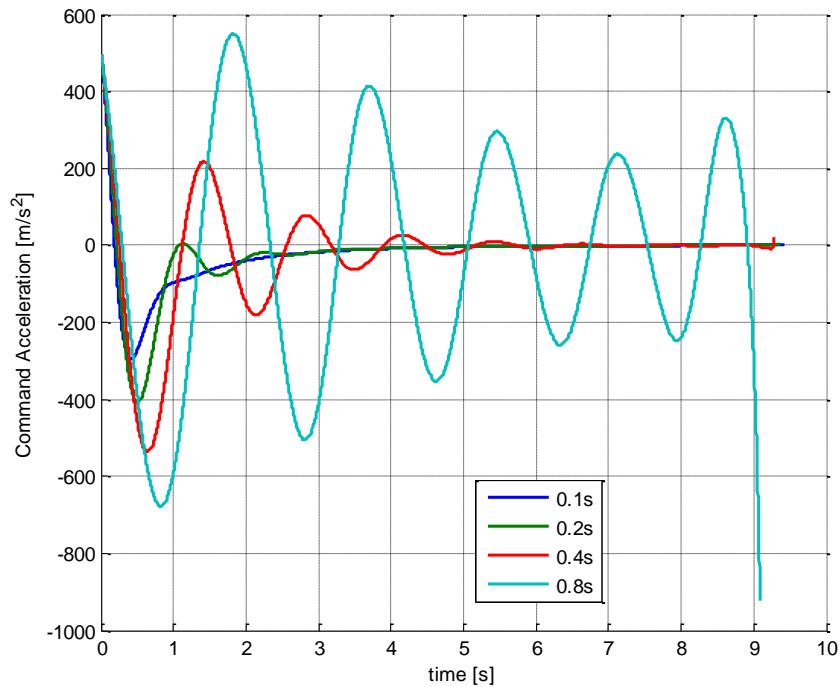


Figure 72. Command Acceleration on pursuer with first order dynamics

The simulation results for pursuer having first order dynamics with various time constants are presented in figures from Figure 67 to Figure 72. The spatial trajectories of the pursuer show that target is successfully captured for all cases. However, in last case, successful mission criteria are not satisfied. LOS angles for various time constants can be seen in Figure 68. It can be observed that delay in acceleration commands can affect closed-loop systems response. The slower dynamics can cause oscillations in actualizing guidance commands and indirectly unstable LOS dynamics. The speed of pursuer and acceleration commands can be seen in Figure 71 and Figure 72. As pursuer oscillates around the equilibrium subspace, the speed of the pursuer also changes due to that oscillatory accelerations perpendicular to range vector. It can be observed from figures Figure 68, Figure 69 and Figure 70 that in order to satisfy the successful mission criteria, the pursuer's dynamics time constant can not be higher than 0.5s. In other words, the bandwidth of the pursuer should be higher than approximately 0.3 Hz for successful mission.

Next, the proposed guidance law is tested under limitation. The common primary limitation in practical applications is generally on pursuer acceleration. The high accelerations can cause higher angle of attacks for pursuer which should be limited for autopilot accuracy and control surface mechanical limits. Thus, the proposed guidance law is tested for limitation on acceleration commands perpendicular to range vector. The system has also first order dynamics with 0.2 s time constant and gravitational acceleration to simulate “*real world-like*” behaviour of the system[§]. The guidance constant is chosen similarly as 3 and the acceleration limits of the pursuer is chosen as $10g's$ ($\sim 98.1m/s^2$).

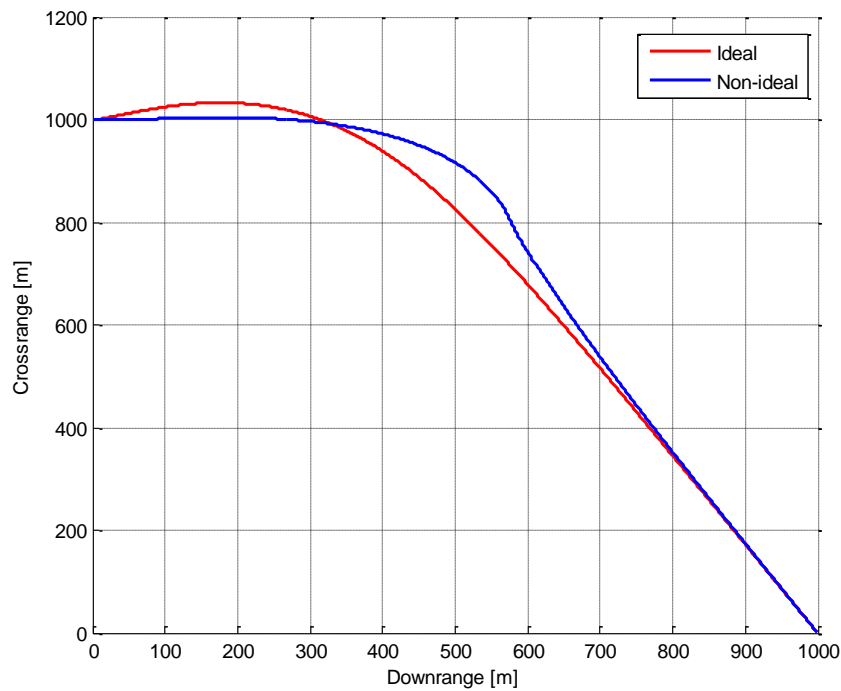


Figure 73. Spatial Trajectory of Pursuer with system lag and limitations

[§] It's convenient to state that the scenarios presented here are produced artificially to show and compare proposed guidance law performance. The results can vary for real systems in practical applications. In other words, there is no claim about being realistic in simulations.

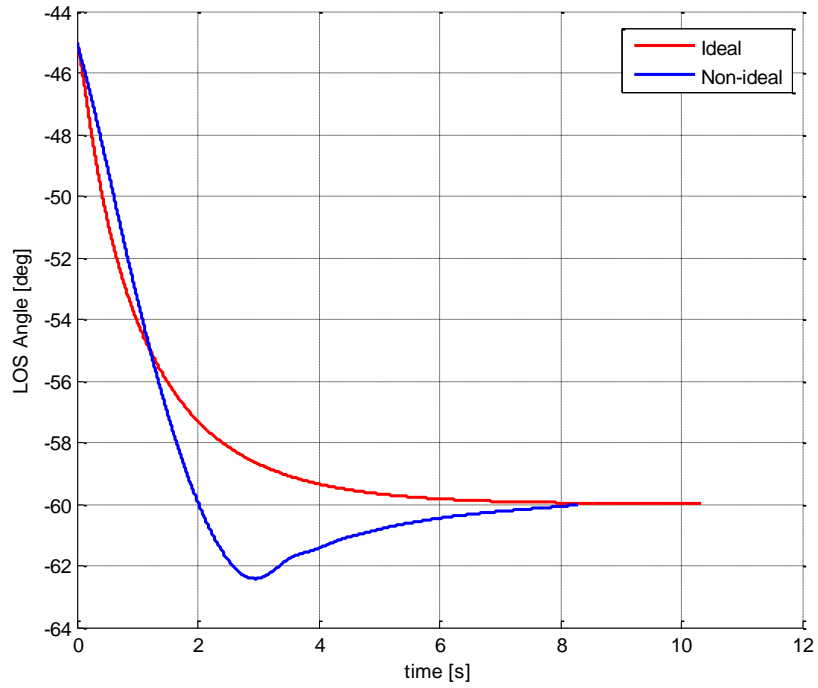


Figure 74. LOS Angle with system lag and limitations

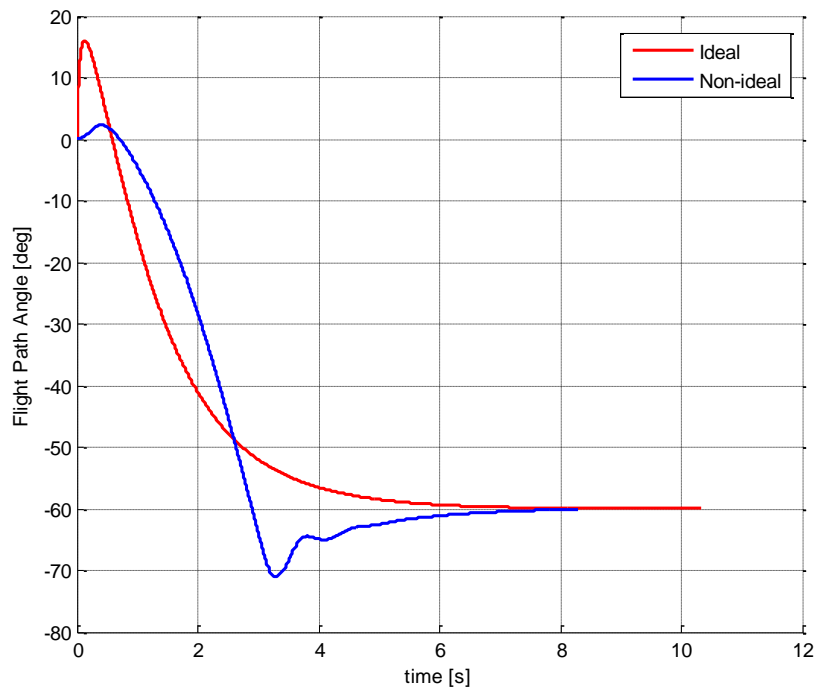


Figure 75. Flight Path Angle with system lag and limitations

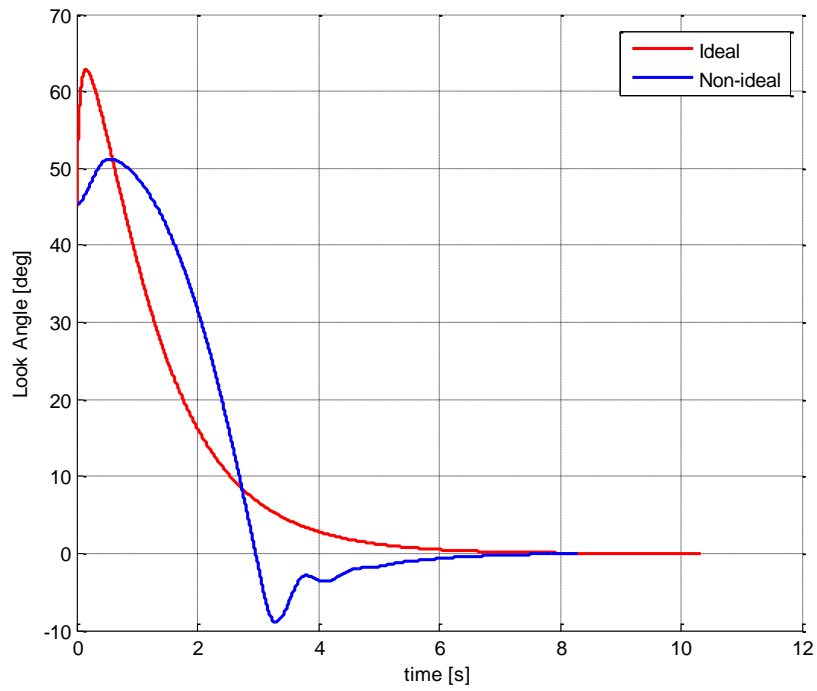


Figure 76. Look Angle with system lag and limitations

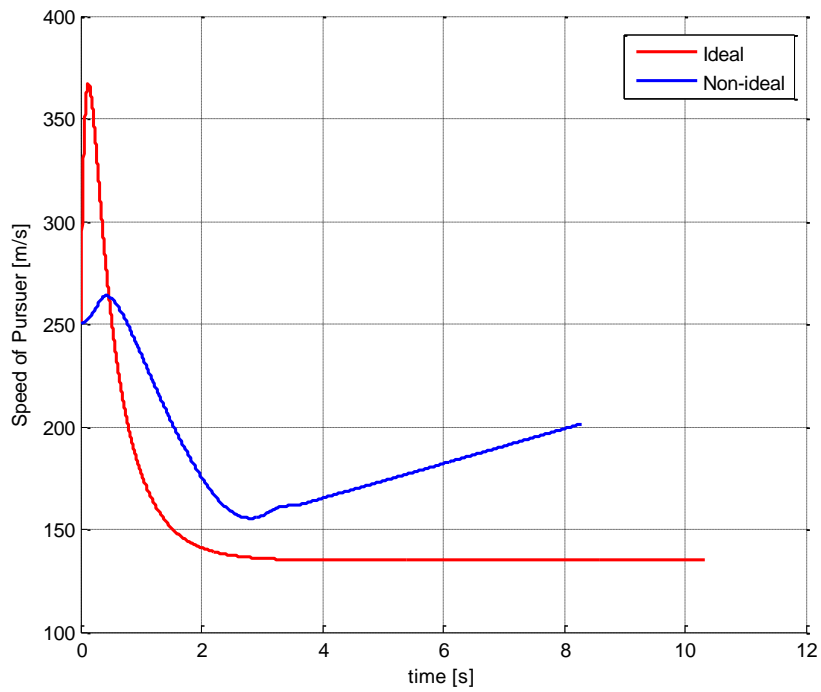


Figure 77. Speed of the Pursuer with system lag and limitations

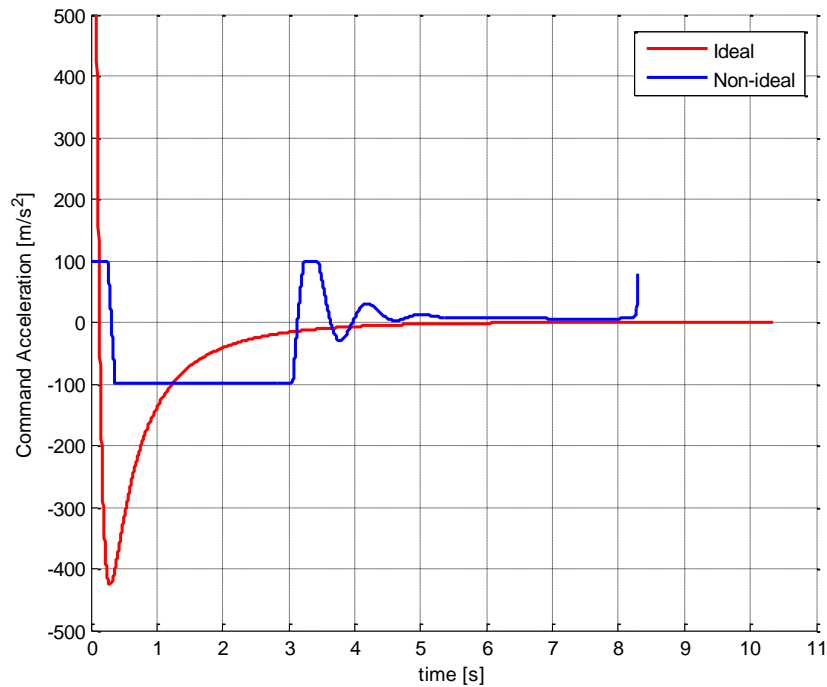


Figure 78. Commanded Acceleration with system lag and limitations

The simulation results for pursuer model with gravity, system lag and acceleration limit can be examined from Figure 73 to Figure 78. The spatial trajectory of the pursuer is shown in Figure 73. Although, the target is successfully captured, the limitation on guidance commands, system lag and gravitational acceleration has a effect on pursuer's trajectory. Due to non-ideal pursuer model, both LOS, flight path and look angles undershoot the desired impact angle during flight. In ideal scenario, the controller-like structure of nonlinear guidance law does not allow undershooting phenomenon. However, the final angles of LOS, flight path and look angle stay between designated values for successful mission criteria. The flight path angle and look angle of the pursuer can be observed from Figure 75 and Figure 76 respectively. The speed of the pursuer is different than ideal system since there are limitations on pursuer acceleration. The speed and commands accelerations of the pursuer can be seen in Figure 77 and Figure 78 respectively. It can be examined that the speed is changing linearly between 0-3 seconds due to limitation. Although the severe

maneuvering to adjust LOS angle at the beginning of the flight is prevented due to limitations, precision on impact angle is not affected by it. Furthermore, again, the constant acceleration commands can be observed to compensate disruptive gravity at the final rendezvous. Nevertheless, the pursuer still successfully intercepts target with desired impact angle in existence of limitations, system lag and gravitational disruptive accelerations.

Some terms that guidance law needs might be hard to provide correctly in practical applications. For that reason, the proposed guidance law is tested with some errors in sensor feedback. The major sources of error in sensors can be briefly categorized as sensor bias and noise. Thus, some sensor bias and white noise values are selected to examine the nominal scenario. The list of scenarios and bias/noise values of the sensor are listed in Table 4. The scenarios are selected considering accelerometer bias and noise, target locator systems' errors and also delays and errors in seeker models. All considered errors are amplified for each scenario to see where the proposed guidance law lose precision or fail to hit the target. All noise values in the Table 4 are the 2σ values of standard deviation. The guidance constant K is selected as 4 in simulations. The seeds of error models selected randomly as day-hour-minute-second data when simulations run.

Table 4. Scenarios for sensor noise & bias

| Scenario | | Accelerometer | Target Position | LOS Angle | Gimbal Dynamics |
|----------|--------------|---------------|-----------------|-----------|-----------------------|
| 1 | Bias | 10 mg | 0.1 m | - | Time constant 0.01 |
| | Noise | 0.001 mg | 0.001 m | 0.5 deg | |
| 2 | Bias | 20 mg | 0.5m | - | Time constant 0.1 |
| | Noise | 0.02 mg | 0.02 m | 1.5 deg | |
| 3 | Bias | 40 mg | 1m | - | Time constant 0.5 |
| | Noise | 0.4 mg | 0.5 m | 4.5 deg | |

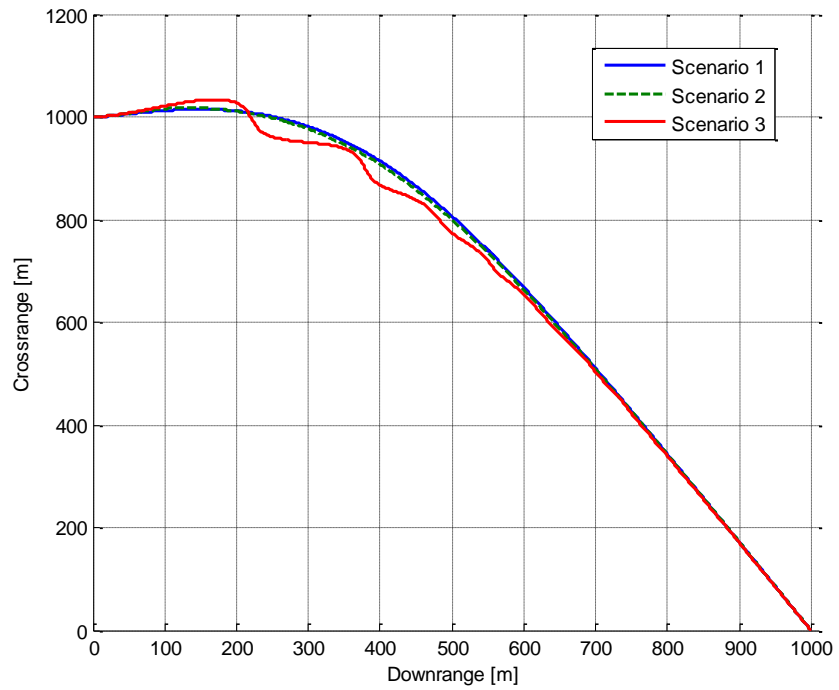


Figure 79. Spatial Trajectory for all three scenarios with sensor errors

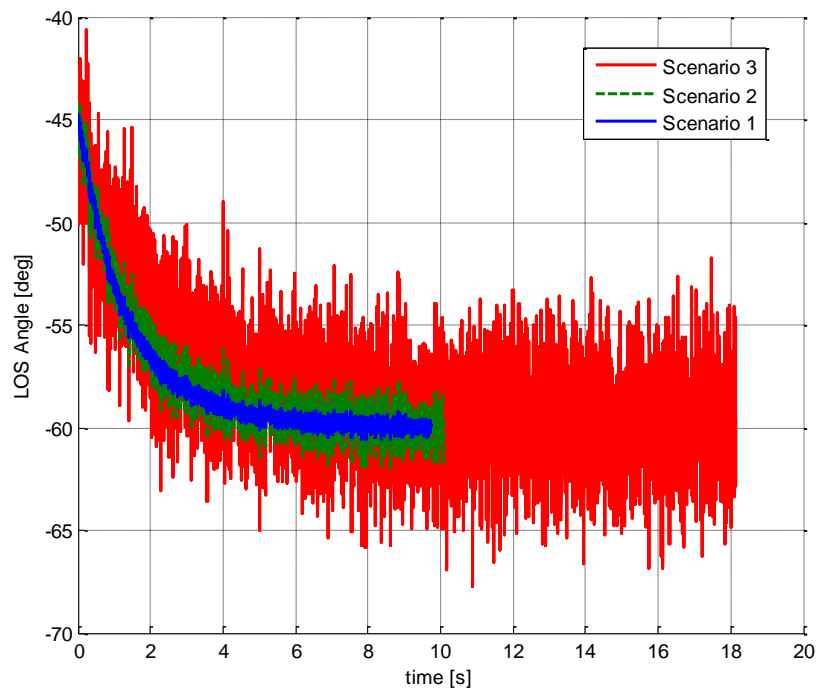


Figure 80. LOS angle for all three scenarios with sensor errors

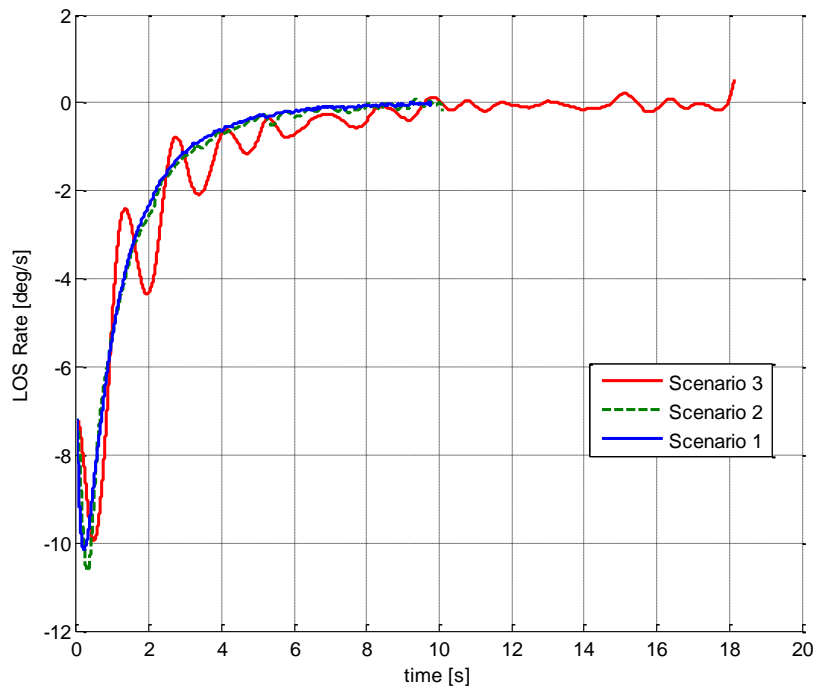


Figure 81. LOS rate for all three scenarios with sensor errors

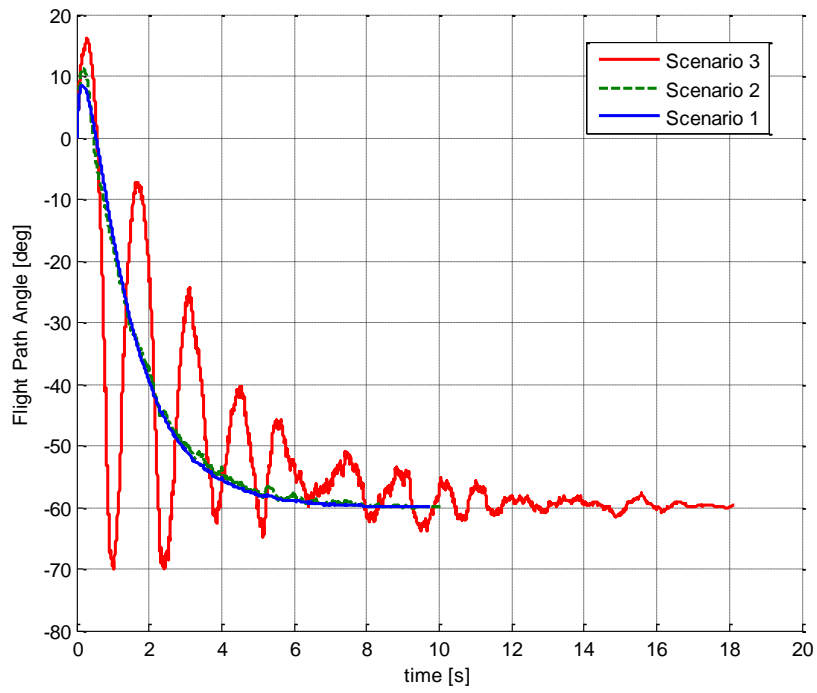


Figure 82. Flight Path Angle for all three scenarios with sensor errors

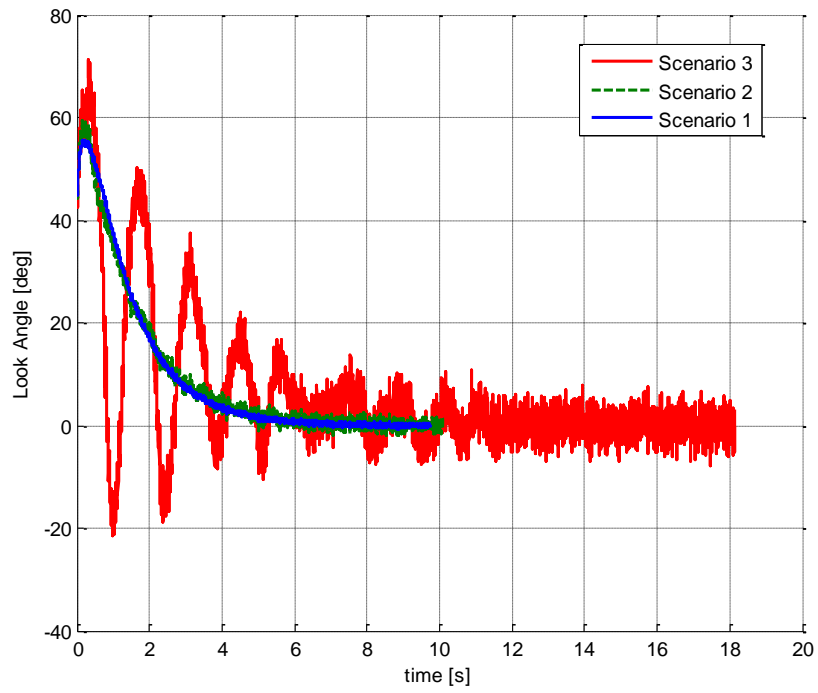


Figure 83. Look Angle for all three scenarios with sensor errors

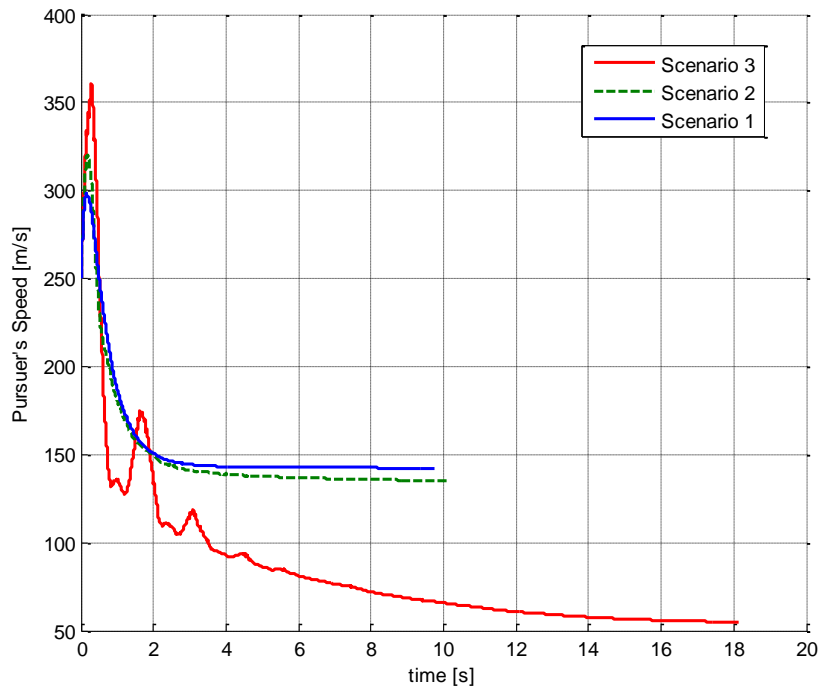


Figure 84. Speed of the pursuer for all three scenarios with sensor errors

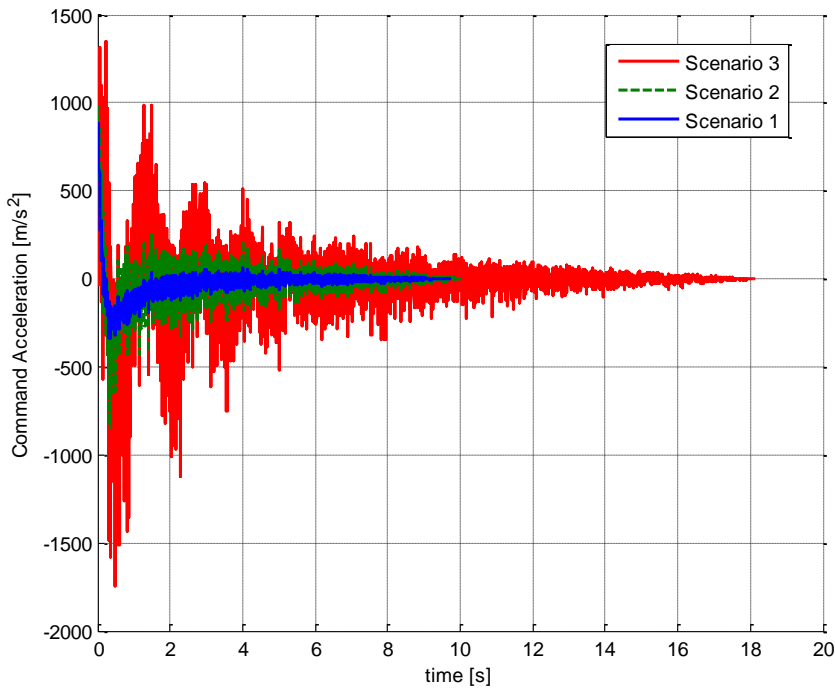


Figure 85. Command Acceleration for all three scenarios with sensor errors

The simulation results for three scenarios to determine the behaviour of proposed guidance law with sensor noise and error is presented in figures from Figure 79 to Figure 85. The spatial trajectories of the pursuer reveals that for all scenarios, target is successfully captured. It can be seen from Figure 80 that LOS angle for first two scenarios are between the acceptable limits for successful mission criteria but the last scenario exceed the limits due to large noise and bias in sensor-feedback. The bias and noise in acceleration can cause shifting and winding up in velocity and position calculations for pursuer, and with combining in errors in target position can amplify the error in range value used in guidance synthesis. The speed and acceleration commands of pursuer can be seen in Figure 84 and Figure 85 respectively. Although the error in LOS angle does not wind-up because the seeker model provides the current data from geometry, look angle calculation includes flight path angle that is shifting due to integration for velocity vector. Thus, closing velocity calculation is

also inaccurate due to that effect. The time constant of first order gimbal dynamics can cause oscillation in stabilization loop of the seeker. Thus, it can effect the sensor feedback for proposed guidance law.

It can be concluded that the proposed guidance law can reject robustly disturbances and noises upto 20 mg bias and white noise with 0.02 mg variance in accelerometer; 0.5 meter error in target estimations with white noise of 0.02 m variance for succesful mission. Moreover, the seeker model's noise characteristics can not exceed approximately 0.5 degree variance for succesfully interception without losing precision. However, note that the proposed guidance law can intercept the target for all scenarios due to its characteristics. Even if the sensor feedbacks have bias and noise, the acceleration commands can still converge to zero for largest part of the interception. Thus, the effects of this erroneous feedback are minimized by proposed guidance law.

It's convenient to state there that the limitations in sensor errors are found for the worst case scenario that errors occur simultaneously. It's appropriate to deduce that the results of the proposed guidance law may vary if errors occurs non-simultaneously. For instance, if the errors in target information is lower than recommended limits, the guidance law can compensate for larger accelerometer errors pursuer may capture the target with desired precision.

Lastly, even if the proposed guidance law is studied for stationary targets, the disturbance rejection analysis shows that the pursuer can handle the error in target position information. This finding can lead to consider testing the effectiveness of the guidance law with moving targets with constant speeds. Thus, the guidance law is simulated for constant speed targets to see the effectiveness and precision in capturing the target. To test that various moving targets are chosen with velocity of -

20, 20, 50 and -50 m/s in x-direction. In other words, the guidance law is tested for targets with escaping towards and against the pursuer. To analyze only the behaviour of the guidance law, the ideal system is used in simulations. Moreover, the guidance constant K is chosen as 4 in simulations.

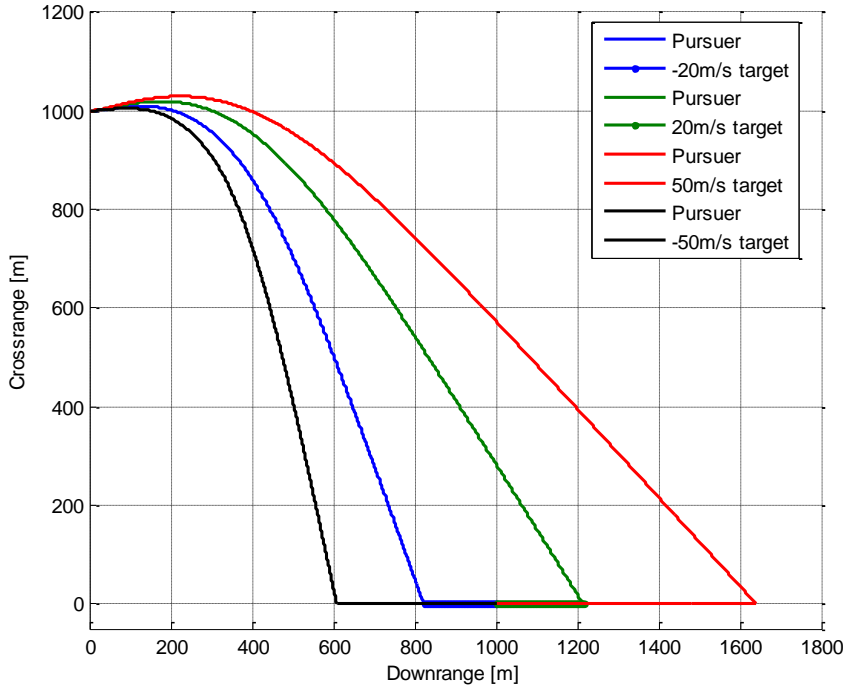


Figure 86. Spatial Trajectories of Pursuer and constant speed targets

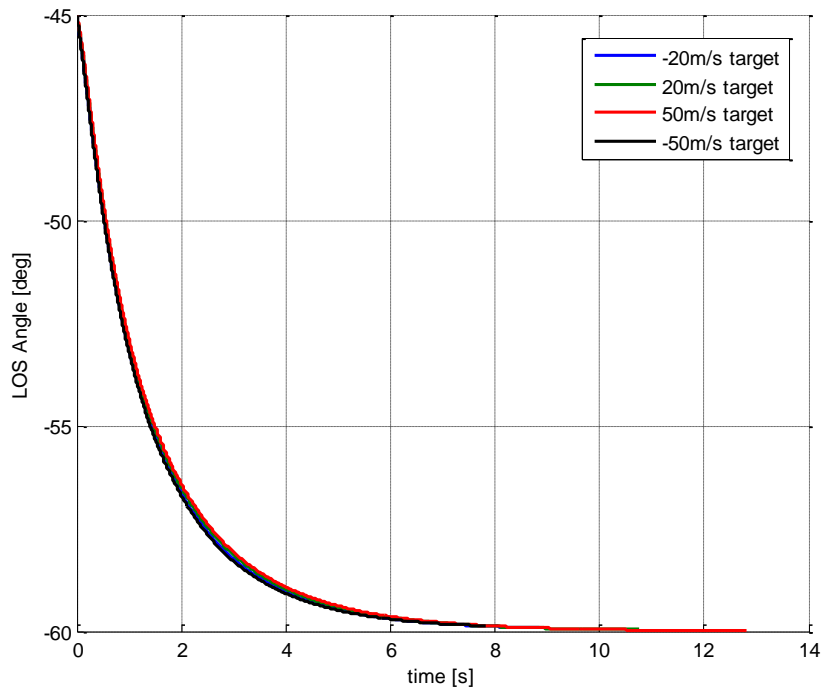


Figure 87. LOS angles between pursuer and constant speed targets

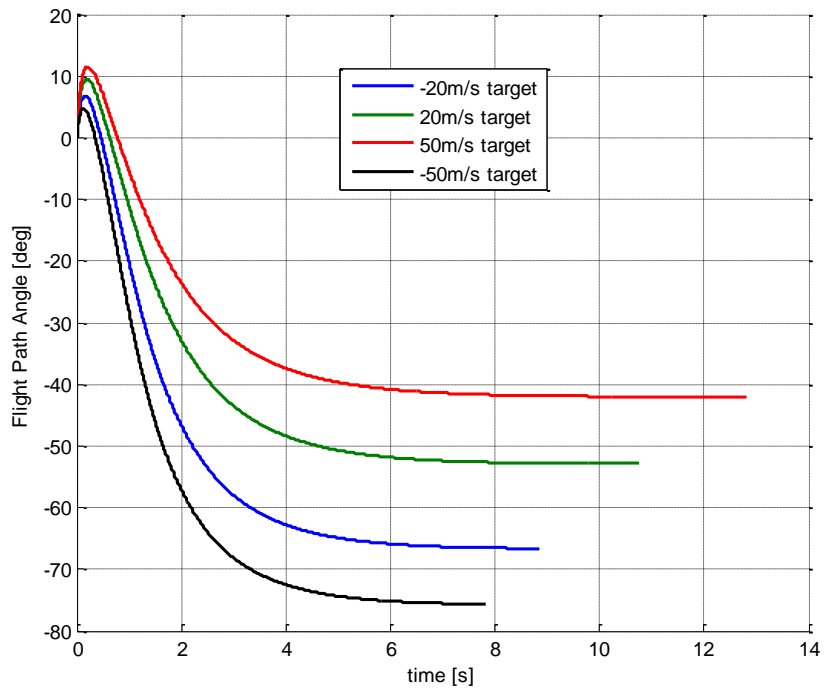


Figure 88. Flight Path Angles of Pursuer and constant speed targets

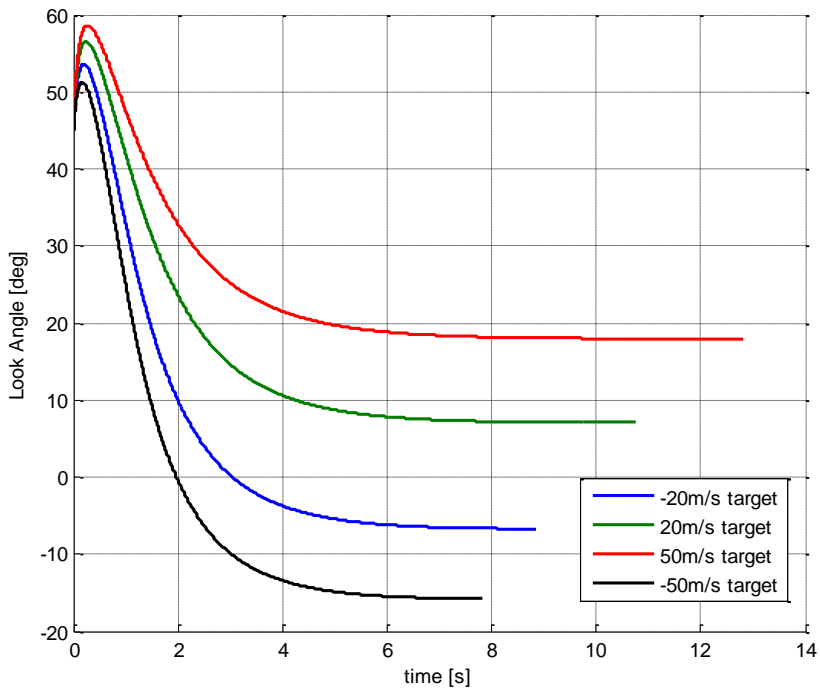


Figure 89. Look Angles of pursuer and constant speed targets

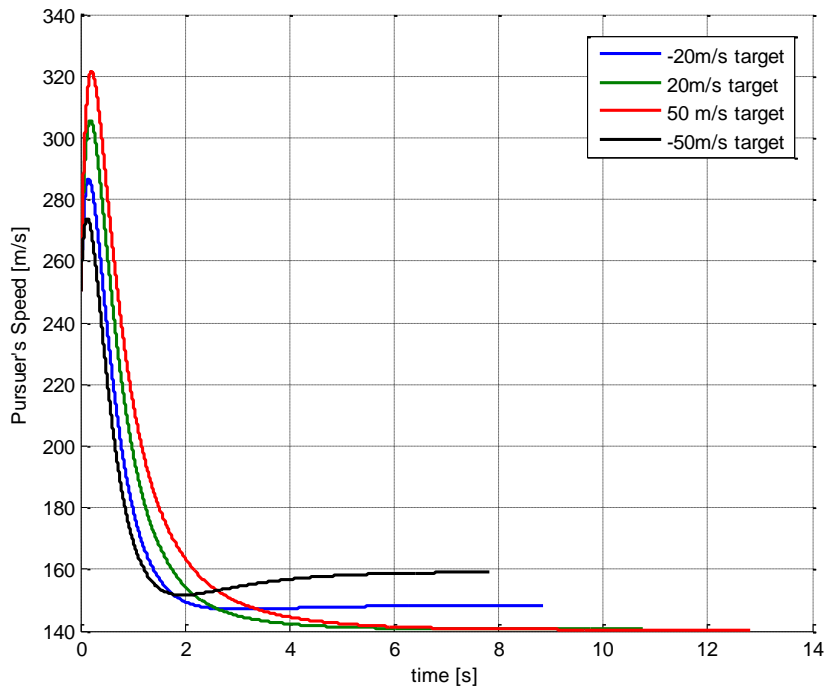


Figure 90. Speed of the pursuer for constant speed targets

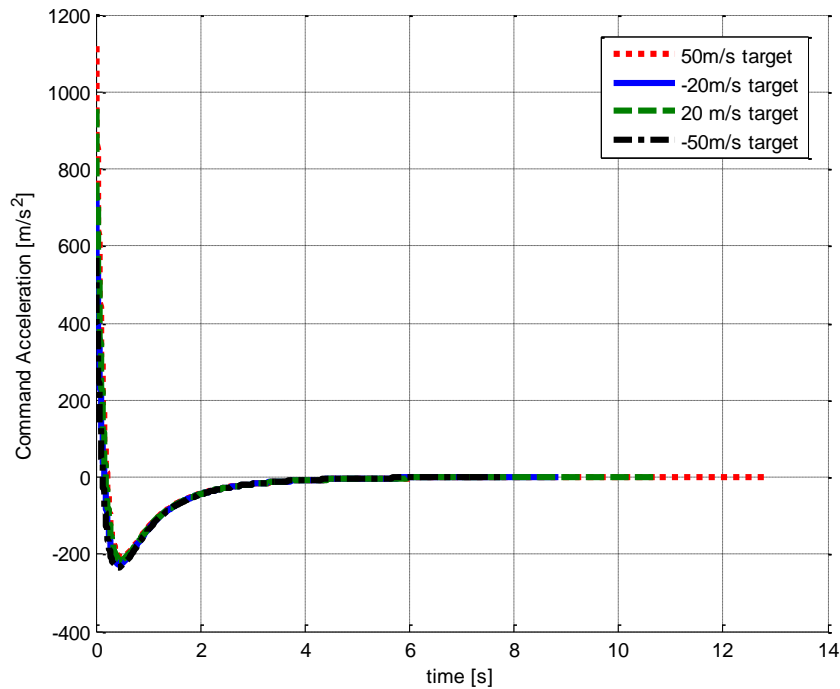


Figure 91. Command Acceleration for pursuer and constant speed targets

The simulation results for various moving targets are presented in figures from Figure 86 to Figure 91. The spatial trajectory of the pursuer reveals that the targets are successfully captured for all scenarios. However, due to target's speed, the flight path angle does not converge the LOS angle. This relationship can be observed from Figure 87, Figure 88 and Figure 89. Although, the relationship between LOS angle, flight path angle and look angle is still reserved, the impact angle –which can be thought as flight path angle– can not be satisfied. However, it can be seen from LOS angle that the proposed guidance law does its job to control LOS angle successfully. In the moving target case, the assumption made in Section 2.2 that the flight path angle of the pursuer converges to the LOS angle at the end of the flight is not satisfied. Hence successful tracking of LOS angle does not yield achievement of desired flight path angle. The look angle of pursuer reveals that the target is captured with non-zero look angle. This is caused by target's motion. It can be seen from Figure 89 that as the escape speed of the target increases, the final constant look

angle of the pursuer also increases. Moreover, the speed and acceleration commands of pursuer can be seen in Figure 90 and Figure 91 respectively. It can be logical to state that if the velocity ratio of the target and pursuer is smaller than 1, the pursuer might catch the target. [1, 3] However, due to guidance commands acting perpendicular to range vector, the speed of the pursuer varies and may decrease lower than target's escaping speed. Thus, the pursuer can not capture target for those conditions. This phenomenon can provide the limits of target speed for successful interception. Although guidance law can satisfy LOS angle for moving target, the simulation results show that the LOS dynamics should be revised with nonlinear control methodology to satisfy impact angle precision.

4.6 Step-size Selection and Integration Scheme

In practical applications, the on-board computer runs in discrete time. Thus, as mentioned before, the integration scheme and step-size selection become vital in capturing target and impact angle precision. In order to test the proposed guidance law's performance, various step-sizes and integration schemes are tried in simulations. Nominally, the step-size is chosen similar in simulation as 0.002 s and integration scheme is forward Euler for previous runs. Thus, the calculations run in a continuous manner with simulations and forward Euler method proves itself for precision and accuracy. In this section, the step-size is reduced to 0.01, 0.1 and 0.2 seconds to compare the results for nominal scenario. All errors, disturbances and integration scheme stay ideal for comparing only effects of step-size selection on precision.

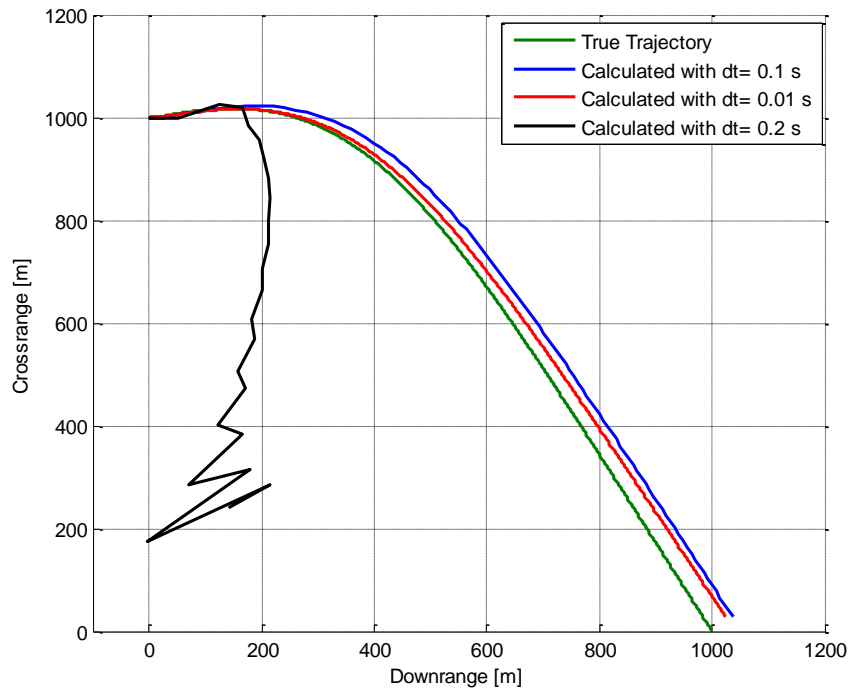


Figure 92. Spatial Trajectories for various step-sizes

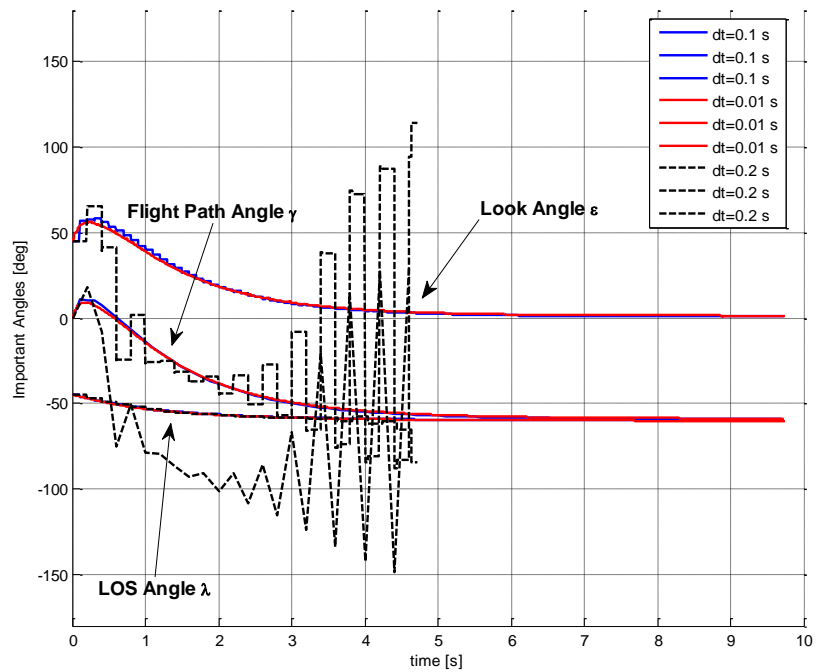


Figure 93. Important angles for various step-sizes

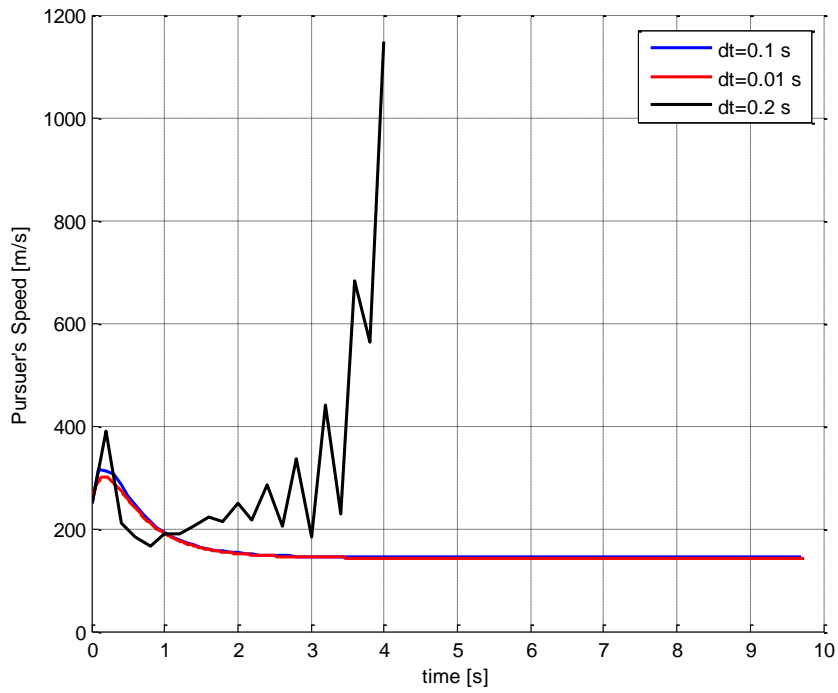


Figure 94. Speed of pursuer for various step-sizes

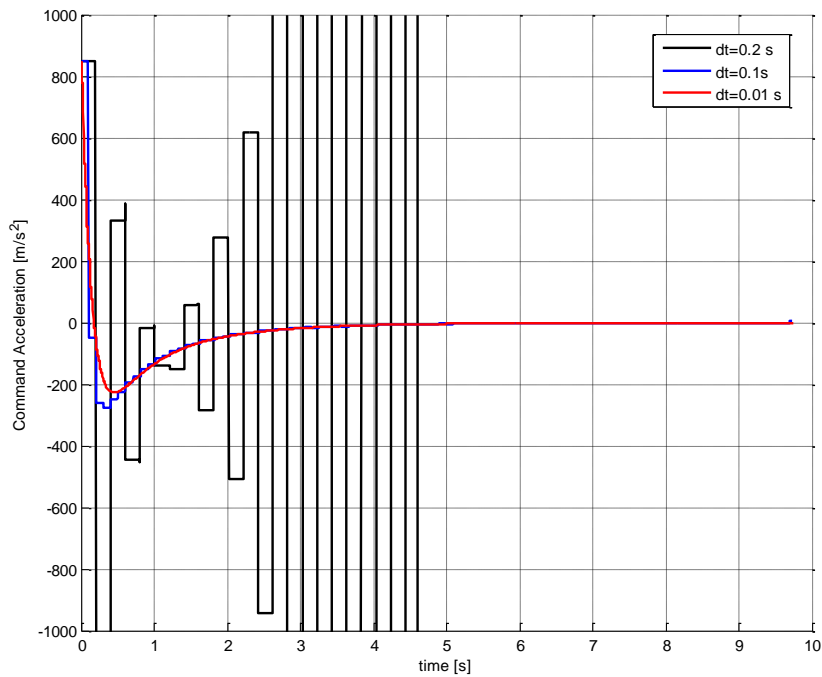


Figure 95. Command Acceleration for various step-size

The spatial trajectories for three scenarios are shown in Figure 92. It can be seen that the third scenario fails to capture the target. Moreover, simulation is terminated due to severe oscillations in mid-run. However, in the first two scenarios, pursuer is successfully captures the target. The important angles for the pursuer-target dynamics for different step-sizes are presented in Figure 93. Reduction in step-size causes oscillations and divergence of the flight path and look angles. Due to that effect, the acceleration commands acting on pursuer diverges instead of converging zero. However, the guidance law manages to control again the LOS angle as its main purpose. The acceleration commands and its effects on pursuer's speed can be observed from Figure 95 and Figure 94 respectively. It is convenient to state here that to accurately calculate the proposed guidance law and avoid divergence caused by step-size selection; the step-size for accurate guidance calculations should be higher than 0.15 seconds ($\sim 7Hz$).

Next, in order to see the effects of integration scheme, the step-size of 0.1 seconds ($\sim 10Hz$) is selected. Various discrete integration schemes are tested in simulations to see the effects of integration scheme on accuracy of guidance calculations.

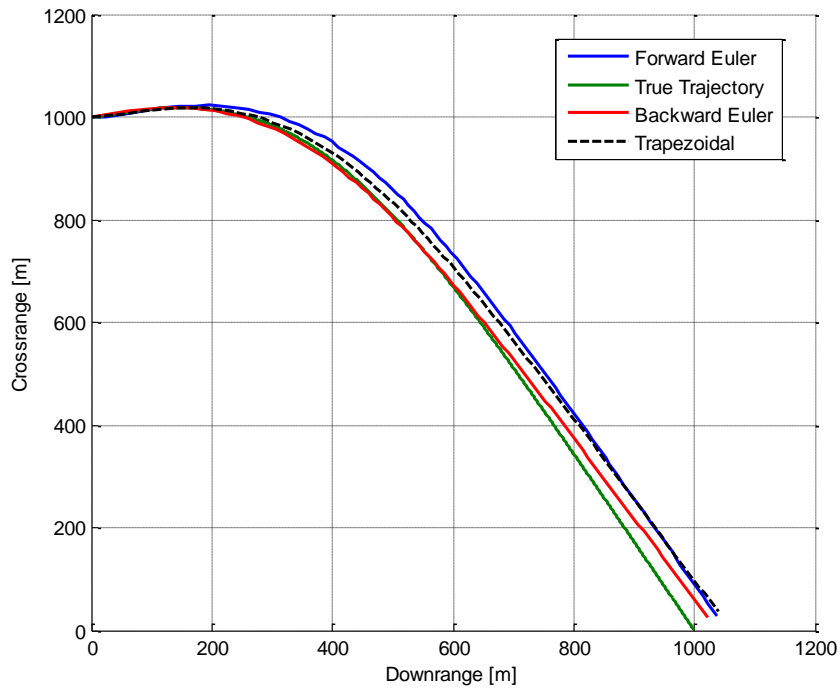


Figure 96. Spatial Trajectories for integration schemes

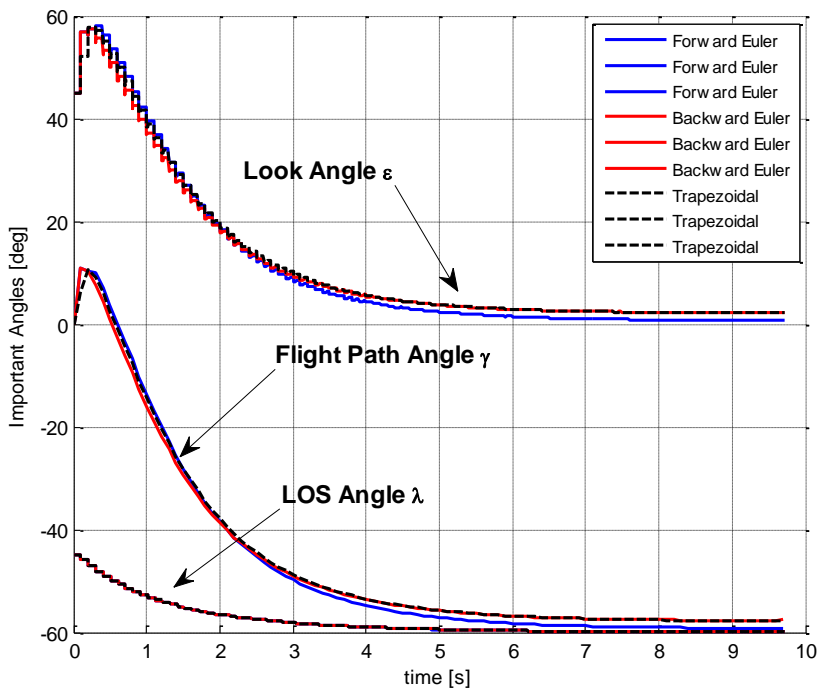


Figure 97. Important angles for integration schemes

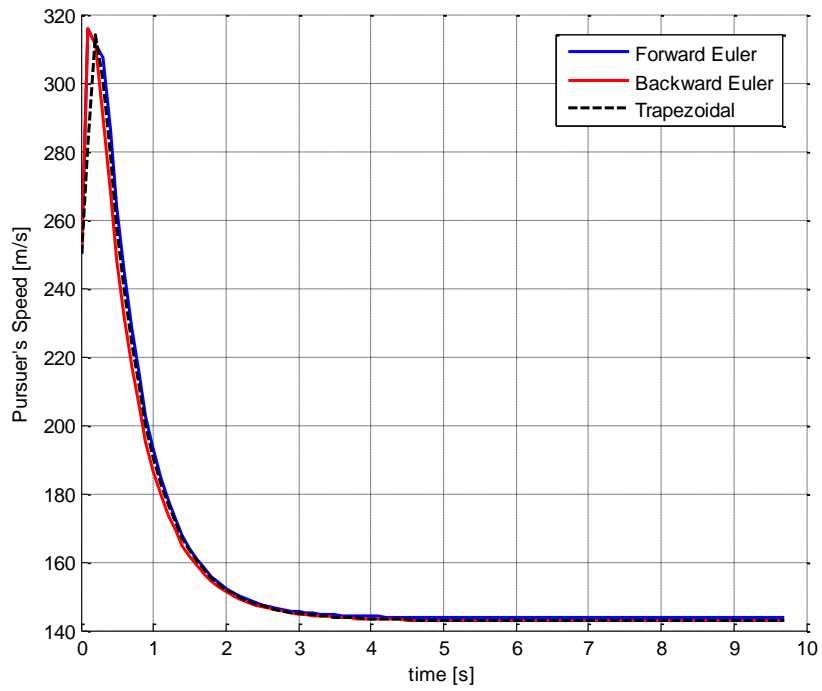


Figure 98. Speed of pursuer for integration schemes

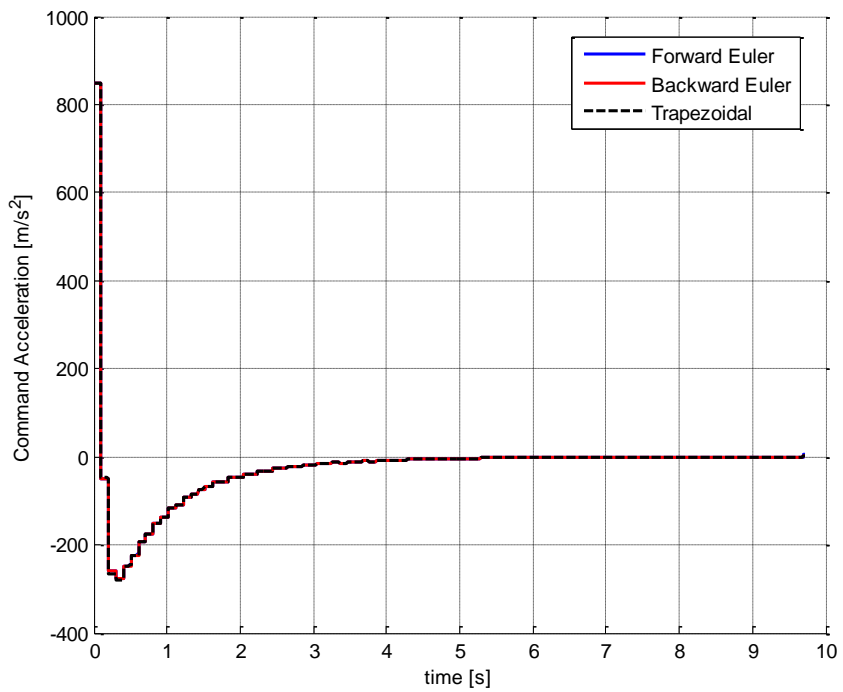


Figure 99. Command Acceleration for integration schemes

The spatial trajectories for scenarios with three different integration schemes are shown in Figure 96. It can be seen that the target is successfully intercepted for all scenarios. The calculated position of the pursuer on flight computer shifts from true trajectory since the step-size is selected as relatively lower to see the effects of integration scheme. However, it can be seen that backward Euler methodology follows true trajectory much longer than other integration schemes. Even if the calculations of position and velocity of the pursuer has an accuracy error, the true trajectories for all scenarios show that the target is captured within successful mission criteria. Note that in the guidance law relative position of target with respect to pursuer obtained by the seeker is used. Therefore, errors in position calculations due to integration do not have a direct effect on capture performance. The important angles for the pursuer-target dynamics for different integration schemes are presented in Figure 97. It can be observed that the LOS controlling proposed guidance law achieves controlling LOS angle with large step-size and different integration schemes successfully. However, due to various methodologies in discrete integration, the other angles are slightly different than each other. The acceleration commands and their indirect effects on pursuer's speed can be observed from Figure 99 and Figure 98 respectively. The acceleration commands on all scenarios are identical since the guidance law can follow same LOS dynamics for different discrete integration schemes. However, the speed of the pursuer changes again due to the different integration schemes.

It can be concluded that guidance law designer should select the most suitable integration scheme and fastest step-size for proposed guidance law in order to achieve impact angle and accuracy in on-board guidance & navigation calculations. Even if the proposed guidance law can control LOS angle for almost all integration schemes and step-sizes, other calculations may affect the mission success.

CHAPTER 5

CONCLUSION

In this study, novel Lyapunov based nonlinear impact angle control guidance law for stationary targets is presented. In addition to that a capturability analysis is performed for proposed guidance law to investigate the capture conditions to intercept the various targets. Guidance law is analyzed in simulation environment to obtain and verify its behavior under disturbances via numerical analyses. Lastly, some aspects which may occur in practical applications are discussed.

In order to control impact angle for stationary targets, first, nonlinear line-of-sight dynamic of the engagement geometry and kinematics between target and pursuer is investigated. The line-of-sight angle which converges the final flight path angle of the pursuer at the final rendezvous is aimed to be controlled to satisfy impact angle constraints in this thesis.

To control final line-of-sight angle stably, a first order sliding manifold is constructed in order to force the line-of-sight dynamical system to slide towards equilibrium subspace with exponential stability. Then, a novel nonlinear method with robust control Lyapunov function is used to force the system towards the defined exponentially stable sliding surface. The asymptotical stability of the closed-loop system is provided via using robust control Lyapunov functions. Then, the control inputs of the dynamical system, which is the acceleration commands perpendicular to range vector; is found for asymptotically stable closed-loop system. This kind of perpendicular to range vector guidance commands are found appropriate and similar to True-Proportional Navigation method, which is a widely recognized guidance law.

Next, to assure the capturability of the target with proposed guidance law, a nonlinear capturability analysis is performed. Since, the dynamics and guidance law is developed in nonlinear environment; a capturability analysis of guidance law should also be nonlinear. Thus, a Lyapunov based capturability analysis which is proven for Pure-Proportional Navigation, True-Proportional navigation and Augmented-Proportional Navigation methods by Ryoo et. al. is used. [48] The results of the capturability analysis show that the proposed guidance law can capture target successfully for defined domains. This defined domain is suitable for both air-to-ground and ground-to-ground missions for stationary targets. Therefore, the capturability of the guidance law is proven.

After proving the capturability of the proposed guidance law, some test scenarios are simulated in MATLAB®/Simulink environment. First, 10 scenarios with various air-to-ground and ground-to-ground missions are tested for ideal systems to verify the capturability of the guidance law. In addition to that some insights about the proposed guidance law characteristics are also obtained from ideal test scenarios. The tunable parameters in guidance law are also studied. The effects of these parameters on guidance performance and characteristics are investigated. The studies showed that the parameters which affect guidance law response could be tuned adequately by guidance engineer.

Next, robustness and disturbance rejection characteristics of the system with proposed guidance law are investigated. In order to analyze the system numerically, successful mission criteria are set for pursuer-target engagements. To test the proposed guidance law; disturbing gravitational acceleration, system lag and acceleration command limitations are applied to the system. The limits of time constants are found for first-order system. Moreover, it's shown that the gravitational acceleration is compensated in closed-loop system without calculating and subtracting gravity from commands externally. This feature may grants some advantages for calculation errors in gravity in practical applications. Then, even though the proposed guidance law requires severe accelerations in the beginning of

the flight, it's demonstrated that the pursuer can also capture the target with desired impact angle in essence of acceleration limits.

Then, some sensor errors are introduced to investigate the behavior of the system under erroneous sensor feedback. The error limitations for guidance law to successfully intercept with target are found numerically. The limitation values for sensors are found to be acceptable considering successful mission criteria.

Moreover, results of behavior of the system with erroneous target information are led to test the proposed guidance law with moving targets. The simulations show that the target is successfully captured for all cases. However, due to target speed, the flight path angle and look angle vary from mentioned desired values for successful mission criteria. However, the LOS angle and angular rate is controlled successfully as expected for all moving target cases. Therefore, it's concluded that the LOS dynamics and control topology should be revised for moving target. Thus, it can be said that the future works will proceed towards capturing moving and maneuvering targets.

Lastly, the proposed guidance law is tested for integration scheme and step-size selection. The results show that selection of the step-size is vital to accurately calculate necessary values used in guidance law. Moreover, in general to remain the safe side, the step-size of the on-board calculations should be selected as $1/5$ or $1/10$ of the fastest dynamics. As expected, simulations results show that as the size-step is bigger, the accuracy in calculations and desired impact angle decreases. Thus, the step-size should be selected as low as hardware allows for accurate calculations.

The integration scheme which is used in discrete navigation calculations are also vital part in mission success. The simulation results show that not only step-size selection but also the integration method should be revised for most suitable case for mission. Note that the backward Euler method is found to be less erroneous method for low step-sizes. Thus, if the hardware can't allow using lower step-sizes and

higher frequency calculations, the discrete backward Euler integration is advised to use in navigation calculations.

Future efforts for the proposed guidance law are planned to import pursuer, autopilot and sensor dynamics into the derivation of LOS dynamics. This integrated guidance and control methodology can grant some more robustness and precision. Moreover, the 3-D implementations of the proposed guidance law can provide more insights about pursuer-target kinematics and more realistic results for rigid body dynamics. Thus, point-mass pursuer assumption can be eliminated with 3-D implementation of the proposed guidance law. Furthermore, the LOS dynamics and impact angle relationships for maneuvering and moving targets are planned to analyze as mentioned before.

The immediate plan for future work is to modify the guidance law to command accelerations perpendicular to pursuer velocity vector. Although accelerations perpendicular to range vector is proven to be valid, most of the pursuers in practical applications are controlled aerodynamically. Also, thrust control of the pursuers for stationary targets may not be available most of the time. For these reasons, the more applicable versions of the guidance laws will be prepared.

REFERENCES

- [1] N. A. Shneydor, *Missile Guidance and Pursuit: Kinematics, Dynamics and Control*, Horwood Publishing Limited, Horwood, Chichester, West Sussex, England, 1998
- [2] M. W. Fossier, *The Development of Radar Homing Missiles*, Journal of Guidance, Control and Dynamics, Vol. 7, No. 6, 1984, pp. 641-651
- [3] P. Zarchan, *Tactical and Strategic Missile Guidance, 6th Ed.*, Progress in Astronautics and Aeronautics, Atlanta, Georgia, 2012.
- [4] C. L. Yuan, *Homing and Navigation Courses of Automatic Target-Seeking Devices*, RCA Labs, Rept. PTR-12C, Princeton, New Jersey, 1942.
- [5] C. L. Yuan, *Homing and Navigation Courses of Automatic Target-Seeking Devices*, Journal of Applied Physics, Vol. 19, 1948, pp. 1122-1128
- [6] A. E. Bryson, and Y. C. Ho, *Applied Optimal Control*, Blaisdell, Waltham, Massachusetts, 1969
- [7] M. Guelman, *Closed-Form Solution of True Proportional Navigation*, IEEE Transaction on Aerospace and Electronics Systems, Vol. AES-12, No. 4, 1979.
- [8] K. Becker, *Closed-Form Solution of Pure Proportional Navigation*, IEEE Transactions on Aerospace and Electronics Systems, Vol. 26, No. 3, 1990.
- [9] U. S. Shukla, and P. R. Mahapatra, *The Proportional Navigation Dilemma – Pure or True?*, IEEE Transactions on Aerospace and Electronics Systems, Vol. 26, No.2, 1990
- [10] G. M. Siouris, *Comparison between Proportional and Augmented Proportional Navigation*, Nachrichtentechn. Z., Vol. 27, No.7, 1974, pp. 278-280

- [11] M. Kim, and K. V. Grider, *Terminal Guidance for Impact Attitude angle constrained flight trajectories*, IEEE Transactions on Aerospace and Electronics Systems, Vol. AES-9, No. 6, 1973, pp. 852-859
- [12] B. S. Kim, J. G. Lee, and H. S. Han, *Biased PNG Law for Impact with Angular Constraint*, IEEE Transactions on Aerospace and Electronics Systems, Vol. 34, No. 1, 1998, pp.277-288
- [13] C. H. Lee, T. K. Kim, and M. J. Tahk, *Interception Angle Control Guidance using Proportional Navigation with Error Feedback*, Journal of Guidance, Control and Dynamics, Vol. 36, No. 5, 2013, pp. 1556-1561
- [14] K. S. Erer, and O. Merttopçuoğlu, *Indirect Impact-Angle-Control Against Stationary Targets Using Biased Proportional Navigation*, Journal of Guidance, Control and Dynamics, Vol. 35, No. 2, 2012, pp.700-703
- [15] G. W. Cherry, *A General, Explicit, Optimizing Guidance Law for Rocket-Propelled Spaceflight*, AIAA Paper No. 64, 638, AIAA/ION Astrodynamics Guidance and Control Conference, 1964, August 24-26
- [16] E. J. Ohlmeyer, and C. A. Phillips, *Generalized Vector Explicit Guidance*, Journal of Guidance, Control and Dynamics, Vol. 29, No. 2, 2006, pp. 261-268
- [17] C. F. Lin, *Modern Navigation, Guidance, and Control Processing*, Prentice Hall, Englewood Cliffs, New Jersey 07632, Chapter 8, 1991
- [18] R. G. Cottrel, *Optimal Intercept Guidance for Short-Range tactical Missiles*, Journal of Guidance, Control and Dynamics, Vol. 5, No. 10, 1971, pp.1414-1415
- [19] E. J. Holder, and V. B. Sylvester, *An analysis of modern versus classical homing guidance*, IEEE Transactions on Aerospace and Electronic Systems, Vol. 26, No. 4, 1990, pp. 599-605
- [20] I. Rusnak, and L. Meir, *Optimal Guidance for high order and acceleration constrained missile.*, Journal of Guidance, Control and Dynamics, Vol. 14, No. 3, 1991, pp. 589-596

- [21] I. Rusnak, *Advanced guidance laws for acceleration constrained missile, randomly maneuvering target and noisy measurement*, Proceedings of the IEEE regional conference aerospace control system, Westlake, California, 1993
- [22] C. K. Ryoo, H. Cho, and M. J. Tahk, *Optimal Guidance law with Terminal Impact angle Constraint*, Journal of Guidance, Control and Dynamics, Vol. 28, No. 4, 2005, pp.724-732
- [23] R. J. York, and H. L. Pastrick, *Optimal Terminal Guidance with Constraints at Final Time*, Journal of Spacecraft and Rockets, Vol. 14, No. 6, 1977, pp. 381-182
- [24] T. L. Song, and J. S. Shin, *Time Optimal Impact Angle Control for Vertical Plane Engagements*, IEEE Transactions on Aerospace and Electronics System, Vol. 35, No.
- [25] S. Gutman, *On Optimal guidance for homing missiles*, Journal of Guidance, Control and Dynamics, Vol. 2, No. 4, 1979, pp.296-300
- [26] Y. Lipman, J. Shinar, and Y. Oshman, *Stochastic analysisi of the interception of maneuvering antisurface missiles*, Journal of Guidance, Control and Dynamics, Vol. 20, No. 4, 1997, pp.707-714
- [27] I. R. Manchester, and A. V. Savkin, *Circular-Navigation-Guidance Law for Precision Missile/Target Engagements*, Journal of Guidance, Control and Dynamics, Vol. 29, No. 2, 2006, pp.314-320
- [28] Y. C. Chiou, and C. Y. Kuo, *Geometric Approach to Three Dimensional Missile Guidance Problem*, Journal of Guidance,Control and Dynamics, Vol. 21, No. 7, 2003, pp. 819-832
- [29] A. V. Savkin, P. Pathirana, and F. A. Faruqi, *The Problem of Precision Missile Guidamce: LQR and H^∞ Frameworks*, IEEE Transactions on Aerospace and Electronics System, Vol. 39, No. 3, 2003, pp. 901-910
- [30] T. W. Hwang, and M. J. Tahk, *Integrated Backstepping Design of Missile Guidance and Control with Robust Disturbance Observer*, Proceedings of the SICE-

ICASE International Joint Conference, IEEE Publications, Piscataway, New Jersey, 2006, pp. 4911-4915

[31] M. Xin, S. N. Balakrishnan, and E. J. Ohlmeyer, *Integrated Guidance and Control of Missile with θ -D Method*, IEEE Transactions on Control Systems Technology, Vol. 14, No. 6, 2006, pp. 981-992

[32] B. H. Sang, and C. S. Jiang, *Integrated Guidance and Control for a Missile in the Pitch Plane Based upon Subspace Stabilization*, Proceedings of the 2009 Chinese Control and Decision Conference (CCDC 2009), IEEE Publications, Piscataway, New Jersey, 2009, pp. 5409-5414

[33] P. K. Menon, G. Sweriduk, E. J. Ohlmeyer, and D. Malyevac, *Integrated Guidance and Control of Moving Mass Actuated Kinetic Warheads*, Journal of Guidance, Control and Dynamics, Vol. 27, No. 1, 2004, pp. 118-126

[34] S. S. Vaddi, P. K. Menon, and E. J. Ohlmeyer, *Numerical State-Dependent Riccati Equation Approach for Missile Integrated Guidance Control*, Journal of Guidance, Control and Dynamics, Vol. 32, No. 2, 2009, pp. 699-703

[35] I. Shkolnikov, Y. Shtessel, and D. Lianos, *Integrated Guidance Control Systems of a Homing Interceptor-Sliding Mode Approach*, AIAA Guidance, Navigation and Control Conference and Exhibit, AIAA 2001-4218, 2001

[36] Y. B. Shtessel, I. A. Shkolnikov, *Integrated Guidance and Control of Advanced Interceptors Using Second Order Sliding Modes*, Proceedings of the 42nd IEEE Conference on Decision and Control, IEEE Publications, Piscataway, New Jersey, 2003, pp. 4587-4592

[37] Y. Y. Wei, M. Z. Hou, and G. R. Duan, *Adaptive Multiple Sliding Surface Control for Integrated Missile Guidance and Autopilot with Terminal Angular Constraint*, Proceedings of the 29th Chinese Control Conference, IEEE Publications, Piscataway, New Jersey, 2010, pp. 2162-2166

- [38] D. C. Foreman, C. H. Tournes, and Y. B. Shtessel, *Integrated Missile Flight Control Using Quaternions and Third-Order Sliding Mode Control*, Proceedings of the American Control Conference, IEEE Publications, Piscataway, New Jersey, 2010, pp. 1332-1337
- [39] J. G. Guo, and J. Zhou, *Integrated Guidance and Control of Homing Missile with Impact Angular Constraint*, Proceedings of 2010 International Conference on Measuring Technology and Mechatronics Automation, IEEE Publications, Piscataway, New Jersey, 2010, pp. 480-483
- [40] H. B. Oza, and R. Padhi, *Nonlinear Suboptimal Guidance Law with 3D Impact Angle Constraints for Ground Targets*, AIAA Guidance, Navigation and Control Conference and Exhibit, AIAA 2010-8185, 2010
- [41] X. Wang, and X. Wang, *Partial Integrated Guidance and Control with Impact Angle Constraints*, Journal of Guidance, Control and Dynamics, AIAA Early Edition, 2014
- [42] R. T. Yanushevsky, and W. J. Boord, *A New Approach to Guidance Law design*, AIAA Guidance, Navigation and Control Conference and Exhibit, AIAA 2003-5577, Austin Texas, 2003
- [43] R. Yanushevsky, *Modern Missile Guidance*, CRC Press, Taylor & Francis Group, New York, 2008
- [44] N. Lèchevin, and C. A. Rabbath, *Lyapunov-Based Nonlinear Missile Guidance*, Journal of Guidance, Control and Dynamics, Vol. 27, No 6, 2004, pp.1096-1101
- [45] D. S. Sang, B.M. Min, and M.J.Tahk, *Impact Angle Control Guidance Law using Lyapunov Function and PSO Method*, SICE Annual Conference, 2007, pp. 2253-2257
- [46] M. Guelman, *A Qualitative Study of Proportional Navigation*, IEEE Transactions on Aerospace and Electronics Systems, Vol. AES-7, No. 4, 1971, pp. 637-643

- [47] R. A. Freeman, and P. V. Kokotović, *Robust Nonlinear Control Design State-Space and Lyapunov Techniques*, Modern Birkhäuser Classics, Reprint of the 1996 Edition, Boston, 2008
- [48] C. K. Ryoo, Y. H. Kim, and M. J. Tahk, *Capturability Analysis of PN Laws Using Lyapunov Stability Theory*, AIAA Guidance, Navigation and Control Conference and Exhibit, AIAA 2004-4883, 2004
- [49] H. U. Ateş, *Sabit Hedefler İçin Lyapunov Tabanlı Doğrusal Olmayan Vuruş Açısı Kontrollü Güdüm Kanunu*, Havacılıkta İleri Teknolojiler Konferansı HİTEK-2014
- [50] H. U. Ateş, *Lyapunov Based Nonlinear Impact Angle Guidance Law for Stationary Targets*, AIAA SciTech 2015, Guidance, Navigation and Control Conference and Exhibit, 2015
- [51] H. K. Khalil, *Nonlinear Systems*, Prentice-Hall Inc, Upper Saddle River, New Jersey, 2002
- [52] A. M. Lyapunov, *Problème general de la stabilite du mouvement*, Ann. Fac. Sci. Toulouse, 9, 1907, pp. 203-474. *in French*
- [53] J. Kurzweil, *On the inversion of Liapunov's second theorem on stability of motion*, Ann. Math. Soc. Transl. Ser. 2, 24, 1956, pp.19-77
- [54] J. L. Massera, *Contributions to stability theory*, Annals of Mathematics, 64, 1956, pp. 182-206.
- [55] R. E. Kalman, and J. E. Bertram, *Control System Analysis and design via the "second method" of Lyapunov, I: Continuous-time systems*, Journal of Basic Engineering, Vol. 32, 1960, pp. 1241-1253
- [56] A. A. Krasovskiy, *A new solution to problem of a control system analytical design*, Automatica, Vol. 7, 1971, pp.45-50

- [57] D. H. Jacobson, *Extensions of Linear-Quadratic Control, Optimization and Matrix Theory*, Academic Press, London, 1977
- [58] V. Jurdjevic, and J. P. Quinn, *Controllability and stability*, Journal of Differential Equations, Vol. 28, 1978, pp.381-389
- [59] S. H. Song, and I.J. Ha, *A Lyapunov-like Approach to performance Analysis of 3-Dimensional Pure PNG Laws*, IEEE Transactions on Aerospace and Electronic Systems, Vol. 30, No.1, 1994, pp.238-248
- [60] S. Ghosh, D. Ghose, and S. Raha, *Capturability of Augmented Proportional Navigation (APN) Guidance with Nonlinear Engagement Dynamics*, American Control Conference (ACC) , 2013